Characterization of the pathogenicity relevant genes *THI4* and *PA14_2* in *Verticillium dahliae*

Dissertation

zur Erlangung des mathematisch-naturwissenschaftlichen Doktorgrades

"Doctor rerum naturalium"

der Georg-August-Universität Göttingen

im Promotionsprogramm GAUSS

der Georg-August University School of Science

vorgelegt von

Clara Elisabeth Hoppenau

aus Köln

Göttingen 2013

Betreuungsausschuss und Mitglieder der Prüfungskomission

Referent: Prof. Dr. Gerhard Braus, Abteilung für Molekulare Mikrobiologie und Genetik, Institut für Mikrobiologie und Genetik

Korreferentin: Prof. Dr. Ursula Kües, Institut für Forstbotanik

Weitere Mitglieder der Prüfungskommission:

Prof. Dr. Stefanie Pöggeler, Abteilung für Genetik Eukaryotischer Mikroorganismen, Institut für Mikrobiologie und Genetik

Prof. Dr. Rolf Daniel, Abteilung für Angewandte Mikrobiologie, Institut für Mikrobiologie und Genetik

Jun.-Prof. Dr. Kai Heimel, Abteilung für Mikrobielle Zellbiologie, Institut für Mikrobiologie und Genetik

PD Dr. Stefan Irniger, Abteilung für Molekulare Mikrobiologie und Genetik, Institut für Mikrobiologie und Genetik

Tag der mündlichen Prüfung: 04.12.2013

Die vorliegende Arbeit wurde in der Arbeitsgruppe von Prof. Dr. Gerhard H. Braus in der Abteilung Molekulare Mikrobiologie und Genetik des Instituts für Mikrobiologie und Genetik der Georg-August-Universität Göttingen angefertigt.
Teile dieser Arbeit wurden veröffentlicht in:

Clara E. Hoppenau, Van Tran Tuan, Harald Kusch, Kathrin P. Aßhauer, Manuel Landesfeind, Peter Meinicke, Blagovesta Popova, Susanna A. Braus-Stromeyer, and Gerhard H. Braus (2014) *Verticillium dahliae VdTHI4* involved in thiazole biosynthesis, stress response and DNA repair functions is required to induce vascular disease in tomato. *Environmental and experimental botany* (in press)

Meinen Eltern und Geschwistern

Table of contents Page

Abbreviations ..... **VIII**

Summary **1**

Zusammenfassung **2**

1 Introduction **4**

1.1 *Verticillium* is a soil borne plant pathogen 4

1.1.1 Morphology of *Verticillium* 7

1.1.2 *Verticillium* is a monocyclic phytopathogenic fungus 7

1.1.3 Genetics of *Verticillium* 9

1.2 *THI4*, a gene of the essential thiamine pathway 10

1.3 Secreted proteins are required for the first contact to the host 16

1.4 Aim of this work 19

2 Materials and methods **21**

2.1 Chemicals 21

2.2 Prokaryotic microorganisms 21

2.3 Eukaryotic microorganisms 21

2.3.1 Yeast strains 21

2.3.2 Plant lines 22

2.3.3 *Verticillium* strains 22

2.4 Plasmids 30

2.4.1 Construction of plasmids for *V. dahliae* knock-out strains 31

2.4.2 Construction of plasmids for complementation of *VdΔTHI4* and *VdΔPA14_2* 31

2.4.3 Construction of *GFP*-tagged plasmids 32

2.5 Recombinant DNA methods 33

2.6 Fungal nucleic acid purification and hybridization 33

2.7 Genetic manipulations 35

2.7.1 *E. coli* transformation 35

2.7.2 *S. cerevisiae* transformation 35

2.7.3 *Agrobacterium tumefaciens*-mediated transformation in *Verticillium* spp. 35

2.7.4 Transformation of DNA in *Verticillium dahliae* via protoplastation 35

2.8 Sequence analysis 36

2.9 Microscopy analysis 36

2.10 UV-irradiation assay 37

2.11 Plant infection assay 37
2.11.1 Plant growth and cultivation 37
2.11.2 Spore solutions 38
2.11.3 Planting and infection process 38
2.11.4 Growth conditions 38
2.11.5 Documentation of infection symptoms 38
2.11.6 Sample collection 38
2.11.7 Fungal out-growth of infected plant material 39
2.11.8 Fungal DNA extraction and quantification of infected plant material 39
2.12 Experimental setup for *V. longisporum* omics (big batch) 40
2.12.1 Fungal growth and transfer procedure 40
2.13 Transcriptomics of *V. longisporum* 43 40
2.13.1 RNA transcriptomics by deep sequencing 40
2.13.2 Reads per kilobase per million of mapped reads (RPKM) data processing 40
2.13.3 MarVis analysis 41
3 Results 42
3.1 *V. dahliae* Thi4 shows amino acid sequence similarities to *S. cerevisiae* and *F. oxysporum* proteins involved in thiazole biosynthesis 42
3.1.1 Knockout of *V. dahliae THI4* evokes reduced growth on thiamine-free medium 44
3.1.2 *Verticillium* Thi4p is localized in mitochondria 50
3.1.3 DNA damage repair and oxidative stress response is affected by *Verticillium* Thi4 51
3.1.4 *Verticillium* Thi4 is involved in plant pathogenicity 54
3.2 Secreted *Verticillium dahliae* Pa14_2 protein is involved in infection process 57
3.2.1 The *VdPA14_2* knockout is deficient in black colored microsclerotia formation 58
3.2.2 *Verticillium* Pa14_2 is localized at the fungal membrane 62
3.2.3 *Verticillium* Pa14_2 increases oxidative stress in the cell 63
3.2.4 *Verticillium* Pa14_2 is involved in the infection process of the host 64
3.3 Transcriptomic analysis of *in situ* and *in vitro* expressed transcripts of *Verticillium longisporum 43* 67
3.3.1 Core regulated transcripts of *V. longisporum* in *in situ* (xylem-sap) and *in vitro* (SXM) cultivation 69

3.3.1.1 Cellular localization of core transcripts 69
3.3.1.2 Comparison of functional classes and predicted domains of the core transcriptome 71
3.3.2 Specific regulated transcripts of *V. longisporum* in *in situ* (xylem-sap) and *in vitro* (SXM) cultivation 74
3.3.2.1 Cellular localization of specific regulated transcripts 75
3.3.2.2 Comparison of xylem-sap and SXM specific up-regulated transcripts 77
3.3.2.3 Comparison of xylem-sap and SXM specific 20 highest up-regulated transcripts 82
3.3.2.4 Comparison of predicted domains in xylem-sap and SXM specific up-regulated transcripts 86
4 Discussion 89
4.1 Thi4, the mitochondrial localized thiazole synthase in *Verticillium dahliae* 89
4.1.1 Involvement of Thi4 in DNA repair mechanism and oxidative stress-response 92
4.1.2 Thiazole synthase mutant of *Verticillium dahliae* is impaired in pathogenicity 93
4.2 The secreted Pa14_2 is involved in melanization and in response to ROS of *Verticillium dahliae* 95
4.2.1 *Verticillium dahliae* Pa14_2 mutant is impaired in infection process on host plants 98
4.3 Protoplastation as established DNA transformation method in *Verticillium dahliae* 100
4.4 *Verticillium longisporum* 43 specific and core-set regulated transcripts belong to the same protein familys 101
4.4.1 Core-regulated transcripts 102
4.4.2 Specific regulated transcripts 103
5 References 107
6 Appendices 125
6.1 Specific up-regulated transcripts – top 20 of most different main categories 125
6.2 Specific and core regulated transcript functional categories comparison 136
6.3 Specific up-regulated transcripts – regulated subcategories only in xylem-sap 137
6.4 Pfam domains of xylem-sap and SXM specific up-regulated transcripts 143
Danksagung 148

List of tables

Page

Table 1: Bacterial strains 21

Table 2: Yeast strains 22

Table 3: Plant lines 22

Table 4: *Verticillium* strains 24

Table 5: Primers used for amplifications and fusions 25

Table 6: Primers used for amplifications and fusions 29

Table 7: Plasmids constructed and used in this study 30

Table 8: Primers for Southern-hybridization probes 34

Table 9: Phylogenetic similarities of ScThi4p, FoxSti35, VlThi4-1, VlThi4-2, VdThi4 and VaaThi4 44

Table 10: Number of RNA-seq mappable reads on the genome of *V. longisporum* 43 67

Table 11: First 30 functional subcategories for xylem-sap (xyS) and SXM same regulated transcripts 72

Table 12: First 30 up-regulated KEGG functional subcategories for xylem-sap (xylS) and SXM different up-regulated transcripts 80

Table 13: Xylem-sap up-regulated top 20 transcripts of *Vl*43 84

Table 14: SXM up-regulated top 20 transcripts of *Vl*43 85

Table 15: Domains predicted for xylem-sap up- and SXM up-regulated transcripts 86

Table 16: Transcripts up-regulated in xylem-sap or SXM medium 125

Table 17: “Metabolism” top 20 Transcripts up-regulated in xylem-sap 126

Table 18: “Metabolism” top 20 Transcripts up-regulated in SXM 127

Table 19: “Protein fate” top 20 Transcripts up-regulated in xylem-sap 128

Table 20: “Protein fate” top 20 Transcripts up-regulated in SXM 129

Table 21: “Cell rescue” top 20 Transcripts up-regulated in xylem-sap 130

Table 22: “Cell rescue” top 20 Transcripts up-regulated in SXM 131

Table 23: “Interaction with the environment” top 20 Transcripts up-regulated in xylem-sap 132

Table 24: “Interaction with the environment” top 20 Transcripts up-regulated in SXM 133

Table 25: “Energy” top 20 Transcripts up-regulated in xylem-sap 134

Table 26: “Energy” top 20 Transcripts up-regulated in SXM 135

Table 27: Functional protein categories of regulated transcripts 136

Table 28: First 30 up-regulated KEGG functional subcategories for xylem-sap (XylS) and SXM specific up-regulated transcripts 137

Table 29: “Nucleotide/nucleoside/nucleobased metabolism” 139

Table 30: “Extracellular metabolism” 140

Table 31: “Metal binding” 140

Table 32: “Cellular signalling” 141

Table 33: “Nucleus” 142

Table 34: First 120 domains of different up-regulated transcripts 143

List of figures

Page

Figure 1: *Verticillium* wilting symptoms and morphology 5

Figure 2: Lifecycle of *Verticillium dahliae* on *Solanum tuberosum* 8

Figure 3: Thiamine metabolism in eukaryotes and prokaryotes 12

Figure 4: Thiazole synthesis in eukaryotes and prokaryotes 13

Figure 5: Thi4 enzymatic reaction in *S. cerevisiae* 14

Figure 6: Alignment of deduced amino acid sequences of Thi4-like proteins of vascular pathogenic fungi in comparison to *S. cerevisiae* Thi4p and *F. oxysporum* Sti35. 43

Figure 7: Phylogenetic tree of thiazole synthase of *V. dahliae*, *V. albo-atrum*, *F. oxysporum* and *S. cerevisiae* 44

Figure 8: Southern hybridization of *THI4 V. dahliae* wt, Δ*THI4*, Δ*THI4* :: *VdTHI4* and Δ*THI4* :: *VlTHI4-1*, *Vl* wt and *Vaa* wt 45

Figure 9: *Vd*Δ*THI4*, Δ*THI4* :: *VdTHI4* and Δ*THI4* :: *VlTHI4-1* strains show wild type-like phenotype 46

Figure 10: Growth rate of *Vd*Δ*THI4* deletion strain in comparison to wild type *V. dahliae ex planta* and without supplemented thiamine visualizes a reduced growth phenotype using small spore inoculum 47

Figure 11: *Vd*Δ*THI4* is involved in thiamine pathway 49

Figure 12: Restriction map and Southern hybridization of *THI4* - *GFP* strain 50

Figure 13: Mitochondrial localization of C-terminal Gfp-tagged Thi4 in *Verticillium dahliae* 51

Figure 14: UV-illumination assay 52

Figure 15: Oxidative stress tests on gradient plates. 53

Figure 16: Plant infection assay 56

Figure 17: Alignment of deduced amino acid *Verticillium* Pa14_2 sequence. 58

Figure 18: Southern hybridization of *VdPA14_2* wt, Δ*PA14_2*, Δ*PA14_2* :: *VdPA14_2* and Δ*PA14_2* :: *VlPA14_-1l*, *Vl* wt and *Vaa* wt 59

Figure 19: Phenotype of *Vd* wt, *Vd*Δ*PA14_2*, Δ*PA14_2* :: *VdPA14_2* and Δ*PA14_2* :: *VlPA14_2-1* 60

Figure 20: *PKS1* expression is not detectable in Δ*PA14_2* mutant and in Δ*PA14_2* :: *VdPA14_2* 61

Figure 21: Growth on different carbon sources of *Vd* wt, Δ*PA14_2*, Δ*PA14_2* :: *VdPA14_2 and* Δ*PA14_2* :: *VlPA14_2-1* 61

Figure 22: Restriction map and Southern hybridization of *PA14_2* - *GFP* strain 62

Figure 23: Plasma membrane localization of C-terminal Gfp-tagged Pa14_2 in *Verticillium dahliae* 63

Figure 24: Stress tests for oxidative and cell wall stress on gradient plates. 64

Figure 25: Plant infection assay 66

Figure 26: Experimental setup and HCA dendrogram of specific up-regulated transcripts of *Verticillium longisporum* 43 global approach RPKM data sets 68

Figure 27: *Verticillium longisporum* 43 transcripts up-regulated in xylem-sap and in SXM 69

Figure 28: Cellular localization of core set transcripts predicted by WoLF PSORT and YLoc+ 70

Figure 29: *Verticillium longisporum* 43 transcripts specific up-regulated in xylem-sap and SXM 75

Figure 30: Cellular localization of predicted proteins from specific xylem-sap or SXM up-regulated transcripts predicted by WoLF PSORT and YLoc+ 76

Figure 31: Functional categories of predicted proteins specifically up-regulated in xylem-sap and SXM 78

Figure 32: *Verticillium longisporum* 43 transcriptome reveals SXM not to reflect xylem-sap conditions. 88

Figure 33: Model of VdThi4 function in thiamine biosynthesis 91

Figure 34: *VdTHI4* encodes a protein with function in thiamine synthesis that has additional repair function and is required to induce disease on tomato 94

Figure 35: Pa14_2 is involved in melanization and reduces resistance against ROS 98

Figure 36: Non-melanizing Δ*PA14_2* mutant lost the ability to infect the host 99

Abbreviations

1 D-SOM	one-dimensional self-organizing map
°C	degree Celsius
Δ	deletion
λ	wavelength
Amp^R	ampicillin resistance
ATMT	*Agrobacterium tumefaciens*-mediated transformation
bp	base pair
CAZy	carbohydrate-active enzyme
CDM	Czapek-Dox medium
cDNA	complementary DNA
cm	cenimeter
DAPG	2,4-Diacetylphloroglucinol
DIC	differential interference contrast
DMSO	dimethyl sulfoxide
DNA	deoxyribonucleic acid
DXP	1-deoxy-dxylulose 5-phosphate
E. coli	*Escherichia coli*
EDTA	ethylenediaminetetraacetate
EST	expressed sequence tags
FAD	flavin adenine dinucleotide
FLO	flocculin
g	gram
Gb	giga byte
GFP	green fluorescent protein
GPI	glycosyl phosphatidylinositol
h	hour
HMP-PP	4-amino-5-hydroxymethyl-2-methylpyrimidine
H_2O	water
H_2O_2	hydrogen peroxide
hph	hygromycin B phosphotransferase
Hyg^R	hygromycin resistance
ITS	internal transcribed spacer
Kan^R	kanamycin resistance

kb	kilobase
kDa	kilodalton
l	liter
LB	Luria Bertani medium
LiAc	Lithium acetate
min	minute
ml	milli liter
mM	milli molar
MM	minimal medium
NAD	nicotinamide adenine dinucleotide
nat	nourseothricin acetyltransferease gene
Clo*Nat*^{R}	nourseothricin resistance
Nm	nanometer
OD	optical density
ORF	open reading frame
PCR	polymerase chain reaction
PDA	potato dextrose agar
PDB	potato dextrose both
PEG	polyethylene glycol
pH	power of hydrogen
PP_i	pyrophosphate
rDNA	ribosomal DNA
RFLP	restriction fragment length polymorphism
RNA	ribonucleic acid
RPKM	reads per kilobase per million of mapped reads
rpm	revolutions per minute
rRNA	ribosomal RNA
s	second
S	Svedberg unit
SC-Ura	synthetic complete without uracil medium
SDS	sodium dodecyl sulphate
SXM	simulated xylem medium
TE	Tris-Cl and EDTA
TDP	Thiamine diphosphate

TH-P	5-(2-hydroxyethyl)-4-methylthiazole
THZ	4-methyl-5-β- hydroxyethylthiazole
TMP	Thiamine monophosphate
TMP-PPase	thiamine-phosphate pyrophosphorylase
Tris	tris(hydroxymethyl)aminomethane
TPP	Thiamine pyrophosphate
U	unit
UV	ultraviolet
Vaa	*Verticillium albo-atrum*
Vd	*Verticillium dahliae*
Vl	*Verticillium longisporum*
v/v	volume per volume
wt	wild type
w/v	weight per volume
YPD	yeast extract peptone dextrose
µl	microliter
µm	micrometer

Summary

Verticillium is a soil-borne plant pathogen including species that are distributed all over the word. Up to now no fungicides could avoid an infection on host plants. In resting structures, (microscrlerotia, melanized hyphae) the fungus can survive for many years in the soil of infected fields and even after a long period they can germinate and the fungus can infect host plants. This made *Verticillium* species to become an economical problem. The infection occurs through the roots, and after entering the xylem vessels of the plant, the fungus grows only inside this vascular system. On infected plants, the fungus can cause symptoms like premature foliar chlorosis, necrosis and vascular discoloration in stems and roots. That is why investigations on plant-pathogen interactions have a high impact for agriculture, and finding putative points of attack on the fungus are important research goals. This thesis is focused on two genes that are relevant for pathogenicity in *Verticillium dahliae* and focused on the transcriptome of *Verticillium longisporum*. The aim is to analyze the adaption of the fungus to the life inside the central cylinder in the xylem-sap where the saprotrophic fungus has only access to a limited number of nutrients. The investigated *V. dahliae* VdThi4 protein, is involved in the essential pathway of thiamine biosynthesis. This mitochondrial localized protein has additional functions in DNA repair and the response induced by reactive oxygen species (ROS). Lacking VdThi4 leads to impaired plant pathogenicity of the fungus on *Solanum lycopersicum* host plants. Besides proteins of essential biosynthetic pathways, secreted proteins are important for the infection process. They are the first contact of a pathogen with the host and are released by both organisms. Therefore, functions of VdPa14_2 as a membrane-bound protein are described in the second part of this work. Infection assays revealed the protein to be required for infection of *S. lycopersicum* plants. VdPa14_2 seems to decrease the resistance against oxidative stress and to be involved in the synthesis of black colored melanin. In *V. dahliae* lots of different proteins form several pathways are required for the infection host plants and for being pathogenic. Two of them are the analyzed VdThi4 and VdPa14_2, which have different functions in the cell, but are both needed by the fungus for pathogenicity. For a more comprehensive view of the plant-fungus interaction, gene regulation in *V. longisporum* has been analyzed in a transcriptomic approach. In detail, specific up- and core-regulated transcripts have been reviewed during *in situ* growth in *B. napus* xylem-sap and *in vitro* growth in simulated xylem medium (SXM). The transcriptomic approach revealed that gene expression of xylem-sap and SXM grown fungus are highly different. Therefore SXM does not reflect the nutritional conditions of the *in vivo* vascular fluid inside host plants.

Zusammenfassung

Die bodenbürtigen, pflanzenpathogenen Pilze der *Verticillium* Familie sind über die ganze Welt verteilt. Bislang gibt es keine Fungiszide, die einen Befall der Wirtspflanzen verhindern können. Auf infizierten Feldern ist dem Pilz für viele Jahre ein Überleben im Boden in sogenannten Dauerformen (Mikrosklerotien, melanisierte Hyphen) möglich. Auch nach langer Zeit können diese auskeimen und der Pilz dann die Wirtspflanzen befallen, was ihn zu einem wirtschaftlichen Problem macht. Die Infektion der Wirtspflanzen erfolgt durch die Wurzeln; und nachdem der Pilz in die Xylemgefäße der Pflanze eingedrungen ist, wächst er innerhalb dieser vasculären Leitungsbahnen. Die infizierten Pflanzen zeigen Infektionssymptome wie frühzeitige Chlorose der Blätter, absterbendes Gewebe sowie verfärbte Gefäße in Stamm und Wurzel. Für die Landwirtschaft ist die Erforschung der Interaktionen zwischen Pflanzen und dem pathogenene Pliz von großer Bedeutung um mögliche Angriffspunkte zur Pilzbekämpfung zu finden. Diese Arbeit fokussiert sich auf zwei spezifische Gene in *Verticillium dahliae*, die für die Pathogenität des Pilzes eine Rolle spielen. Des Weiteren wurde die Gen-Regulation in *Verticillium longisporum* durch Analyse eines Transkriptoms untersucht. Die Studie hat zum Ziel die hohe Anpassung des Pilzes an die Bedingungen innerhalb des vaskulären Systems der Wirtspflanze zu zeigen, in dem dem saprophytischen Pilz nur eine limitierten Menge an Nährstoffe zugänglich ist. Das untersuchte *V. dahliae* Protein VdThi4 ist Teil der Thiamin Biosynthese (Vitamin B1). Dieses Mitochondriell lokalisierte Protein ist mit seinen weiteren Funtktionen in den DNA Reparaturmechanismus und die zelluläre Antwort auf oxidativen Stress (induziert durch ROS) eingebunden. Das Fehlen des Proteins führt im Pilz zum Verlust der pathogenen Eigenschaften auf der Wirtspflanze *Solanum lycopersicum*. Neben Proteinen wichtiger Stoffwechselwege spielen sekretierte Proteine eine große Rolle bei der Wirtsinfektion. Solche Proteine sind der Erste Kontakt zwischen Pathogen und Wirt und werden von beiden Seiten abgesondert. Infektionsversuche an *S. lycopersicum* zeigten, dass der Pilz das membrangebundene *V. dahliae* Protein VdPa14_2 für die Wirtspflanzeninfektion benötigt. Dieses Protein scheint die Resistenz gegen oxidativen Stress in der Zelle zu verringern in der Synthese schwarzen Melanins involviert zu sein. Für die Infektion von Wirtspflanzen und die Pathogenität benötigt *V. dahliae* viele verschiedene Proteine aus verschiedenen Stoffwechelwegen, wie die analysierten Proteine VdThi4 und VdPa14_2, die in der Zelle verschiedene Funktionen haben, aber beide für die Pathogenität des Pilzes benötigt werden. Um ein umfassenderes Bild der Interaktion zwischen Pilz und Pflanze zu bekommen, wurde die Genregulation in *V. longisporum* untersucht. Hierfür wurde ein Transkriptom erstellt. Es

wurden sowohl die spezifisch- als auch die gleich-regulierten Transkripte während der *in situ* Kultivierung des Pilzes in Xylem-Saft aus *Brassica napus*, sowie der *in vitro* Kultivierung in simuliertem Xylem medium (SXM) untersucht. Beide Medien stellten sich während der Analyse als grundverschieden heraus. Das SXM stellt hingegen früherer Annahmen keine Simmulation der *in vivo* Konditionen innerhalb des vaskulären Systems einer Pflanze dar.

1 Introduction

1.1 *Verticillium* is a soil borne plant pathogen

The investigation of plant-pathogen interactions is a major topic in research due to the important impact of plant diseases on energy supply and human nutrition. Among the most devastating plant diseases worldwide are vascular wilt diseases caused by soil-borne pathogens (Tjamos & Beckman, 1989). The main vascular wilt pathogens are distributed in four fungal genera: *Ceratocystis*, *Fusarium*, *Ophiostoma,* and *Verticillium* (Agrios, 2005).

Verticillium species are a soil-borne vascular plant pathogenic fungi belonging to the phylum of ascomycota. The species of *Verticillium* are broadly distributed over the world and cause symptoms as wilting, early flowering and senescence with a wide host range including economically important crops like alfalfa, cotton, lettuce, hops, olive trees, oilseed rape, cabbages, potato, tomato, strawberries and many more. Infection and wilting symptoms lead annually to huge crop decreases in agriculture caused by *Verticillium dahliae, Verticillium albo-atrum* and *Verticillium longisporum* (Agrios, 2005; Inderbitzin *et al.*, 2011b; Isaac, 1949; Pegg & Brady, 2002; Zeise & von Tiedemann, 2002). In contrast to other vascular pathogens, fungi of the genus *Verticillium* could not be characterized by infecting the same host ranges. *V. longisporum* infect hosts belonging to the family of *Cruciferaceae* like cabbage (*Brassica oleracea* var. *capita*), cauliflower (*Brassica oleracea*) and rapeseed (*Brassica napus*). *V. dahliae* and *V. albo-atrum* have a host range of over 200 dicotyledonous species, including important crops, with an overlap in host specificity. In these host ranges *V. albo-atrum* has a specific host adaption to *Canabaceae* family members (lucerne, leguminoses and hops) (Agrios, 2005; Inderbitzin *et al.*, 2011b; Klosterman *et al.*, 2009; Pegg & Brady, 2002).

The name *Verticillium* is derived from the verticillate shaped around the conidiophores and the branches of the conidiophores which occur also in whorls at some levels. The vascular pathogen was first found in Europe and described in 1879 by Reinke and Berthold on potato plants (*Solanum tuberosum*) at the botanic laboratory of the University of Göttingen and named *Verticillium albo-atrum* (Hastie, 1973; Klosterman *et al.*, 2009; Reinke & Berthold, 1879). Klebahn described a second species with morphological distinction to *V. albo-atrum* in 1913 that causes wilt on *dahlia* (family of *Asteraceae*) and named it *Verticillium dahliae* (Hastie, 1973; Isaac, 1947). In 1961 Stark was the first who isolated a *V. dahliae*-like fungus from wilted horseradish in Hamburg, Germany, that had microsclerotia and conidia

approximately twice as long as those of *V. dahliae* (Stark, 1961). The strain was named *V. dahliae* var. *longisporum*. Karapapa suggested the long-spored isolates as a new species on the basis of morphological characteristics of many similar strains (Karapapa *et al.*, 1997). The numbers of isolates from crucifers of *V. longisporum* are increasing and include horseradish from Illinois (Eastburn & Chang, 1994), oilseed rapes from Europe and Canada (Heale & Karapapa, 1999; Steventon *et al.*, 2002; Zeise & von Tiedemann, 2001) or cauliflower from California (Koike *et al.*, 1994).

After comprehensive revision, seven plant pathogenic species of *Verticillium* are now generally accepted (Barbara & Clewes, 2003b). Besides *V. dahliae*, *V. albo-atrum* and *V. longisporum* the species *V. tricorpus*, *V. nigrescens*, *V. nubilum* *V. theobromae* are accepted as *Verticillium* species. They are similar but weaker plant pathogens or soil saprophytes. On the basis of molecular evidences from rRNA, *V. nigrescens* and *V. theobromae* were classified into the genera *Gibellulopsis* and *Musicillium* (Zare *et al.*, 2007). Furthermore, with *V. zaregamsianum*, *V. isaacii*, *V. klebahnii*, *V. alfalfae* and *V. nonalfalfae* another five new *Verticillium* species were found recently (Inderbitzin *et al.*, 2011a)

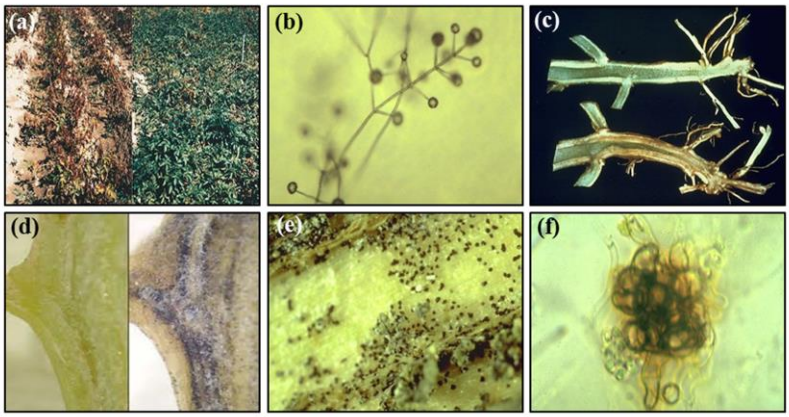

Figure 1: *Verticillium* wilting symptoms and morphology. (a) Solanum tuberosum plants. Left: uninfected, right: necrosis of V. dahliae infected plants. **(b)** Phialides of Verticillium arranged in whorls (verticillate shaped), **(c)** Vascular discoloration in Solanum lycopersicum stems (upper: uninfected, lower: infected), (d) Small black microsclerotia of V. dahliae in the vascular tissue of the infected Spinacia oleraceae (right), (e) Microsclerotia on S. tuberosum, (f) Structure of V. dahliae microsclerotium. Figures modified after Berlanger & Powelson, 2000; Davis *et al.*, 1996; Rowe & Powelson, 2002; mtvernon.wsu.edu.

The differentiation of *Verticillium* species is difficult because the infection symptoms vary in dependency of the hosts and the diagnostic techniques for *Verticillium* pathogens are limited (Rowe & Powelson, 2002). However, premature foliar chlorosis, necrosis and vascular discoloration in stems and roots are characteristic for all hosts. Although, the name *Verticillium* wilt would implicate wilting as a symptom of *Verticillium* infection, not always a

true wilt occurs on infected plants. The temperature plays an important role for this wilting. In several plant species, wilting of young shoots can occur during warmer periods of the day with recovery at night. Temperatures above 30°C inhibit *Verticillium* infection; so it is generally restricted to temperate climates (Mace *et al.*, 1981) and in contrast to *V. dahliae*, *V. albo-atrum* is not able to grow in culture or induce wilting on plants at 30°C (Rowe & Powelson, 2002). Typical symptoms of wilting are first detectable in the oldest parts of the plant and proceed acropetal (from base to apex). On tomato, infected by *V. dahliae*, lower leaves turn yellow while tips and edges die. Ultimately the whole leaf wilts and may abscise. Alternatively, leaves may develop yellow blotches that later turn necrotic and brown, and the veins may appear brown or purple. On infected leaves, wilting normally occurs only at one half of the leaves (Fradin & Thomma, 2006). Annuals being infected often survive the season but may be chlorotic, stunted, early senescent and have a smaller yield. In stem sections a brown discoloration of the vascular tissues can be seen. Stunting occurs in some host as a symptom of *Verticillium* infection in various degrees (Fradin & Thomma, 2006; Kim *et al.*, 2001; Pegg & Brady, 2002). Symptoms caused by *Verticillium* appear slowly and only on the lower or outer parts of the infected plants. Overall, *Verticillium* induced symptoms are difficult to diagnose based on symptom expression, especially because several *Fusarium* species cause similar symptoms (Babadoost *et al.*, 2004).

The vascular pathogenic fungus *Fusarium oxysporum* is also soil-borne and exists as a saprophyte inside the soil with the ability to degrade lignin and complex carbohydrates associated with the soil debris (Christakopoulos *et al.*, 1995; Christakopoulos *et al.*, 1996; Michielse *et al.*, 2012; Rodriguez *et al.*, 1996; Sutherland *et al.*, 1983). It survives in the soil in form of mycelium and in three types of asexual spores: microconidia, macroconidia and chlamydospores (Snyder & Hansen, 1940). In contrast to *Verticillium* species which spread in infected seeds or in dead plant material back into the soil, *F. oxysporum* spreads in short distances by water splash, by planting equipment and long distances by infected transplants and seeds. Both fungi infect healthy plants by penetrating and entering the plants trough the root tips, root wounds or lateral roots. After root penetration the fungal mycelium advances intracellularly through the root cortex and into its vascular living department, the xylem vessels. *Verticillium* and *Fusarium* stay a long time of their lives inside this medium and thereby need to be highly adapted. Further investigations illustrated these adaptions of *V. longisporum* for a life in the xylem-sap of its host *Brassica napus* by the detection of up-regulated catalase-peroxidase activity in the fungus growing inside the xylem-sap (Singh *et al.*, 2012).

1.1.1 Morphology of *Verticillium*

Both species, *Verticillium dahliae* and *Verticillium albo-atrum* are producing colonies with conidiophores, which are more or less erect and hyaline, with verticillate branches and arranged on the 3-4 phialides at each node. These phialides are asexual spore carrying structures forming branches at each node of the conidiphores (Kim *et al.*, 2001). The two distict species are closely related in morphology (Inderbitzin *et al.*, 2011a). As resting structures, *V. albo-atrum* forms melanized hyphae, whereas the hyphae of *V. dahliae* are not black. Instead *V. dahliae* forms black microsclerotia as resting forms, which are melanized clumps formed by budding of mycelial cells (Goud *et al.*, 2003). The formation of these outliving structures is the most distinctive feature for morphological separation (Pegg & Brady, 2002).

The species *Verticillium longisporum*, isolated from crucifer family of Brassicaceae (Stark, 1961), forms preferentially only three phialides per node and survives by means of black and elongated microsclerotia, comparable to structures of *V. dahliae*. The produced asexual spores (conidia) are with 7-9 µm twice as long as those from *V. dahliae* (3.5-5.5 µm) (Inderbitzin *et al.*, 2011a; Karapapa *et al.*, 1997; Zeise & von Tiedemann, 2001).

1.1.2 *Verticillium* is a monocyclic phytopathogenic fungus

Verticillium wilt is a monocyclic disease that has only one disease cycle and inoculum per season. From season to season *V. dahliae*, *V. albo-atrum* and *V. longisporum* survive inside the soil or free embedded in dead plant material in outliving structures as microsclerotia and melanized hyphae (Eynck *et al.*, 2007; Karapapa *et al.*, 1997; Rowe & Powelson, 2002).

In those resting structures, *V. dahliae* and *V. longisporum* can survive up to 14 years without hosts (Wilhelm, 1955). The dark hyphae of *V. albo-atrum* are only viable for 2-5 years (Sewell & Wilson, 1964). Possibly triggered by root exudates, microsclerotia germinate in the soil and penetrate the roots through the root tip or via wounds and sides of lateral root formation. Here, the effective influence of the roots rhizosphere on microsclerotia is about 100 µm on average (Huisman, 1982). After crossing the root endodermis, the fungus enters the xylem vessels and produces conidia that are transported by the water stream throughout the plant. The fungus emerges from the xylem vessels to colonize neighboring vascular and cortical tissues. A rapid systemic infection of the plant soon occurs and foliar symptoms of wilting, clorosis and necrosis become apparent. When the foliage begins to senescence, the fungus leaves the xylem elements and colonizes the surrounding nonvascular tissues and

microsclerotia are soon formed in the dying leaves and stems. Following the incorporation of dead tissues into the soil during subsequent cultivations, the microsclerotia are slowly released as the tissues decay (Fradin & Thomma, 2006; Rowe & Powelson, 2002). On average, based on this infection cycle, the largest contribution to the soil inoculum density is reached during the second growing season after incorporation of crop refuse.

Currently, only this asexual lifecycle is known and no sexual stage has been found in *Verticillium* genus (Klosterman *et al.*, 2009; Pegg & Brady, 2002).

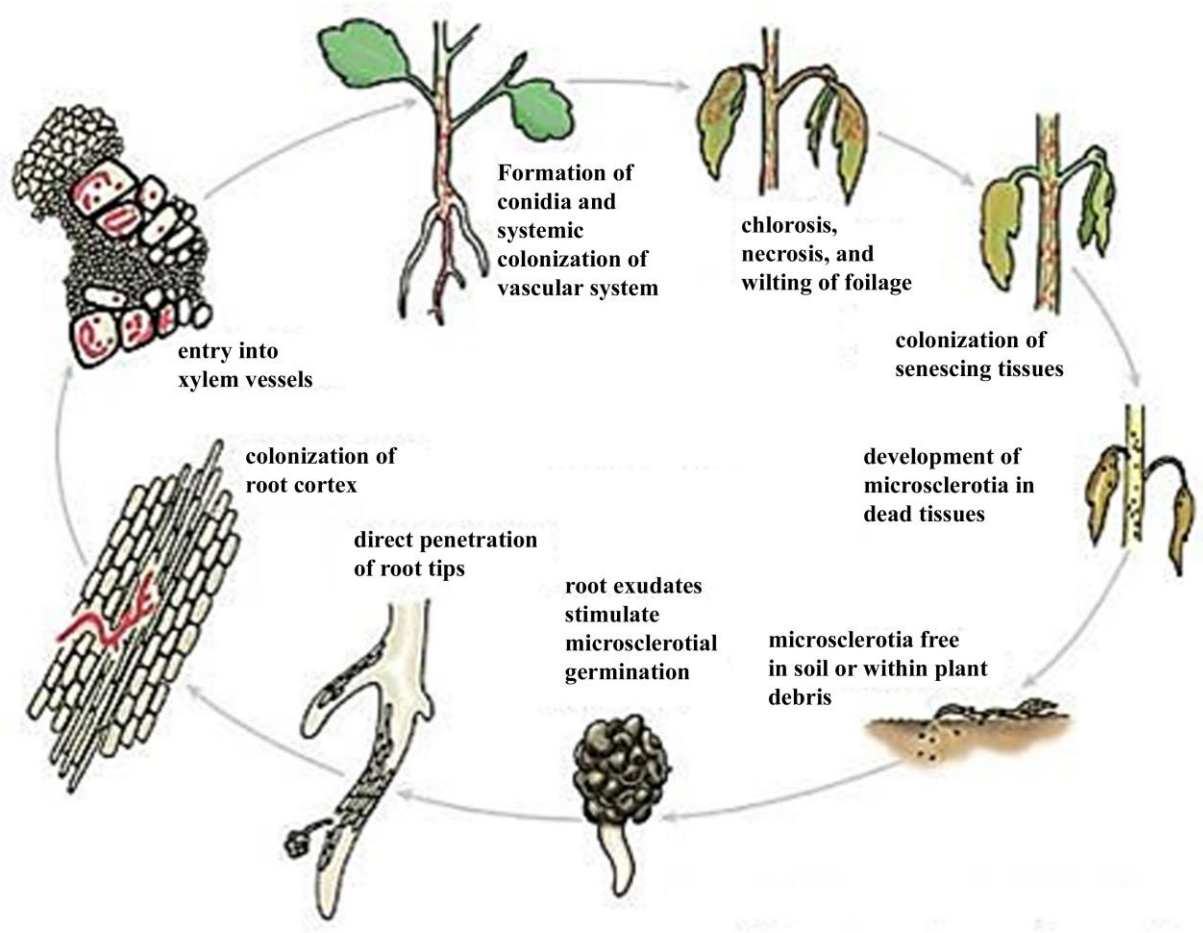

Figure 2: Lifecycle of *Verticillium dahliae* on *Solanum tuberosum*. When hosts are planted into the soil, root exudates stimulate Verticillium microsclerotia germination. Hyphae grow towards the roots and penetrate the root cortex. The fungus enters the vascular system (xylem vessels), builds asexual conidia and colonizes the whole vascular stissue of the plant. Symptoms like wilting of the leaves, chlorosis and necrosis appear early. Microsclerotia are soon formed in the dying leaves and stems. In dead material or inside the soil, the pathogen survives until the next infection cycle. Figure modified after Berlanger & Powelson, 2000.

Instead of a sexual cycle, genome evolution in the *Verticillium* species seems to occur by transposable elements and chromosomal reshuffling (Amyotte *et al.*, 2012; de Jonge *et al.*, 2013)

Vascular wilt diseases caused by soil-borne pathogens are particularly notorious since, in the vascular system of host plants, the pathogens cannot be reached by many fungicides and few fungicides exist to cure plants once they are infected. The long survival without hosts in the persistent resting structures generates a problem for agriculture of huge extent. The only effective control, soil fumigation, is expensive and has harmful environmental effects. Their high economic impact, combined with the absence of curative treatments, justifies increased attention for vascular wilt diseases. However, to design novel control strategies, understanding the biology of vascular pathogens is of fundamental importance (Fradin & Thomma, 2006; Fradin *et al.*, 2009; Rowe, 1987).

1.1.3 Genetics of *Verticillium*

Little is known about the genetics and molecular biology of *Verticillium*-host interactions. The genomes of *V. dahliae* and *V. albo-atrum* have been sequenced by the Broad Institute, and are available at http://www.broad.mit.edu/annotation/genome/verticillium_dahliae/MultiHome.html. *V. dahliae* contains a genome size of 33.8 Mb split up on 8 chromosomes, and for *V. albo-atrum* a genome size of 32.8 Mb split up on 7-8 chromosomes was detected by sequencing. The two genomes are highly similar and share about 92% similarities (Klosterman *et al.*, 2011).

Over the years, a perception of genetic homogenicity in *V. dahliae* has changed (de Jonge *et al.*, 2013; Klosterman *et al.*, 2009). It has been shown that genetically diverse groups exist within the species by using vegetative compatibility analysis (Puhalla & Hummel, 1983). Populations of isolates with the same vegetative compatibility are referred to as vegetative compatibility groups (VCG1-6) (Katan, 2000; Leslie, 1993) and are identified by using specific mutant tester isolates (Joaquim & Rowe, 1990; Joaquim & Rowe, 1991; Katan, 2000). Vegetative compatibility is the ability of hyphae from two isolates of the same species to anastomose and form a stable heterokaryon. This trait is genetically controlled. Hyphal anastomosis followed by formation of a heterokaryon is the only known means of genetic exchange among individuals of *Verticillium*. In contrast, strains that are incapable of anastomosing with one another and fail to establish heterokaryons are vegetatively incompatible (Elena, 1999). By this incompatibility isolates are thought to be genetically separated from each other and isolates in different VCGs may vary in many characteristics, including those related to pathogenicity and aggressiveness (Rowe & Powelson, 2002). The VCGs include *V. dahliae* strains from different hosts and geographic origins and the members

of each group often share specific traits related to pathogenicity and aggressiveness (Bhat *et al.*, 2003; Dobinson *et al.*, 2000; Jimenez-Diaz *et al.*, 2006; Klosterman *et al.*, 2009).

V. albo-atrum isolates were separated on the basis of morphological and rDNA analysis into two groups called Grp1 and Grp2. Most strains are referred to Grp1 (Barbara & Clewes, 2003a; Klosterman *et al.*, 2009; Morton *et al.*, 1995; Robb *et al.*, 1993; Robinson *et al.*, 2007). Sequence analysis of the ITS region (fungus specific internal transcribed spacer between structural ribosomal RNAs) revealed, that the ITS of Grp2 isolates contain 17 bases that are not found in Grp1 isolates (Mahuku & Platt, 2002; Robb *et al.*, 1993). The differences are significant enough to classify Grp2 strains as a separate species. Currently they are only recognized as a distinct taxonomic unit of *V. albo-atrum* (Mahuku & Platt, 2002).

The two haploid species *V. dahliae* and *V. albo-atrum* resemble the putative parents of the allodiploid fungus *V. longisporum* (Clewes *et al.*, 2008; Collado-Romero *et al.*, 2010; Inderbitzin *et al.*, 2011b; Timpner *et al.*, 2013; Tran *et al.*, 2013). Recent molecular evidences indicated that *V. longisproum* is an allodiploid hybrid with three different lineages (Inderbitzin *et al.*, 2011b; Tran *et al.*, 2013). Sequencing of *V. longisporum* and a screen for genome size and number of chromosomes are in progress by the research group of Prof. Braus in Göttingen, Germany.

Transcriptome profiling of interaction between *V. dahliae* and tomato has been carried out to study incompatible and tolerant interactions to identify genes that play a role in host defense (Robb *et al.*, 2007; Van Esse *et al.*, 2009). However, little is known about general interaction between *V. longisporum* and the host *Brassica napus*. To gain basic understanding of the host-pathogen interaction, transcriptomic data of *V. longisporum* growing in xylem-sap of *B. napus* (*in situ*) and in the synthetic pectin medium SXM (*in vitro*) were generated by deep sequencing (RNAseq) (see 2.13.1).

1.2 *THI4*, a gene of the essential thiamine pathway

Living in the central cylinder in the vascular medium xylem-sap leads to a limited number of nutrients for the saprotrophic fungus *Verticillium.* This leads to the fact, that the filamentous fungus needs to synthesize essential nutrients that are not contained in the xylem-sap and have to be assimilated for surviving and to be pathogenic. The fungus is highly adapted to live inside the vascular system. Further investigations illustrated these adaptions of *V. longisporum* for livinf in the xylem-sap of its host *Brassica napus* by detection of

up-regulated catalase-peroxidase activity which might be a precaution for a defensive plant response causing oxidative stress (Singh *et al.*, 2012; Timpner *et al.*, 2013). This catalase-peroxidase is rather required for late than for early stages of the plant disease. The synthesis of essential nutrients by the fungus while living inside the vascular system was demonstrated in former studies, revealing a bradytrophic mutant of *V. longisporum* with reduced pathogenicity on *Brassica napus* in a strain with reduced activity of the aromatic amino acid enzyme chorismate synthase (Singh *et al.*, 2010). The chorismate synthase is highly conserved and produces the first branch point intermediate of biosynthesis of aromatic amino acids.

Like amino acids, the fungus also needs to synthesize vitamins if they are not sufficiently provided by the host. Vitamine synthesis or uptake by diet, like vitamine B1 (thiamine) is essential for all organisms. Thiamine (vitamine B1) is a water-soluble vitamin found in appreciable quantities in wholegrain cereals, yeast and some legumes (Butterworth, 2003). The thiamin content of these foods is sensitive to pH and to high temperatures. The most common human thiamine-deficiency disorders are beriberi and Wernicke's encephalopathy (WE; the Wernicke – Korsakoff syndrome). Thiamine plays a key role in the maintenance of brain function. Thiamine diphosphate is co-factor for several enzymes involved in glucose metabolism, whereas thiamine triphosphate has distinct properties at the neuronal membrane (Butterworth, 2003). It was first isolated from rice bran in 1926 by Jansen and Donath, its structure was elucidated in 1936 by R. R. Williams and its synthesis was reported soon after (Jansen, 1972; Jansen & Donath, 1926; Spenser & White, 1997; Williams & Spies, 1938). The biochemical function of the compound was recognized 1937 when the corresponding pyrophosphate (Brown, 1970; Brown, 1971; Leder, 1975) was identified as the cocarboxylase, the conenzyme of pyruvate decarboxylase, the pyruvate dehydrogenase, the transketolase and several other enzymes (Spenser & White, 1997).

Biosynthesis of thiamine occurs in most microorganisms and higher plants (Bocobza *et al.*, 2013), but also many eukaryotes cannot biosynthesized all vitamins, so they have to take them up by diet. Beneath the synthesis of thiamine, acquisition of exogenously available thiamine occurs in *S. cerevisiae* by the plasma membrane thiamine carrier Thi7 (Thi10) (Enjo *et al.*, 1997; Singleton, 1997). The annual world production of synthetic vitamin B (thiamine) exceeds 4000 metric tons and the recommended daily intake for humans is approximately 1.5 mg and to prevent the recurrence of deficiency diseases, in the Western world the synthetic compound is routinely added to bread (Spenser & White, 1997).

The molecule consists of two components, a thiazole and a pyrimidine moiety, which are initially synthesized by separate pathways (Young, 1986). In a series of well-documented steps the two components, hydroxymethyl pyrimidine (4-amino-5-hydroxymethyl-2-methylpyrimidine) (HMP) and hydroxyethyl thiazole (5-(2-hydroxyethyl)-4-methylthiazole) (HEP), are first phosphorylated and then condensed to form thiamine monophosphate. Thiamine monophosphate (TMP) is converted to thiamine prior to phosphorylation by the thiamine-phosphate pyrophosphorylase (TMP-PPase) to form thiamine diphosphate (pyrophosphate) (ThDP), the active form of the co-factor (Jurgenson *et al.*, 2009).

Thiamine is a co-factor for several enzymes involved in carbohydrate metabolism. In its active predominant form, the thiamine diphosphate (ThDP), it functions as a co-factor for enzymes that catalyzes the decarboxylation of α-keto acids and some transfer reactions with aldehyde derivatives, such as the transketolase reaction in the phosphogluconate pathway (Young, 1986). Furthermore, ThDP is a Co-factor for decarboxylases and other key enzymes that mediate C–C bond formation or cleavage (Müller *et al.*, 2009).

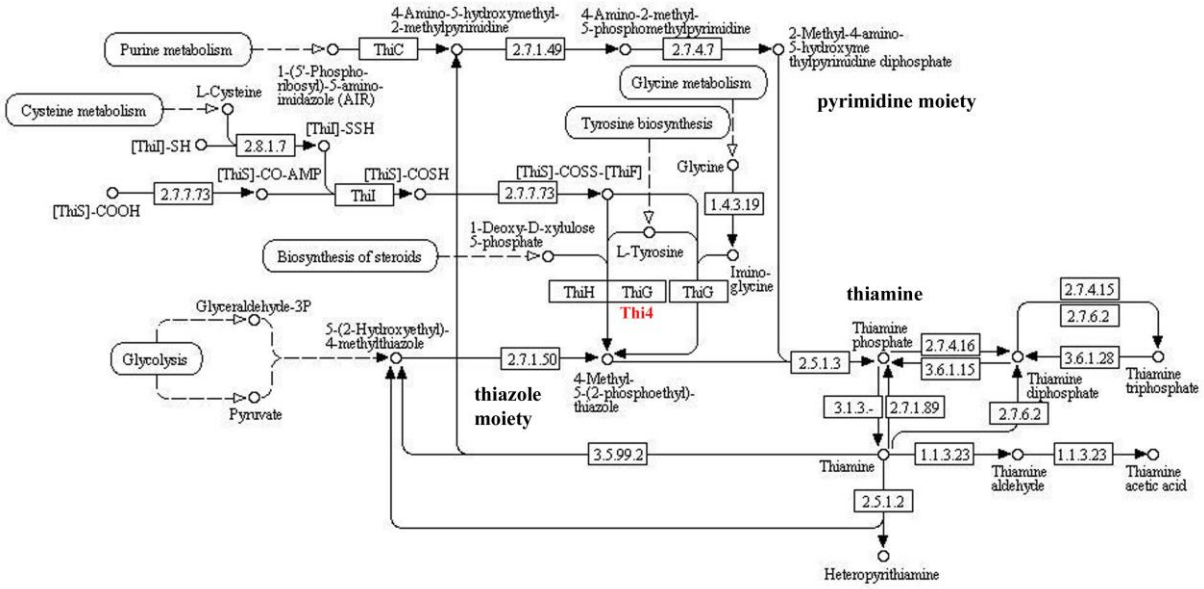

Figure 3: Thiamine metabolism in eukaryotes and prokaryotes. Thiamine (vitamin B1) is synthesized in the cells of prokaryotes and eukaryotes. The molecule consists of two components, a thiazole and a pyrimidine moiety, which are initially synthesized by separate pathways (Young, 1986). In the cell it is a co-factor for several enzymes involved in carbohydrate metabolism. The KEGG numbers for the enzymatic reactions of the pathway are in rectangles. Figure adapted from KEGG database http://www.genome.jp/kegg/pathway/map/map 00730.html.

In eukaryotes thiamine biosynthetic studies are still at an early stage. The bacterial biosynthesis of the pyrimidine moiety is also still poorly understood (Jurgenson *et al.*, 2006). Labeling studies in *Saccharomyces cerevisiae* have demonstrated that the thiamine thiazole is biosynthesized from a five-carbon carbohydrate, glycine, and cysteine (White & Spenser, 1979a; White & Spenser, 1979b; White & Spenser, 1982).

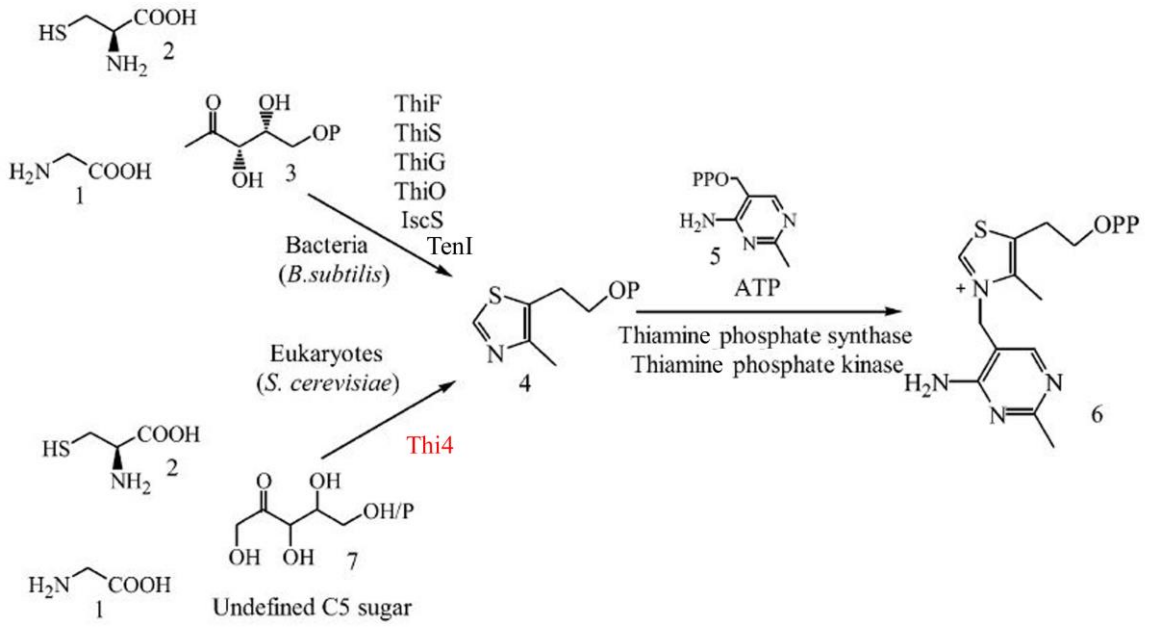

Figure 4: Thiazole synthesis in eukaryotes and prokaryotes. In eukaryotes the thiazole moiety is biosynthesized from five-carbon carbohydrate 7, glycine 1, and cysteine 2 (White & Spenser, 1979a; White & Spenser, 1979b; White & Spenser, 1982). In bacteria six biosynthetic enzymes are required for the thiazole synthesis, in eukaryotes one (Thi4 in S. cerevisiae). Figure adapted from Jurgenson *et al.*, 2006.

In bacteria, formation of thiazole requires six gene products. The best-studied thiamine biosynthetic pathways are those of *Escherichia coli* and *Bacillus subtilis*, which utilize very similar pathways. The thiazole moiety (4-methyl-5-β- hydroxyethylthiazole or HET) is synthezised through three distinct steps. First, glyceraldehyde 3-phosphate and pyruvate are coupled together by a phosphate synthase to give 1-deoxy-dxylulose 5-phosphate (DXP). Next, the sulfur carrier protein ThiS undergoes an adenylation by ThiF, followed by a sulfur transfer step using ThiI (*E. coli*) and IscS (NifS) to yield a thiocarboxy group at its C-terminus. This sulfur atom is incorporated into the HET ring of thiamine. Finally, glycine (by ThiO in *B. subtilis*) or tyrosine (by ThiH in *E. coli*) is converted to dehydroglycine. The thiocarboxy C-terminus of ThiS, along with DXP and dehydroglycine, are all coupled together by the thiazole synthase ThiG, to give the thiazole phosphate carboxylate tautomer.

The enzyme TenI (*B. subtilis*) then aromatizes the thiazole tautomer to the thiazole phosphate carboxylate (Jurgenson *et al.*, 2009).

Only one eukaryotic thiazole biosynthetic enzyme (Thi4p in *S. cerevisiae*, Thi1p in *A. thaliana*) has been identified to be required for the formation of the thiazole (Machado *et al.*, 1996; Machado *et al.*, 1997; Praekelt *et al.*, 1994). In *S. cerevisiae* this enzyme is a 35 kDa protein composed of 326-amino acid and sequence analysis suggests a conserved dinucleotide binding motif (Praekelt & Meacock, 1992). In the enzymatic mechanism for thiazole synthesis the co-factor nicotinamide adenine dinucleotide (NAD), that is transduced from the undefined C5 sugar, is converted into adenosine diphospho-5-(β-ethyl)-4-methylthiazole-2-carboxylic acid (ADT) (Chatterjee *et al.*, 2006). Jurgenson (Jurgenson *et al.*, 2006) proposed the detailed chemical reaction of Thi4 in *S. cerevisiae*.

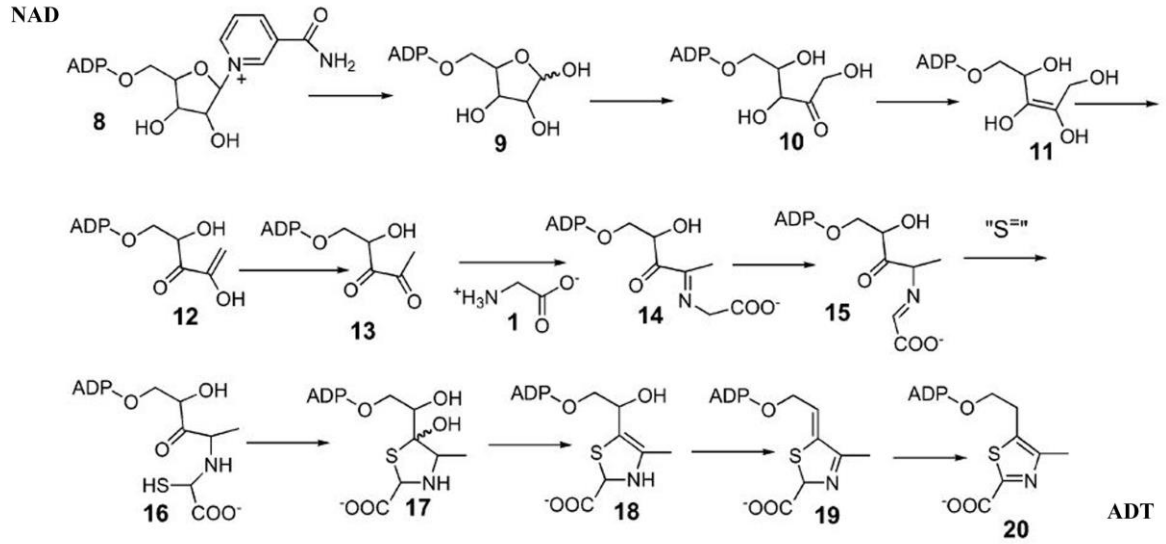

Figure 5: Thi4 enzymatic reaction in *S. cerevisiae*. In the thiazole synthesis by Thi4 the Co-factor nicotinamide adenine dinucleotide (NAD) is converted into adenosine diphospho-5-(β-ethyl)-4-methylthiazole-2-carboxylic acid (ADT) (Chatterjee *et al.*, 2006). Figure adapted from Jurgenson *et al.*, 2006.

In this mechanism NAD is converted to adenylated thiatole (ADT) in a complicated chemical mechanism. ADT was found tightly bound to the active site of *S. cerevisiae* Thi4p and can be released *in vitro* only upon protein denaturation. This identification suggested NAD as the probable precursor to ADT and provided key insights into the mechanism of thiazole biosynthesis in eukaryotes (Chatterjee *et al.*, 2006; Jurgenson *et al.*, 2006). Fully active recombinant wild type yeast Thi4p was prepared by Chatterjee in 2011 (Chatterjee *et al.*, 2011). In contrast to the earlier findings recent mass spectrometric protein studies implicated that *S. cerevisiae* Thi4p acts as a co-substrate rather than an enzyme (Chatterjee *et al.*, 2011).

The crystal structure of the yeast Thi4 protein revealed that it is a homooctamer with two monomers. The Thi4p monomer consists of 10 β-strands and 9 α-helices. It consists of a central five-stranded parallel β-sheet flanked on one side by three α-helices and on the other by an antiparallel three-stranded β-sheet that lies between 8 and 9 Å above the plane of the central β-sheet and is rotated by an angle of approximately 30°. Long α-helices are found on both the N-terminal and C-terminal ends of the monomer (Jurgenson *et al.*, 2006).

In the eukaryotic kingdom the thiazole synthase protein is highly conserved (Ruiz-Roldan *et al.*, 2008). This protein family includes Thi4p from *S. cerevisiae* (Praekelt *et al.*, 1994), Sti35 from the vascular wilt fungus *Fusarium oxysporum* (Choi *et al.*, 1990; Ruiz-Roldan *et al.*, 2008; Thanonkeo *et al.*, 2000), Nmt2p from *Schizosaccharomyces pombe* (Manetti *et al.*, 1994) and Thi1p from *Arabidopsis thaliana* (Machado *et al.*, 1996) as well as others (Belanger *et al.*, 1995; Faou & Tropschug, 2003; Jacob-Wilk *et al.*, 1997; Ribeiro *et al.*, 1996). More recently, the *Neurospora crassa* ortholog CyPB37 was identified (Faou & Tropschug, 2003; Faou & Tropschug, 2004). Besides their role in thiamine biosynthesis, members of this family have been associated with additional, apparently unrelated cellular functions such as tolerance to DNA damage in *A. thaliana* (Machado *et al.*, 1996), maintenance of mitochondrial genome stability in *S. cerevisiae* (Machado *et al.*, 1997) or function in oxidative stress response in *F. oxysporum* (Choi *et al.*, 1990). Recent studies have shown that yeast Thi4p is also involved in the stress response of the cell. The gene expression and enzymatic activity level generally showed an increased production of thiamine biosynthesis enzymes like Thi4p subjected to oxidative and osmotic stress (Kowalska *et al.*, 2012). The expression level of thiamine in the cell is highly regulated. For *S. cerevisiae THI4* expression it was shown that the presence of 1 µM thiamine represses gene expression (Praekelt *et al.*, 1994). The thiamine diphosphate (ThDP) production was revealed to be regulated by riboswitches (Croft *et al.*, 2007). These are short sequences in mRNAs that bind metabolites directly, without the need for intermediary proteins. Binding of the ligand alters the secondary structure of the RNA, thereby regulating expression of the gene, typically by premature transcription termination and/or initiation of translation. Riboswitches have been found to regulate the ThDP production in prokaryotes like *Bacillus subtilis* (Mandal *et al.*, 2003; Winkler *et al.*, 2002) and in the 5'-UTR of the eukaryotic organisms *Aspergillus oryzae* and *Neurospora crassa* where they appear to operate by causing alternative splicing of the transcripts (Cheah *et al.*, 2007; Kubodera *et al.*, 2003). In the higher plant *Arabidopsis thaliana*, a ThDP riboswitch was identified in the 3'-UTR, and this has been characterized structurally (Sudarsan *et al.*, 2003; Thore *et al.*, 2006). Recent analyses suggest

that in *A. thaliana*, the *THIC* promoter (it participates in the synthesis of thiamine monophosphate) and the thiamine-diphosphate riboswitch act simultaneously to tightly regulate thiamine biosynthesis in a circadian manner and consequently sense and control vital points of core cellular metabolism (Bocobza *et al.*, 2013). In algae riboswitches were also detected to regulate the TPP production (Croft *et al.*, 2007).

In the plant pathogenic fungus *Fusarium oxysporum* the disruption of *sti*35 has no effect on normal growth and development (Choi *et al.*, 1990; Ruiz-Roldan *et al.*, 2008). In addition, all disruptants retained pathogenicity to tomato plants, suggesting that *sti*35 is dispensable for fungal pathogenicity to the host plants, although it is induced by phytoalexin produced by the infected plants (Thanonkeo *et al.*, 2000).

In *Verticillium longisporum* a thi4 domain containing gene was originally found in a cDNA library screen for putative fungal adhesins in *Saccharomyces cerevisiae*. However, later analysis revealed the gene not to be involved in adhesion. Sequence similarities to the thiazole synthase of *S.s cerevisiae* and *Fusarium oxysporum* hypothesized instead an involvement in the essential thiamine pathway. The Thi4 homolog in *V. dahliae* is analyzed in this study regarding its role in thiamine metabolism and pathogenicity on the same *Solanum lycopersicum* (tomato) host plants.

1.3 Secreted proteins are required for the first contact to the host

In addition to the adaptions of cellular processes for the life inside the vascular system, the fungus needs to be highly specified for the interaction with the host plant. Protein secretion plays here an important role in filamentous fungi with both, enzymes and structural proteins being secreted. Enzymes are released from the surface of the plasma membrane into the periplasmic space, where they may be incorporated into the cell wall or in many instances may be secreted across the cell wall into the external medium. Secreted structural proteins are incorporated into the plasma membrane as well as the cell wall, where they may be involved in recognition processes (Peberdy, 1994). Except membrane proteins most secreted proteins are glycosylated. Secretion of a protein is determined by the information embodied in the signal sequence, an N-terminal domain attached to the protein molecule. In yeast, mammalian cell and plant cell proteins destined for secretion are synthesized on ribosomes associated with the membranes of the ER (rough ER).

Pathogenic fungi are absolutely dependent on adhesins in order to recognize and adhere to host tissues. Such adhesins can also mediate invasion of host tissues and even invasion of host

cells (Linder & Gustafsson, 2008; Sheppard *et al.*, 2004). Small proteins secreted by plant pathogenic fungi in their hosts are important to recognize and respond to the host environment (Rep, 2005). Filamentous fungi secrete a broad spectrum of enzymes, of which the majority is hydrolytic. The secreted proteins play important roles in food and textile processing, in the manufacture of paper and pulp, and their production is an important and growing sector of the fermentation industries. With the development of gene-transfer systems for a number of fungi, which are used as production organisms in the fermentation industry (Feldbrügge *et al.*, 2013; Van den Hondel & Punt, 1991), considerable progress could be made by using these organisms for the overproduction of proteins from fungal origin, but also for the production of non-fungal proteins (Hasan *et al.*, 2013; Van den Hondel *et al.*, 1991). For the production of fungal proteins commercially attractive protein yields have been accomplished up to several grams per liter of culture fluid (Punt *et al.*, 1994). For example, *Aspergillus niger* is used to produce glucoamylase at 20g/1, and *Trichoderma reesei* produces 30g/1 cellulase (Peberdy, 1994). Microbial plant pathogens like fungi or prokaryotes secrete enzymes capable of degrading the polysaccharides of plant cell walls (Albersheim *et al.*, 1969; Hasan *et al.*, 2013). Recently, in *V. dahliae* secreted proteins were found, which are associated with the cell wall degradation and are required for pathogenicity (Klosterman *et al.*, 2011; Liu *et al.*, 2013b). At the time when pathogens are grown with isolated cell walls as the sole carbon source, polysaccharide-degrading enzymes are secreted into the medium. Several fungal pathogens secrete degradative enzymes in a temporal sequence with regard to culture age (Albersheim & Valent, 1974; Liu *et al.*, 2013a). These enzymes are mainly glycosidases or glucanases. Glycosidases of the pathogen can function either in releasing active molecules from the fungal cell wall by modifying polysaccharide polymers to produce active compounds, or in the inactivation of active or potentially active substances by degradation (Young & Pegg, 1982). Tomato host plants also release glycosidases with a role as a defense mechanism of the plant against the pathogen infection by *V. albo-atrum* (Castroverde *et al.*, 2010; Van Loon *et al.*, 2006; Young & Pegg, 1982). This is supported by the demonstration that the increase of glycosidase activity is correlated temporally with a reduction in fungal colonization (Pegg & Young, 1981). In higher plants, 1,3-β-glucanase appears to be ubiquitous as well as chitinases (Balasubramanian *et al.*, 2012). Most fungi contain chitin and β-1,3 linked glucan as major cell wall components (Bartnicki-Garcia, 1968; Zhou *et al.*, 2013b). This was also shown for *Verticillium* spp.(Ahrazem *et al.*, 2006).

A β-barrel domain was found in a variety of bacterial and eukaryotic glycosidases and glycosyl transferases like bacterial toxins, enzymes, adhesins and signaling molecules.

Furthermore, the domain occurs in proteins involved in cell adhesion including medically important surface adhesins of *Candida glabrata* (Cormack *et al.*, 1999; Frieman *et al.*, 2002) and in human polycystic kidney and hepatic disease protein (Onuchic *et al.*, 2002; Ward *et al.*, 2002; Xiong *et al.*, 2002). The domain was exhibited by BLAST searches to be located in the N-terminal pro-peptide fragment of the protective antigen (PA_{20}) of the anthrax toxin complex. It was named PA14 after the theoretical molecular domain weight of 14 kDa in protective antigen (PA); based on the analogy with the nomenclature of PA fragments (Rigden *et al.*, 2004). The PA14 domain is a structure comprising two β-sheets of six and five strands with no significant structural similarity with any other domain of known structure and forms the core of the PA_{20} fragment. The N- and C-termini of the domain are close together, presumably, thereby facilitating the insertion of the PA14 domain into other recognized domains without structural disruption. The PA14 domain occurs in many domain combinations and is a lectin-like ligand-binding domain. Most of the experimentally characterized PA14-containing proteins are involved in carbohydrate binding and/or metabolism (Rigden *et al.*, 2004). Several of these proteins participate in adhesion. This ability is consistent with their ability to bind carbohydrate-containing ligands. Among sequences lacking obvious catalytic domains, a carbohydrate-binding function has been shown for *S. cerevisiae* flocculation proteins Flo1p, Flo5p, Flo9p and Flo10p (Kobayashi *et al.*, 1998; Linder & Gustafsson, 2008; Rigden *et al.*, 2004; Zupancic *et al.*, 2008) and their distant homologs in the pathogenic yeast *Candida glabrata* that mediate adherence to human cells (Cormack *et al.*, 1999). In the *C. glabrata* adhesin Epa1p (epithelial adhesion) (Frieman *et al.*, 2002; Ielasi *et al.*, 2012) and *S. cerevisiae* flocculins (Goossens & Willaert, 2010) carbohydrate binding is associated with the N-terminal third of the protein (Rigden *et al.*, 2004). For the conserved PA14 domains of two related Epa proteins in *C. glabrata* a pentapeptide that determines binding specificity and cell adherence was evidenced to be located on a surface loop of the PA14 domain (de Groot & Klis, 2008). Studies on a β-glucosidase protein from yeast species *Kluyveromyces marxianus* unequivocally demonstrate the interaction between the PA14 domain and a carbohydrate, whereas structure-based mutational analyses revealed that the PA14 domain plays a critical role in determining the substrate specificity at subsite (Yoshida *et al.*, 2010).

The not well described so called GLEYA (named after the contained amino acid sequence) sequence containing domain, found by sequence analysis approaches, is localized C-terminal in putative fungal adhesins and is related to the the lectin-like ligand-binding PA14 domain. It was identified in a family of putative adhesins in *Schizosacharomyces pombe* and the related

fission yeast *Schizosaccharomyces japonicas* (Linder & Gustafsson, 2008; Rigden *et al.*, 2004). This domain containing family of adhesins does not appear to be dependent on C-terminal GPI (glycosyl phosphatidyl inositol) anchors for their attachment to the cell wall. In addition, the C-terminal location of their ligand-binding domains would suggest an alternative form of cell wall attachment (Linder & Gustafsson, 2008). None of the GLEYA domain containing proteins are currently recognized as being part of the PA14 domain protein family in the Pfam Database (release 21.0) or the NCBI Conserved Domain Database (CDD, (Marchler-Bauer *et al.*, 2005)). Multiple sequence alignment and quality assessment of the sequences identified a shorter region conserved between the GLEYA sequence containing domain and the lectin-like ligand-binding Pa14 domains that argued for homology of the two domain families. Until now it is not completely excluded that these two domain families evolved independently into fungal adhesins from the PA14 superfamily of carbohydrate-binding proteins (Linder & Gustafsson, 2008). Therefore this domain is called PA14_2 (Pfam number PF10528). In this study a PA14_2 domain containing protein is analyzed in *V. dahliae* regarding its role in pathogenicity on tomato plants. The analysis of putative adhesive functions and their relation to the infection process was interesting to analyze.

1.4 Aim of this work

Soil-borne plant pathogenic fungi causing vascular wilt diseases are among the most devastating plant diseases worldwide and are a huge problem for agriculture. The soil-borne plant pathogen *Verticillium* is a vascular wilt causing fungus with a wide host range. The infection by penetrating and entering the plants trough the root tips, root wounds, or lateral roots and the following wilting symptoms lead annually to huge crop decreases in agriculture caused by *Verticillium dahliae*, *Verticillium albo-atrum* and *Verticillium longisporum*. On infected plants premature foliar chlorosis, necrosis and vascular discoloration in stems and roots are characteristic for all hosts. After root penetration the fungal mycelium advances intracellularly through the root cortex and into the xylem vessels. *Verticillium* stays a long time of its life inside this vascular medium and thereby needs to be highly adapted. Further investigations illustrated these adaptions of *V. longisporum* for a life in the xylem-sap of its host *Brassica napus* by the detection of up-regulated catalase-peroxidase activity in the fungus growing inside the xylem-sap (Singh *et al.*, 2010).

In the first part of this work, the *V. dahliae* VdThi4 protein belonging to the pathway of thiamine biosynthesis is characterized. Originally, the *Verticillium THI4* gene was found in an assay for adhesion and adhesion in *V. longisporum* should be analyzed, but *THI4* later turned out to be involved in other cellular functions. Further investigations of the homologous protein in *Fusarium oxysporum* revealed that absence of this corresponding protein still causes disease on tomato plants (Thanonkeo *et al.*, 2000). In this study the focus was to show the high adaption of *Verticillium* for living inside the central cylinder in the xylem-sap which results in the importance of this thiazole synthase to receive pathogenicity on host plants.

Protein secretion and adhesion plays an important role in filamentous fungi, with both enzymes and structural proteins being secreted. These proteins are the first contact of a pathogen with the host. Pathogenic fungi are absolutely dependent on adhesins in order to recognize and adhere to host tissues. In the second part of this work, a secreted protein containing a PA14_2 domain regarding also putative adhesive functions is described. The closely related PA14 domain occurs in a variety of bacterial and eukaryotic glycosidases, glycosyl transferases (bacterial toxins, enzymes, adhesins and signaling molecules) and proteins involved in cell adhesion. The aim of studying the unknown VdPa14_2 protein was to identify its putative functional role using the new adapted method of DNA transfer via protoplast based transformation.

In order to get deeper insights into the general regulation of *V. longisporum* genes and the high adaption of the fungus to the vascular system, a transcriptomic approach was performed using RNA-seq. In this approach, fungal transcript regulation in two media was investigated under *in situ* cultivation conditions in harvested *Brassica napus* xylem-sap and under *in vitro* conditions in simulated-xylem-medium (SXM). To compare the datasets, specific up-regulation and the core set of genes were analyzed.

2 Materials and methods

2.1 Chemicals

All chemicals and authentic standards were obtained from Sigma-Aldrich (Deisenheim, Germany), Merck (Darmstadt, Germany) or Carl Roth (Karlsruhe, Germany) unless stated otherwise.

2.2 Prokaryotic microorganisms

Bacterial strains *E. coli* DH5α and MACH-1 (Woodcock *et al.*, 1989) as well as *Agrobacterium tumefaciens* AGL1 (Lazo *et al.*, 1991) were used for transformation procedures in this study. They were cultivated at 37°C and 28°C, respectively. Both strains were cultivated in Luria Bertani (LB) medium (0.5% yeast extract, 1% tryptone, 0.5% NaCl). Strains used in this study were listed in Table 1.

Table 1: Bacterial strains

Organism	Name	Genotype	Company / Citation
Escherichia coli	DH5α	F^- endA1 glnV44 *thi-1 recA1 relA1 gyrA96 deoR nupG* Φ80d*lacZ*ΔM15 Δ(*lacZYA-argF*)U169, hsdR17(r_K^- m_K^+), λ–	Invitrogen GmbH Karlsruhe / Germany
Escherichia coli	MACH-1	F^- endA1 glnV44 *thi-1 recA1 relA1 gyrA96 deoR nupG* Φ80d*lacZ*ΔM15 Δ(*lacZYA-argF*)U169, hsdR17(r_K^- m_K^+), λ–	Invitrogen GmbH Karlsruhe / Germany
Agrobacterium tumefaciens	AGL1		(Lazo *et al.*, 1991)

2.3 Eukaryotic microorganisms

2.3.1 Yeast strains

Yeast strains were cultivated in YEPD (yeast extract peptone dextrose: 2% peptone, 1% yeast extract, 2% glucose), YNB (1.5 g/l yeast nitrogen base lacking amino acids and ammonium sulfate, 5 g/l ammonium sulfate, 2% glucose or galactose, supplemented with the appropriate amino acids) or SC-Ura medium (a synthetic complete medium lacking uracil, (Guthrie & Fink, 2004) at 30°C.

Strains used and constructed in this study were listed in Table 2.

Table 2: Yeast strains

Acc. No	Strain	Background	Gene name / plasmid	Genotype	Source
Y00000	BY4741	S288C		*MATa; his3Δ 1; leu2Δ 0; met15Δ 0; ura3Δ 0*	Euroscarf
Y04774	YGR144	S288C	*THI4* ESP35 MOL1	BY4741; *MATa; his3Δ1; leu2Δ0; met15Δ0; ura3Δ0; YGR144w::kanMX4*	Euroscarf
Y06107	BY4741	S288C		BY4741; *MATa; his3D1; leu2D0; met15D0; ura3D0; YER109c::kanMX4*	Euroscarf
RH3521	BY4741	S288C	pME2791		this study
RH3522	YGR144	S288C	pME2791		this study
RH3523	YGR144	S288C	pME2791	::*VdTHI4* gDNA	this study
RH3524	YGR144	S288C	pME2791	::*VdTHI4* cDNA	this study
RH3525	YGR144	S288C	pME2791	:*VlTHI4* cDNA	this study

2.3.2 Plant lines

Plants were grown as described in 2.11.1.

Plant lines used in this study were listed in Table 3.

Table 3: Plant lines

Organism	Line	Genotype	Company / Origin
Solanum lycopersicum	Moneymaker		Kiepenkerl® (Volmary GmbH Münster, Bruno Nebelung GmbH Everswinkel, Germany)
Brassica napus	Rapid-cycling	ACaacc	Prof. Williams (Department of Plant Pathology, University of Wisconsin, Madison, WI, USA)

2.3.3 *Verticillium* strains

Verticillium isolates were kindly provided by Prof. Andreas von Tiedemann (Department of Crop Sciences, Division of Plant Pathology and Crop Protection, Georg-August-University, Göttingen, Germany) (Zeise & von Tiedemann, 2001; Zeise & von Tiedemann, 2002).

Verticillium dahliae JR2 was kindly provided by the group of Bart Thomma (Laboratory of Phytopathology, University of Wageningen, Netherlands) (Fradin & Thomma, 2006).

The strains were cultivated in simulated xylem medium (SXM) (Neumann & Dobinson, 2003), potato dextrose broth (PDB) (Sigma-Aldrich Chemie GmbH, Munich, Germany) or Czapek-Dox medium (CDM) (Smith, 1949). The strains were incubated at 25°C for 7-14 days on a rotary shaker at 140 rpm.

Fungal conidia were harvested from 150 ml liquid cultures (SXM, CDM or PDB) after 4-7 days by filtering through miracloth membrane (Calbiochem, Darmstadt, Germany) and the spores containing medium was centrifuged 10 min at 2,000 rpm (4°C) (Sigma Centrifuge, Osterode am Harz, Germany). The supernatant was discarded and the spore pellet solved in 96% NaCl 0.05% Tween80 and centrifuged again. Spores were concentrated to 10^8 spores/ml and stored at -80°C in 30% glycerin or in 0.96% NaCl with 0.05% Tween80 at 4°C, respectively.

Spore counting was performed with Beckmann Coulter$_{TM}$ Z2 Coulter® Particle and Size Analyzer (Beckman Coulter, Krefeld, Germany).

Strains generated and used in this study are listed in Table 4.

Table 4: *Verticillium* strains

Strain	Genotype	Species	Host	Origin / Reference
Vd JR2	wild type	*V. dahliae*	*Solanum lycopersicum*	Canada
Vd 73	wild type	*V. dahliae*	*Linum usitatissimum*	Mecklenburg / Germany
Vl 32	wild type	*V. longisporum*	*Brassica napus*	Mecklenburg / Germany
Vl 43	wild type	*V. longisporum*	*Brassica napus*	Mecklenburg / Germany
Va 1	wild type	*V. albo-atrum*	*Solanum tuberosum*	Wisconsin / USA
Vd JR2 Δ*THI4*	*VdTHI4* :: ^{P}*gpdA-nat*	*V. dahliae*	*Solanum lycopersicum*	this study
Vd JR2 Δ*THI4* :: *VdTHI4*	*VdΔTHI4* :: *VdTHI4 – trpC* - ^{P}*gpdA* - *hph*	*V. dahliae*	*Solanum lycopersicum*	this study
Vd JR2 Δ*THI4* :: *VlTHI4-1*	*VdΔTHI4* :: *VlTHI4-1 – trpC* - ^{P}*gpdA* - *hph*	*V. dahliae*	*Solanum lycopersicum*	this study
Vd JR2 *THI4-GFP*	*VdTHI4* :: *VdTHI4 – GFP – trpC* - ^{P}*gpdA* - *hph*	*V. dahliae*	*Solanum lycopersicum*	this study
Vd JR2 Δ*PA14_2*	*VdPA14_2* :: ^{P}*gpdA* - *nat*	*V. dahliae*	*Solanum lycopersicum*	this study
Vd JR2 Δ*PA14_2* :: *VdPA14_2*	*VdΔPA14_2* :: *VdPA14_2 –* t*rpC* - ^{P}*gpdA* - *hph*	*V. dahliae*	*Solanum lycopersicum*	this study
Vd JR2 Δ*PA14_2* :: *VlPA14_2-1*	*VdΔPA14_2* :: *VlPA14_2-1 – trpC* - ^{P}*gpdA* - *hph*	*V. dahliae*	*Solanum lycopersicum*	this study
Vd JR2 *PA14_2-GFP*	*VdPA14_2* :: *VdPA14_2 – GF – trpC* - ^{P}*gpdA* - *hph*	*V. dahliae*	*Solanum lycopersicum*	this study
Vd JR2 *GFP*	^{P}*gpdA – GFP - nat*	*V. dahliae*	*Solanum lycopersicum*	this study

:: = replaced by, - = fused with

Table 5: Primers used for amplifications and fusions

Designation	Sequence	Basepairs
CH93 fw	5'-TGT ACA GTG ACC GGT GAC TCT T-3'	22
CH93 rev	5'-CGT GTC GTC GAG GGT GGC CAT GGT GAT GTC TGC TCA AGC-GG-3'	41
CH94 fw	5'-CCG CTT GAG CAG ACA TCA CCA TGG CCA CCC TCG ACG ACA-3'	39
CH94 rev	5'-TCA GGG GCA GGG CAT GCT-3'	18
CH105fw	5'-TCT AGA ATG AAG TCA TTC ATT GCT GCT TTC G-3'	31
CH105 rev	5'-ACT AGT TCA AGC AGC AAC CTG CTC ACT-3'	27
CH112 rev	5'-GGT GAT GTC TGC TCA AGC GG-3'	20
CH119 fw	5'-GAT ATC AGT ACA AGA ACG GCG ACG TCG-3'	27
CH119 rev	5'-GAT ATC AGT ACA AGA ACG GCG ACG TCG-3'	27
CH120 fw	5'-AGC ATG CCC TGC CCC TGA GGG GTG TTG GGA TAA CTT GCA T-3'	40
CH120 rev	5'-CCT GCA GGG ACA TCA GGA TAC CAG CTA GTC-3'	30
CH123 fw	5'-GAA TTC AGT AGA GGA CGG CTG TAC AGC-3'	27
CH123 rev	5'-AAG AGT CAC CGG TCA CTG TAC AGG AGA TGG AAT CTG ATG-ATA TCG A-3'-	46
CH124 fw	5'-GAG CAT GCC CTG CCC CTG AAT GCT CTC GCA CTT GGT TCG C-3'	40
CH124 rev	5'-TCT AGA TGC ACC AGA TCC ATC TCG ACT T-3'	28
CH127fw	5'-ATG GCC ACC CTC GAC GAC A-3'	19
CH134 fw	5'-ATG GCC CCC TCC GCT ACC-3'	18
CH134 rev	5'-CTA GAT CTC GTT CTC CTT CTT GC-3'	23
CH136fw	5'-TCT AGA ATG GCC CCC TCC G-3'	19
CH138 fw	5'-GAA TTC AGT AGA GGA CGG CTG TAC AGC-3'	27
CH141 rev	5'-GGC ACC GGC TCC AGC GCC TGC ACC AGC TCC GAT CTC GTT-CTC CTT CTT GCG G-3'	52
CH142 fw	5'-AAT TGT ACA AAG GAT CTT AAT GCT CTC GCA CTT GGT TCGC-3'	40
CH143 rev	5'-CCT GCA GGT GCA CCA GAT CCA TCT CGA CTT-3'	30
CH146 rev	5'-GGC ACC GGC TCC AGC GCC TGC ACC AGC TCC AGC AGC AAC-CTG CTC ACT CTC-3'	51
CH147 fw	5'-GGA GCT GGT GCA GGC GCT GGA GCC GGT GCC TCT AAA GGT-GAA GAA TTA TTC ACT GGT-3'	57
CH148 rev	5'-CCT GCA GGG ACA TCA GGA TAC CAG CTA GTC-3'	30
CH149 rev	5'-CGA GGT AGC GGA GGG GGC CAT TGT AGC TAT AGG TGG GTT-GAG GT-3'	44
CH150 fw	5'-TCA ACC CAC CTA TAG CTA CAA TGG CCC CCT CCG CTA CC-3'	38
CH150 rev	5'-CGA ACC AAG TGC GAG AGC ATC TAG ATC TCG TTC TCC TTC-TTG C-3'	43
CH151 fw	5'-AGA AGG AGA ACG AGA TCT AGA TGC TCT CGC ACT TGG TTC-GC-3'	41
CH152 fw	5'-GAT ATC ACT CAA GCA CTA CCG CTC AGC-3'	27

Table 5 continued

Designation	Sequence	Basepairs
CH152 rev	5'-AGC AGC AAT GAA GGA CTT CAT GTT TGG AGA AGA CGT GCT-TGA CA-3'	44
CH153 fw	5'-CAA GCA CGT CTT CTC CAA ACA TGA AGT CCT TCA TTG CTG-CTT TC-3'	44
CH153 rev	5'-GCA AGT TAT CCC AAC ACC CCT CAA GCA GCA ACC TGC TCA-CTC-3'	42
CH154 fw	5'-GTG AGC AGG TTG CTG CTT GAG GGG TGT TGG GAT AAC TTG-CAT T-3'	43
CH155 rev	5'-GAG TCA CCG GTC ACT GTA CAT TAA GAT CCT TTG TACA ATT-CAT CCA TAC-3'	49
CH156 fw	5'-AAT TGT ACA AAG GAT CTT AAT GTA CAG TGA CCG GTG ACT-CTT-3'	42
CH157 rev	5'-CGA ACC AAG TGC GAG AGC ATT CAG GGG CAG GGC ATG CTC-3'	39
CH158 rev	5'-ATG CAA GTT ATC CCA ACA CCC CTC AGG GGC AGG GCA TGC T-3'	40
CH159 rev	5'-GTC GCG GTG AGT TCA GGC ATG GTG ATG TCT GCT CAA GCG G-3'	40
CH160 fw	5'-CCG CTT GAG CAG ACA TCA CCA TGC CTG AAC TCA CCG CGA C-3'	40
CH161 rev	5'-CGA ACC AAG TGC GAG AGC ATC TAT TCCT TTG CCC TCG GAC-G-3'	41
CH162 fw	5'-GTC CGA GGG CAA AGG AAT AGA TGC TCT CGC ACT TGG TTC-GC-3'	41
CH163 rev	5'-TGC AAG TTA TCC CAA CAC CCC CTA TTC CTT TGC CCT CGG-ACG-3'	42
CH164 fw	5'-GTC CGA GGG CAA AGG AAT AGG GGG TGT TGG GAT ACT TGC-AT-3'	42
CH165 fw	5'-GAT ATC TGT ACA GTG ACC GGT GAC TCT T-3'	28
CH165 rev	5'-AAT AAT TCT TCA CCT TTA GAG GTG ATG TCT GCT CAA GCG G-3'	40
CH166 fw	5'-CCG CTT GAG CAG ACA CAC CAT GTC TAA AGG TGA AGA ATT-ATT CAC TG-3'	48
CH166 rev	5'-GTG TCG TCG AGG GTG GCC ATT TAA GAT CCT TTG TAC AAT-TCA TCC ATA C-3'	49
CH167 fw	5'-GGA TGA ATT GTA CAA AGG ATC TTA AAT GGC CAC CCT CGA-CGA CA-3'	44
CH167 rev	5'-CCT GCA GGT CAG GGG CAG GGC ATG CTC-3'	27
CH168 rev	5'-AGA GTC ACC GGT CAC TGT ACA CTA GAT CTC GTT CTC CTT-CTT GC-3'	44
CH169 fw	5'-GCA AGA AGG AGA ACG AGA TCT GTA CAG TGA CCG TGA CTC-TT-3'	42
CH170 rev	5'-GAG TCA CCG GTC ACT GTA CAT CAA GCA GCA ACC TGC CAC-TC-3'	42
CH171 fw	5'-AGA GTG AGC AGG TTG CTG CTT GTA CAG TGA CCG GTG ACT-CTT-3'	42

Table 5 continued

Designation	Sequence	Basepairs
CH172 fw / OLG70	5'-CAG CGA AAC GCG ATA TGT AG-3' (Eynck *et al.*, 2007)	20
CH172 rev / OLG71	5'-GGC TTG TAG GGG GTT TAG A-3' (Eynck *et al.*, 2007)	19
CH173 fw	5'-CTG CAG GAA TTC GAT GTT TAA CAC TCA AGC CTA CCG CTC-AGC-3'	44
CH173 rev	5'-ATC GAT AAG CTT GAT GTT AAA CTA ATT ACA CCA TCT TCC-GTA ACC TAA A-3'	50
CH174 fw	5'-CAG GTT GCT GCT TGA GGA TCC ACT TAA CGT TAC TGA AAT C-3'	40
CH174 rev	5'-ACC GGT CAC TGT ACA TCG AGT GGA GAT GTG GAG TGG-3'	36
CH175 fw	5'-CTG CAG GAA TTC GAT GTT TAA ACA GTA GAG GAC GGC-TGT ACA GC-3'	44
CH175 rev	5'-TCG ATA AGC TTG ATG TTT AAA CTG CAC CAG ATC CAT-CTC GAC TT-3'	44
CH176 fw	5'-GAG AAC GAG ATC TAG GGA TCC ACT TAA CGT TAC TGA-AAT C-3'	40
CH176 rev	5'-ACC GGT CAC TGT ACA TCG AGT GGA GAT GTG GAG TGG-3'	36
CH177 rev	5'-TTA AGA TCC TTT GTA CAA TTC ATC CAT A-3'	28
CH178 fw	5'-TAC AAA GGA TCT TAA GGA TCC ACT TAA CGT TAC TGA AAT C-3'	40
CH179 fw	5'-CGG CCG CTC TAG AAC TAG TG-3'	20
CH179 rev	5'-ACA AAA GCT GGG TAC CGG GC-3'	20
CH180 fw	5'-CTC GCA GGT CAT CTC CAG TTG-3'	20
CH180 rev	5'-GTC CTC AAG AGA GGG CGA C-3'	19
CH181 fw	5'-ACT GAG TGA GGT TGA CGG CG-3'	20
CH 181 rev	5'-GTG CGA GCG ACC TGC GAC-3'	18
CH182 fw	5'-CTG CAG GAA TTC GAT GTT TAA ACT GTA CAG TGA CCG GTG-ACT CTT-3'	45
CH182 rev	5'-GGT GAT GTC TGC TCA AGC GG-3'	20
CH183 fw	5'-TGA GCA GAC ATC ACC ATG GTG AGC AAG GGC GAG GA-3'	35
CH183 rev	5'-ACG TTA AGT GGA TCC TCA GGG GCA GGG CAT GCT C-3'	34
CH184 fw	5'-GGA TCC ACT TAA CGT TAC TGA AAT C-3'	25
CH184 rev	5'-ATC GAT AAG CTT GAT GTT TAA ACT CGA GTG GAG ATG TGG-AGT GG-3'	44
CH185 fw	5'GAA TTC TGT ACA GTG ACC GGT GAC TCT T-3'	28
CH185 rev	5'-CCT GCA GGT CGA GTG GAG ATG TGG AGT GG-3'	29
CH186 fw	5'-TGC CAG TGC TTT GAT GGT TAC G-3'	22
CH186 rev	5'-CGG GGT GTA GAT TGT CTC CTC TT-3'	23
CH187 fw	5'-GAC CAA CAG CAA CTG GGA TGC-3'	21

Table 5 continued

Designation	Sequence	Basepairs
CH187 rev	5'-GAG TAG GCG GCG GAG AGA CC-3'	20
CH188 fw	5'-AAC ACC CCC AAA CGA AAG TGA C-3'	22
CH188 rev	5'-TCA GCG AAT CCA TAC CAA GTG C-3'	22

Table 6: Primers used for amplifications and fusions

Strain	Transformed strain	Primers for 5'-UTR	Primers for 3'-UTR	Primers for Promotor and resistance	Primers for ORF, Terminator and GFP	Primers for fusion
VdΔTHI4	*V. dahliae JR2*	CH123fw/rev	CH124fw/rev	CH93fw/rev		CH123fw/124rev
				CH127fw/94rev		
VdΔTHI4 :: *VdTHI4*	*V. dahliae JR2*	CH175fw/149rev	CH162fw/143rev	CH169fw/159rev	CH150fw/134rev	CH175fw/134rev
				CH160fw/161rev	CH176fw/rev	CH176fw/175rev
VdΔTHI4 :: *VlTHI4-1*	*V. dahliae JR2*	CH175fw/149rev	CH162fw/143rev	CH169fw/159rev	CH150fw/134rev	CH175fw/134rev
				CH160fw/161rev	CH176fw/rev	CH176fw/175rev
VdTHI4-GFP	*V. dahliae JR2*	CH175fw/141rev	CH178fw/157rev	CH178fw/157rev	CH178fw/157rev	CH175fw/177rev
					CH142fw/177rev	CH178fw/157rev
VdΔPA14_2	*V. dahliae JR2*	CH119fw/rev	CH120fw/rev	CH93fw/rev		CH119fw/120rev
				CH127fw/94rev		
VdΔPA14_2 :: *VdPA14_2*	*V. dahliae JR2*	CH173fw/152rev	CH164fw/148rev	CH171fw/159rev	CH153fw/84rev	CH173fw/84rev
				CH160fw/163rev	CH174fw/rev	CH174fw/173rev
VdΔPA14_2 :: *VlPA14_2-1*	*V. dahliae JR2*	CH173fw/152rev	CH164fw/148rev	CH171fw/159rev	CH153fw/84rev	CH173fw/84rev
				CH160fw/163rev	CH174fw/rev	CH174fw/173rev
VdPA14_2-GFP	*V. dahliae JR2*	CH173fw/146rev	CH178fw/173rev	CH178fw/173rev	CH178fw/173rev	CH173fw/177rev
					CH147fw/177rev	CH178fw/173rev
Vd GFP				CH182fw/rev	CH184fw/rev	CH183fw/rev

2.4 Plasmids

Table 7: Plasmids constructed and used in this study

pME	Description	Organism	Marker	Source
	pJET1.2	*E. coli*	*Amp*^{R}	Fermentas
	pKO2	*A. tumefaciens* *Verticillium* spp.	*Kan*^{R}, *Phleo*	Tran 2012
2791		*S. cerevisiae*	*Amp*^{R}, *Ura3*	Fred Winston NAR 1994, 22, 25:5767
3739			Clo*Nat*^{R}	(Gerke *et al.*, 2012)
4105	pJET Δ*THI4*	*V. dahliae*	*Amp*^{R}, Clo*Nat*^{R}	this study
4106	pKO2 Δ*THI4*	*V. dahliae*	*Kan*^{R}, Clo*Nat*^{R}	this study
4107	pJET Δ*PA14_2*	*V. dahliae*	*Amp*^{R}, Clo*Nat*^{R}	this study
4108	pKO2 Δ*PA14_2*	*V. dahliae*	*Kan*^{R}, Clo*Nat*^{R}	this study
	pBluescript®II KS$^+$	*E. coli*	*Amp*^{R}	Invitrogen
	pGS1	*A. tumefaciens* / *Verticillium* spp	*Amp*^{R}, *Hyg*^{R}	Tran 2012
4109	pBl®II KS$^+$ Δ*THI4* :: *VdTHI4*	*E. coli* / *V. dahliae*	*Amp*^{R}, *Hyg*^{R}	this study
4110	pBl®II KS$^+$ Δ*THI4* :: *VlTHI4-1*	*E. coli* / *V. dahliae*	*Amp*^{R}, *Hyg*^{R}	this study
4111	pBl®II KS$^+$ Δ*PA14_2* :: *VdPA14_2*	*E. coli* / *V. dahliae*	*Amp*^{R}, *Hyg*^{R}	this study
4112	pBl®II KS$^+$ Δ*PA14_2* :: *VlPA14_2-1*	*E. coli* / *V. dahliae*	*Amp*^{R}, *Hyg*^{R}	this study
4114	pME2791 *VdTHI4* cDNA	*S. cerevisiae*	*Amp*^{R}, *Ura3*	this study
4115	pME2971 *VlTHI4* cDNA	*S. cerevisiae*	*Amp*^{R}, *Ura3*	this study
	pAN 7-1	*E. coli*	*Amp*^{R}, *Hyg*^{R}	(Mullaney *et al.*, 1985)
	pFA6a - *GFP* (S65T)	*S. cerevisiae*	*Amp*^{R}, *Kan*^{R}	(Bahler *et al.*, 1998)
4116	pBluescript®II KS$^+$ *THI4* - *GFP*	*E. coli* / *V. dahliae*	*Amp*^{R}, *Hyg*^{R}	this study
4117	pBluescript®II KS$^+$ *PA14_2* - *GFP*	*E. coli* / *V. dahliae*	*Amp*^{R}, *Hyg*^{R}	this study
3929	*GFP-Nat* cassette	*E. coli*	*Amp*^{R}, Clo*Nat*^{R}	
4118	pBluescript®II KS$^+$ *GFP*	*E. coli* / *V. dahliae*	*Amp*^{R}, Clo*Nat*^{R}	this study

:: = replaced by, - = fused with

2.4.1 Construction of plasmids for *V. dahliae* knock-out strains

The primers and plasmids for deleting *THI4* and *PA14_2* in *V. dahliae* are listed in Table 5, Table 6 and Table 7.

For deleting thiamine synthase *THI4*, the nourseothricin (*nat*) resistance was amplified from the pME3793 vector with primers CH93fw/rev. The 5'-prime and 3'-prime flanking regions of around 1.5 kb were amplified from *V. dahliae* JR2 genomic DNA by CH123fw/rev and CH124fw/rev. A constitutive *gpdA* promoter was used for the resistance cassette and amplified by CH127fw/94rev from vector pKO2. Fusion PCR was performed with the primer pair CH123fw/124rev. The knockout cassette was cloned blunt end into pJET1.2 and into the pKO2 vector via 5'-prime *Eco*RI and 3'-prime *Xba*I restriction sites (resulting in the vectors pME4105 and pME4106). The knockout cassette was cloned into *V. dahliae* JR2 by *Agrobacterium tumefaciens* mediated transformation (ATMT).

Deletion of the membrane protein *PA14_2* was performed by insertion of nourseothricin (nat^R) resistance into the locus. Amplification of the resistance cassette from the pME3793 vector with the primers CH93fw/rev was performed. The 1.5 kb 5'-prime and 3'-prime flanking regions were amplified from genomic *V. dahliae* JR2 DNA by using CH119fw/rev and CH120fw/rev primers. Fusion PCR was then performed together with the constitutive *gpdA* promotor (CH127fw/94rev from vector pKO2) by using the primers CH119fw/CH120rev. Then the knockout cassette was cloned into pJET1.2 and into pKO2 vector via 5'-prime *Eco*RV and 3'-prime *Sbf*I (*Sda*I) restriction sites (pME4107 and pME4108 were the resulting plasmids). The knockout cassette was transformed linear into *V. dahliae* JR2 via protoplastation.

2.4.2 Construction of plasmids for complementation of *Vd*Δ*THI4* and *Vd*Δ*PA14_2*

Complementation was on the one hand performed by using the original *Vd* JR2 open reading frame (resulting in the plasmids pME4109 and pME4111) and on the other hand by using the *Vl* 43 *dahliae*-like allele (resulting in the plasmids pME4110 and pME4112) for heterologous complementation. For both, flanking regions were derived of the JR2 genome.

For construction the GeneArt® Seamless Cloning & Assembly Kit (life technologies™, Darmstadt, Germany) was used to fuse three parts of the complementation cassette and the pBluescript® II KS^+ vector.

For construction of the Δ*THI4* complementation plasmid *THI4* open reading frame was amplified from genomic DNA using the primers CH150fw/134rev like the 1.5 kb up- and

downstream flanking regions (using the primers CH175fw/149rev and CH162fw/175rev). The constitutive *gpdA* promoter was amplified from pME4105 by using CH169fw/159rev and finally the hygromycin resistance gene (*hph*) was amplified with the primers CH160fw/161rev from the pGS1 vector. The t*rpC* terminator at least was amplified from the pAN7-1 vector using CH176fw/rev as primers. Before using the GeneArt® Seamless Cloning & Assembly Kit the upstream flanking region and open reading frame were fused. The promoter was fused with the resistance and the downstream flanking region by PCR. The *trpC* terminator was used as a single part. The three parts of the complementation cassette were ligated into pBluescript®II KS$^+$ vector via *Pme*I restriction sites.

The complementation cassette of Δ*PA14_2* was constructed like the one of thiamine synthase. The 1.5 kb up- and downstream flanking regions (CH173fw/149rev, CH162fw/173rev) and the *PA14_2* open reading frame (CH153fw/84rev) were amplified from genomic DNA. The constitutive g*pdA* promotor was amplified from the plasmid pME4107 by using the primers CH169fw/159rev and finally the hygromycin resistance gene (*hph*) was amplified with CH160fw/161rev from the pGS1 vector. At least *trpC* terminator was amplified by CH176fw/rev from the pAN7-1 vector. Before using GeneArt® Seamless Cloning & Assembly Kit the upstream flanking region and open reading frame were fused and the promoter was connected with the resistance and the downstream flanking region by PCR. The *trpC* terminator was used as a single part. The three parts of the complementation cassette were fused blunt end into pBluescript®II KS$^+$ vector via *Pme*I restriction sites. Finally all cassettes were transformed linear into *Vd*Δ*THI4* and *Vd*Δ*PA14_2* deletion strains via protoplastation.

2.4.3 Construction of *GFP*-tagged plasmids

Single *GFP* (single green fluorescing protein) was cloned downstream to *VdTHI4* and *VdPA14_2* genes (resulting in the vectors pME4116 and pME4117). Fusing the cassette was done by GeneArt® Seamless Cloning & Assembly Kit (life technologies™, Darmstadt, Germany) with two cassette parts and the pBluescript®II KS$^+$ vector.

For the *VdTHI4-GFP* cassette the plasmid pME4109 was used as template. Upstream flanking region and open reading frame were amplified with the primers CH175fw/141rev from the plasmid pME4109. The *GFP* gene was amplified by CH142fw/177rev from pFA6a-*GFP* plasmid and the two parts were fused (CH175fw/177rev) by PCR. As a second part the terminator, promoter, resistance and downstream flanking region were amplified as one fragment with the primers 178fw/175rev from the plasmid pME4109. The *GFP* cassette was

cloned by fusing the two fragments blunt end into pBluescript®II KS$^+$ vector via *Pme*I restriction sites.

For generating the cassette of *VdPA14_2-GFP* pME4111 was used as template and upstream flanking region together with *VdPA14_2* open reading frame were amplified using primers CH173fw/146rev. The *GFP* was generated by PCR from the pFA6a-*GFP* plasmid using the primes CH147fw/177rev. The two parts were fused with 173fw/177rev by fusion PCR. As a second part the terminator, promoter, resistance and downstream flanking region were amplified as one fragment by the primers 178fw/173rev from the plasmid pME4111. The g*fp* cassette was cloned by fusing the two fragments blunt end into pBluescript®II KS$^+$ vector via *Pme*I restriction sites.

In order to create the positive control, *GFP-gpdA-nat*^{R} was amplified from the plasmid pME3929 by using the primers CH183fw/rev. For generating the constitutive promotor *gpdA* pME 4109 was used as the template and the primers CH182fw/rev and CH184fw/rev. All three fragments were cloned into pBluescript®II KS$^+$ vector blunt end via *Pme*I restriction sites and named pME4118. All cassettes were transformed linear into *V. dahliae* JR2 via protoplastation.

2.5 Recombinant DNA methods

Recombinant DNA technologies were performed according to the standard methods (Sambrook *et al.*, 1989). For PCR reactions *Taq* polymerase, Platinum® *Taq* Polymerase (Fermentas GmbH, St. Leon Rot, Germany), or Phusion® High Fidelity DNA Polymerase (Finnzymes, Vantaa, Finland) were used.

Restriction enzymes and DNA modifying enzymes were obtained from Fermentas GmbH (St. Leon-Rot, Germany). Oligonucleotides were ordered from Eurofins MWG GmbH (Ebersberg, Germany).

For cloning GeneArt® Seamless Cloning & Assembly Kit (life technologies™, Darmstadt, Germany) was used.

2.6 Fungal nucleic acid purification and hybridization

Fungal mycelium was grown in liquid cultures (SXM or PDB) and harvested according to description in 2.3.3. Then the mycelium was retained inside the filter by filtering trough miracloth filters. After directly freezing in liquid nitrogen it was ground to fine powder by

using the Retsch MM 400 Cyro Mill (Retsch, Düsseldorf, Germany). The fungal powder was kept in liquid nitrogen or stored at - 80°C.

Genomic DNA was extracted according to Kolar *et al.*. (Kolar *et al.*, 1988). It was extracted twice with phenol/chloroform (1:1 (v/v)) and subsequently precipitated with isopropanol and 50 mM sodium acetate. Genomic DNA was dissolved in RNAse A treated elution buffer (Qiagen, Hilden, Germany) and stored at 4°C.

For plasmid isolation from *E. coli* QIAprep Spin Miniprep Kit or QIAprep Midiprep Kit (Qiagen, Hilden, Germany) was used according to the manufacturer's protocol.

DNA gel extraction was performed using the QIAquick Gel Extraction Kit (Qiagen, Hilden, Germany).

Total fungal RNA was extracted by using the RNeasy Plant Mini Kit (Qiagen, Hilden, Germany) according to the manufacturer's instructions.

DNA and RNA concentration was measured using NanoDrop *ND*-1000 spectrophotometer (PEQLAB, Erlangen, Germany). The DNA quality was also checked on 1% agarose gel using 5 µl genomic DNA.

Southern-hybridization was performed non-radioactively by following the standard protocol (Busch *et al.*, 2003). Probes were labeled by using the Amersham™ AlkPhos Direct Labelling reagents (GE Healthcare, München, Germany).

For probe preparation, DNA was amplified from genomic DNA by PCR using primers according to the list in Table 8.

Table 8: Primers for Southern-hybridization probes

Probe	**Primers**
Δ*THI4* 5'-UTR	CH123 fw / rev
Δ*THI4* 3'-UTR	CH 124 fw / rev
Δ*PA14_2* 5'-UTR	CH 119 fw / rev
Δ*PA14_2* 3'-UTR	CH 120 fw / rev
GFP	CH 166 fw / rev

2.7 Genetic manipulations

2.7.1 *E. coli* transformation

E. coli transformation was performed with calcium/manganese treated cells (Hanahan *et al.*, 1991) as described by Inoue (Inoue *et al.*, 1990).

2.7.2 *S. cerevisiae* transformation

DNA integration in yeast cells was performed according to Ito (Ito *et al.*, 1983).

2.7.3 *Agrobacterium tumefaciens*-mediated transformation in *Verticillium* spp.

A. tumefaciens-mediated transformation (ATMT) in *Verticillium* spp. was performed like previously described (Jyothishwaran *et al.*, 2007; Timpner *et al.*, 2013).

2.7.4 Transformation of DNA in *Verticillium dahliae* via protoplastation

Transformation by protoplasts was performed with a linear fragment following the protocol of Punt and van den Hondel (Punt & van den Hondel, 1992) including adjustments:
V. dahliae strain was grown for one day (22h) in 10 round flasks (500 ml) filled with 150 ml PDB medium on a rotary shaker at 140 rpm and 25°C. The cultures were inoculated with 1.5 up to 3 x 10^8 fresh spores.
For preparation of fresh lysing-solution, 540 mg VinoFlow FCE (Glösmann, Steinakirchen, Austria) and 150 mg Lysozyme (10 mg/ml) (Serva, Heidelberg, Germany) were solved in 10 ml citrate buffer (150 mM KCl, 580 mM NaCl, 50 mM Na-Citrate, pH 5.5 with citric acid). After filtering the mycelium through miracloth filter (see 2.3.3) it was washed with citrate buffer and transferred together with the lysing-solution in a sterile 300 ml flask to shake with 80 rpm and 30°C for 2.5 h. The solution should be viscous, so the amount of lysing-solution has to be adjusted. The protoplasts were harvested by carefully shaking the solution and filtering through miracloth filter into a 50 ml falcon tube, filled up with ice-cold STC 1700 buffer (1.2 M Sorbitol, 10 mM TRIS (pH 5.5), 50 mM $CaCl_2$ and 35 mM NaCl) and chilled in ice for 5 - 10 min. Then the Falcon was centrifuged for 12 min at 2,500 rpm (4°C), the supernatant was discarded carefully and the protoplasts resuspended in the remaining liquid. The Falcon was filled up with STC 1700 buffer and centrifuged again. Then the resuspended protoplasts were split in 15 ml falcon tubes (250 µl each) and 15–18 µg linear DNA was added (except for the negative control). The mixture was chilled on ice for 37 min and then

PEG4000 (10 mM TRIS (pH 7.5), 50 mM $CaCl_2$ and 60% (w/v) PEG4000) was added in a 250 µl and 1000 µl step and incubated for 35 min, above ice. Finally, the Falcon was filled up with ice-cold STC 1700 buffer and centrifuged for 15 min at 2500 rpm (4°C). The supernatant was discarded and protoplasts were resuspended in the last drop. They were plated on sorbitol plates (10 ml 50% Glucose, 10 ml 50 x AspA pH5.5 ($NaNO_3$ 3.5M, KCl 0.35 M, KH_2PO_4 0.55 M) 1 ml 1 M $MgSO_4$, 0.5 ml 1000 x trace elements ($ZnSO_4$*7 H_2O 22 g/L, H_3BO_4 11 g/L, $MnCl_2$*4 H_2O 5 g/L, $FeSO_4$*7 H_2O 5 g/L, $CoCl_2$*6 H_2O 1.7 g/L, $CuSO_4$*5 H_2O 1*6 g/L, Na_2MoO_4*2 H_2O 1.5 g/L, Na_2-EDTA 50 g/L), 54.5 g Sorbitol and 2% Agar in 500 ml, supplemented with the screening antibiotic) after distributing 250 µl STC 1700 on them. Protoplasts were split up on four plates in 50 µl, 100 µl, 200 µl and the rest. The plates were incubated for 7 - 9 days at 25°C. Then the transformants were plated on new plates to avoid heterokarya.

2.8 Sequence analysis

BLAST search analyses (Altschul *et al.*, 1990) were performed online at NCBI (http://www.ncbi.nlm.nih.gov/).

Sequence alignments were carried out by ClustalW2 (http://npsa-pbil.ibcp.fr/) Geneious 5.6.5 (Biomatter Ltd, Auckland, New Zealand). DNA was sequenced by SANGER TECH at the Labor für Genomanalyse in Göttingen (Germany). Sequences were analyzed by the software Lasergene (DNASTAR, Inc., Madison, WI, USA).

For RNA-Seq total RNA was extracted and sequenced at GATC Biotech (Konstanz, Germany). The analysis will be described in section transcriptomics of *V. longisporum* in chapter 2.13.

2.9 Microscopy analysis

To perform fluorescence microscopy *V. dahliae* strains were grown in PDB for 4 days in liquid culture at 25°C and 140 rpm. For microscopy assays mycelium was taken in an eight chambered borosilicate cover glass system (Nunc, Thermo scientific, Waltham MA, USA) and supplemented with liquid medium (CDM or PDB). Cells were visualized using Zeiss Observer. Z1 microscope equipped with CSU-X1 A1 confocal scanner unit (Yokogawa Germany, Ratigen, Germany), QuantEM:512SC (Photometrics, Tucson AZ, USA) digital camera and SlideBook 5.0 software package (Intelligent Imaging Innovations, Denver CO, USA).

Stainings with the lipophilic dye FM4-64 were performed to observe *Verticillium* membranes as previously described (Vida & Emr, 1995).

To label mitochondria, the cells were incubated for 45 min in the presence of 50 nM MitoTracker® Red (Molecular Probes, Invitrogen GmbH, Karsruhe, Germany), washed once with fresh medium and imaged.

2.10 UV-irradiation assay

To determine DNA repair of mutants compared to wild type, *V. dahliae* and *S. cerevisiae* plates were treated with UV-light. 1000 of *S. cerevisiae* cells or fresh *V. dahliae* spores were plated on PDB or SC-Ura. The yeast strains were cultivated overnight in 10 ml SC-Ura raffinose; after 12 h of incubation strains were transferred in main culture (induction medium SC-Ura galactose) and grown for 5 h at 30°C on a rotary shaker. OD_{600} values of the cultures were measured and cell number calculated by the formula $OD_{600} = 0.1 \approx 1.5 \times 10^6$ cells/ml. Yeast and *V. dahliae* cells were plated on SC-Ura or PDA plates and incubated at room temperature for 1 h before illumination. Then they were arranged upside down on an UV-transilluminator (Biometra, Jena, Germany) and the cells were directly exposed with 302 nm wavelength for 5, 10, 15 and 20 sec. Control plates were not illuminated. The experiment was performed in triplicate. The *V. dahliae* plates were incubated for 4 d at 25°C and *S. cerevisiae* 3 d at 30°C. Fungal colonies were counted and mean value for each time point was calculated.

2.11 Plant infection assay

2.11.1 Plant growth and cultivation

Solanum lycopersicum seeds were surface sterilized with 70% ethanol and sown on silica sand (Vitakraft, Bremen, Germany) mixed with soil (T25 Fruhstorfer Erde, Hawita Gruppe, Vechta, Germany) 1:1. The seeds were kept moist under a 16 h light / 8 h dark (long-day conditions) regime for 10 d.

The seeds of *B. napus* were also sterilized but sown only on sand (Ratzinger *et al.*, 2009) and grown under long-day conditions for 14 days. The seedlings were pre-grown in a light chamber (Binder, Tuttlingen, Germany).

2.11.2 Spore solutions

Spores used for the infection of *S. lycopersicum* have to be freshly. They were grown in 150 ml SXM for 5 d at 25°C on a rotary shaker at 140 rpm and harvested one day before infection (see 2.3.3). Spores were diluted with 0.96% + NaCl 0.05% Tween80 in water to a concentration of 1 x 10^6 spores / ml. Overnight they were stored at 4°C.

2.11.3 Planting and infection process

S. lycopersicum and *B. napus* were carefully released from the soil/silica or silica substrate and the roots were washed with tap water. The roots were incubated for 35 min in 25 ml spore solution or water (mock control). *B. napus* plants for harvesting xylem-sap were not treated and directly planted. After this procedure the plants were planted in a mixture of sand and soil 1:1; one plant per pot. *S. lycopersicum* was grown in 13 x 13 cm (6 pots per tray), and *B. napus* in 9 x 9 cm pots (15 pots per tray). The plants were watered either with 1.5 ml spore solution or water (mock control).

To avoid *Sciaridaes*, one day before planting all pots were treated with VectoBac®WDG (Biohelp, Wien, Austria) in concentration of 0.5 l per 200-300 l water.

2.11.4 Growth conditions

Both plant lines were cultivated in a greenhouse under a 16 h light / 8 h dark (long-day conditions) regime for 28 days post infections (dpi). The infected plats were set under water stress in the first two weeks to enforce the infection process.

2.11.5 Documentation of infection symptoms

S. lycopersicum plant height was measured in cm after 7, 14, 21 and 28 days post *V. dahliae* JR2 infection.

2.11.6 Sample collection

Extraction of xylem-sap (not infected plants)

Xylem-sap extraction was performed on non-infected *B. napus* plants after 42 days (6 weeks). The stems were cut in height of the first true leaf with a sharp blade and emerging drops were collected after washing the cut surface with distilled water and discarding the first drop according to the method for *Arabidopsis thaliana* (Horie *et al.*, 2006). Xylem-sap extraction was most effective in the morning shortly after the lights turned on in the greenhouse.

The harvested sap was sterile filtered in Vivaspin 15R MWCO 10 kDa (Sartorius, Göttingen, Germany) with 3,000g.

Root, hypocotyl and stem (infected plants)

After 28 dpi root, hypocotyl and stem of the infected *S. lycopersicum* were harvested by cutting with a sharp blade. Hypocotyl was defined as green part above the white roots until the cotyledons. Root and hypocotyl samples were washed with distilled water and were immediately frozen in liquid nitrogen. The samples were grounded in a Retsch MM 400 Cyro Mill (Retsch, Düsseldorf, Germany). Later DNA was extracted (see 2.11.8) and stem parts were checked for outgrowth of *V. dahliae* (see 2.11.7).

2.11.7 Fungal out-growth of infected plant material

Harvested stems were sterilized for 15 min with 70% EtOH, 15 min in 10% hypochlorite solution and then rinsed three times with sterile water. The inner parts were sliced in pieces and plated on PDA plates supplemented with chloramphenicol (35 mg/ml). Photos were taken after 14 days with a SamsungST70 camera (Samsung Electronics GmbH, Schwalbach am Taunus, Germany).

2.11.8 Fungal DNA extraction and quantification of infected plant material

DNA was extracted from grounded plant material by DNeasy Plant Mini Kit (Qiagen, Hilden, Germany) according to the manufacturer's instructions and the samples were stored at - 20 °C. For measuring the DNA concentration a NanoDrop *ND*-1000 spectrophotometer (PEQLAB, Erlangen, Germany) was used.

To estimate the content of fungal DNA in 25 ng extracted DNA, OLG70 and OLG71 primers were used as standard (Eynck *et al.*, 2007) for quantitative PCR. To perform qPCR, 5 PRIME (5 PRIME GmbH, Hamburg, Germany) Kit was used. Each reaction contained 25 ng extracted DNA from infected plants that was mixed with 0.5 pM OLG primer (70 and 71), (Eynck *et al.*, 2007) (CH172fw/rev), PRIME MasterMix and H_2O was added to a final volume of 20 µl.

Each reaction was performed at least in triplicates using the Light Cycler 2.0 System (Roche, Manheim, Germany) with the following conditions: 95°C denaturation for 3 min, 42 cycles at 95°C for 10s, 63°C for 15 s and 72°C for 25 s to calculate cycle threshold values, followed by 95°C for 1 min, 55°C for 1 min and 80 times of 55°C for 10 s, increasing temperature by 0.5°C each cycle to obtain melting curves and to enable data analyses. The amount of fungal DNA was estimated by integration of a calibration curve. For this, crossing points of digestions of *Vd* gDNA of 1000 to 0.1 ng were measured with OLG70 and 71 primers.

2.12 Experimental setup for *V. longisporum* omics (big batch)

2.12.1 Fungal growth and transfer procedure

In order to comparatively investigate transcriptomic, metabolomic and proteomic, *V. longisporum* 43 was cultivated in SXM and PDB media and xylem-sap of *B. napus* (see 2.3.3). Samples for all three technical platforms were taken from the same flasks.

Vl 43 was pre-grown in 200 ml PDB with streptomycin in a 500 ml flask for four days at 100 rpm and 25°C. Mycelium was filtered with sterilized miracloth and transferred in sterilized flasks with SXM, CDM or xylem-sap and incubated again for 4 d at 100 rpm and 25°C on a rotary shaker. Then *Vl* 43 was harvested under sterile conditions as described above. Mycelium was immediately frozen in liquid nitrogen and stored at -80°C until use for transcriptomics, metabolomics and proteomics experiments.

2.13 Transcriptomics of *V. longisporum* 43

2.13.1 RNA transcriptomics by deep sequencing

Transcriptomics data of *V. longisporum* 43 were generated by RNA deep sequencing (RNAseq) that is a high-throughput sequencing technology to sequence cDNA.

For sequencing *Vl* 43 RNA was prepared from the cultures of big-batch experiments (chapter 2.12) by using RNeasy Plant Mini Kit (Qiagen, Hilden, Germany) and sent for sequencing (GATC Biotech, Konstanz, Germany). Coding RNA was separated at GATC from noncoding RNA by preparing a poly(A)-library followed by reverse transcription to cDNA and sequencing with High Seq 2000 from Illumina (reads 100 bp length, per pool 180.000.000 read pairs and output of 36 Gb rawdata) (San Diego, USA) was performed. Resulting reads data were mapped to *V. longisporum* 43 genome. For quantitative analysis RPKM data (reads per kilobase per million of mapped reads) were calculated at the Institut für Mathematik und Informatik (Greifswald, Germany) in the group of Prof Mario Stanke.

2.13.2 Reads per kilobase per million of mapped reads (RPKM) data processing

For transcript quantification the sequenced reads were normalized as *reads per kilobase per million of mapped reads*, or RPKM after the model of Mortavazi *et al.*. (Mortazavi *et al.*, 2008). This data normalization was performed by Dr. Tonatiuh Pena Centeno, Institut für Mathematik und Informatik (Greifswald, Germany).

2.13.3 MarVis analysis

The obtained data matrices of RPKM data were imported into the software toolbox MarVis (http://marvis.gobics.de, (Kaever *et al.*, 2012; Kaever *et al.*, 2009)) as CSV-files and samples grouped by condition identifiers (condition specific names) to visualize the expression in clusters in a 1D self-organizing-map (1D-SOM). This was performed in the Department of Bioinformatics (University of Göttingen, Germany) by Alexander Kaever.

The single-sample raw data files were merged using the MarVis-Filter tool ("Merge lists" function, column indices "1 2", delimiter ";", start row "1", attach in front of IDs "vl43-au17.", attach behind IDs ".t1"). The resulting CSV file was imported in MarVis-Filter (raw file import, condition identifiers "SXM, Xylem"), the RPKM values were normalized using the median of non-zero values per sample, and ranked according to the signal-to-level ratio (column "s/l"). Additionally, the data set was re-ranked according to the maximum intensity level (column "maximum") and the ANOVA based false discovery rate (ANOVApValue_FDR). The FDR based on the s/l ratio was calculated (based on 10,000 random permutations, column "s/l_FDR"). au17 transcript IDs were replaced by au16 IDs using the mapping file new_au17t_au16t_map.csv. The data set was exported sorted according to s/l and annotated using the VL43 summary file v.longisporum-43_au16_2012-10-01.csv. For quality control, a Principle Component Analysis (PCA) based on normalized profiles (Euclidean norm) and a hierarchical clustering based on log-scale intensities using the linear correlation distance and average linkage were performed. The complete data set was clustered based on a one-dimensional self-organizing map (1D-SOM) using 50 prototypes and the following aggregation and normalization method: Mean and Euclidean norm (norm-2) (noisy profiles may result in highly differential mean profiles). For an alternative visualization of the data set (with most noise eliminated), the data set was filtered according to a signal-to-level ratio of 0.5 (utilizing the maximum level as signal, file identifier "_maxSL05_") and clustered. For a visualization of the differential profiles, the data set was filtered according to an FDR < 0.05 (based on s/l) and clustered. For analysis of condition-specific candidates, the data set was filtered according to FDR < 0.05 (based on s/l) and a positive directed signal-to-level ratio using as maximum the SXM or XyS conditions. The extracted data sets were sorted according to the directed signal-to-level ratio, exported, and annotated. For clustering of the whole data set, profiles containing only zero value intensities were filtered out.

3 Results

3.1 *V. dahliae* Thi4 shows amino acid sequence similarities to *S. cerevisiae* and *F. oxysporum* proteins involved in thiazole biosynthesis

Originally, the thi4 domain containing deduced protein of *Verticillium longisporum* gene was found in a screen for putative fungal adhesins in *S. cerevisiae*. The screen reveals parts of *VlTHI4*, missing the C-terminal part of the gene, to induce adhesion in the non-adhesive Δ*flo8* yeast strain (Euroscarf). Later analysis revealed the gene not to be involved in adhesion. Instead of the *Verticillium THI4* gene, the additional sequence, apart from *VlTHI4*, being inserted in the plasmid, seems to cause the activation of adhesion or the direct adhesion in the yeast (data not shown).

The thi4 domain containing deduced protein of *V. longisporum* shows sequence similarities to the thiazole synthase of *Saccharamyces cerevisiae* and *Fusarium oxysporum*, leading to the assumption of an involvement in the essential thiamine pathway. In eukaryotes the thiazole synthase protein is highly conserved. The family includes Thi4p from *S. cerevisiae* and Sti35 from the vascular wilt fungus *F. oxysporum* as well as others (Praekelt *et al.*, 1994; Ruiz-Roldan *et al.*, 2008). *S. cerevisiae* Thi4p has a dual function in thiazole biosynthesis and in mitochondrial genome stability (Machado *et al.*, 1997). The *sti35* gene of the vascular pathogen *F. oxysporum* is involved in the thiazole moiety synthesis of the thiamine pathway and in addition in stress response. Sti35 is not required for pathogenicity (Ruiz-Roldan *et al.*, 2008). This suggests that the vascular system might provide enough vitamine B1 for fungal growth in case of *F. oxysporum*.

The deduced protein sequence of *Verticillium* Thi4 shows highest similarity with *F. oxysporum* Sti35 (66%) and significant similarity with *S. cerevisiae* Thi4p (53%), including a common putative NAD-binding site (Figure 6, red) in the thi4-binding domain (Figure 6, blue background) (Moeller & Amons, 1985; Praekelt & Meacock, 1992). In the N-terminal region of the sequences positive charged amino acids were determined what led to a predicted mitochondrial localization of the protein. In contrast to yeast and *Fusarium* sequences (Praekelt & Meacock, 1992), the protein sequence analysis of *Verticillium* Thi4 revealed a C-terminally sequence insertion (Figure 6, green).

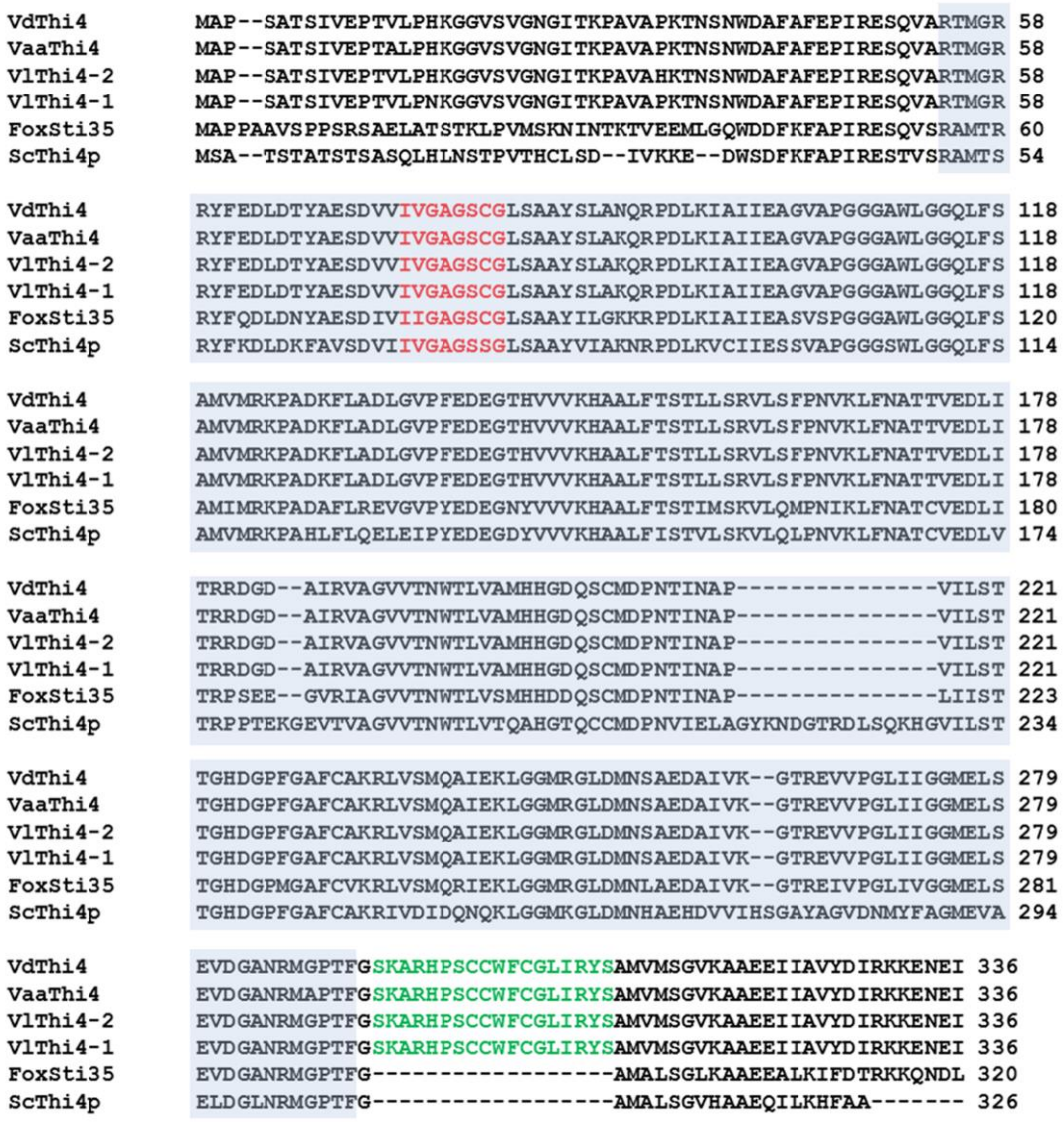

Figure 6: **Alignment of deduced amino acid sequences of Thi4-like proteins of vascular pathogenic fungi in comparison to *S. cerevisiae* Thi4p and *F. oxysporum* Sti35.** S.cerevisiae Thi4p and F. oxysporum Sti35 were aligned with V. dahliae VdThi4 (HG425077 EMBL), V. albo-atrum VaaThi4 (HG425078 EMBL) and V. longisporum VlThi4-1 (HG425079 EMBL) and VlThi4-2 (HG425080 EMBL). The conserved NAD-binding domain is marked in red. Verticillium sequences contain C-terminal an insertion (green) in contrast to yeast Thi4p and F. oxysporum Sti35. Analysis performed with ClustalW2 (http://www.ebi.ac.uk/Tools/msa/clustalw2/).

The phylogenetic comparison of Thi4 (Figure 7 and Table 9) reveals that the protein is highly similar between the *Verticillium* strains (99% identities). Furthermore, sequence comparison of the DNA revealed more similarities between *VdTHI4* and the *VlTHI4-1* isogene. The same situation occurs by comparing *VaaTHI4* with the *VlTHI4-2* isogene (data not shown).

Table 9: Phylogenetic similarities of ScThi4p, FoxSti35, VlThi4-1, VlThi4-2, VdThi4 and VaaThi4

Identity in %	ScThi4p	FoxSti35	VlThi4-2	VlThi4-1	VdThi4	VaaThi4
ScThi4p (NP_011660.1)		55.8	53.3	53.0	53.0	53.0
FoxSti35 (BAA85305.1)	55.8		66.4	66.4	66.1	66.1
VlThi4-1 (HG425079)	53.0	66.4		99.4	99.4	99.1
VlThi4-2(HG425080)	53.0	66.4	99.4		99.4	99.1
VdThi4 (HG425077)	53.0	66.1	99.4	99.4		99.1
VaaThi4 (HG425078)	53.0	66.1	99.1	99.1	99.1	

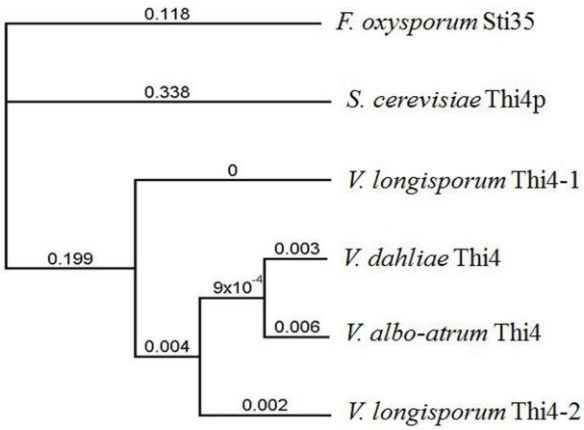

Figure 7: Phylogenetic tree of thiazole synthase of *V. dahliae*, *V. albo-atrum*, *F. oxysporum* and *S. cerevisiae*. *Verticillium* Thi4 deduced protein sequences are highly similar. They share more identities with *F. oxysporum* Sti35 than with *S. cerevisiae* Thi4p.
Accession numbers:
ScThi4p: NP_011660.1 (NCBI),
FoxSti35: BAA85305.1 (NCBI),
VdThi4: HG425077 (EMBL),
VaaThi4: HG425078 (EMBL),
VlThi4-1: HG425079 (EMBL) and
VlThi4-2: HG425080 (EMBL).

3.1.1 Knockout of *V. dahliae THI4* evokes reduced growth on thiamine-free medium

The plant vascular system provides only limited supply of nutrients and former studies revealed a bradytrophic mutant of *V. longisporum* with reduced pathogenicity on *Brassica napus* in a strain with silenced chorismate synthase of the essential amino acid pathway (Singh *et al.*, 2010). Living in the central cylinder in the vascular medium xylem-sap with a reduced number of nutrients results in the fact that the filamentous fungus needs to synthesize essential nutrients itself for survival and pathogenicity. In order to analyze the functions of *V. dahliae* Thi4, a knockout was constructed to investigate the role of VdThi4

ex planta and *in planta*, in the absence or presence of vitamine B1 and under DNA damaging conditions. To analyze the *THI4* deletion strain phenotype *ex planta*, different growth tests were performed before testing the strain for pathogenicity on *Solanum lycopersicum* plants.

The deletion of the *V. dahliae THI4* locus was performed by *Agrobacterium*-mediated transformation and the complementation via protoplastation method. In this study, the protocol for DNA insertion of protoplasts (Punt & van den Hondel, 1992) was adjusted for *Verticillium dahliae*.

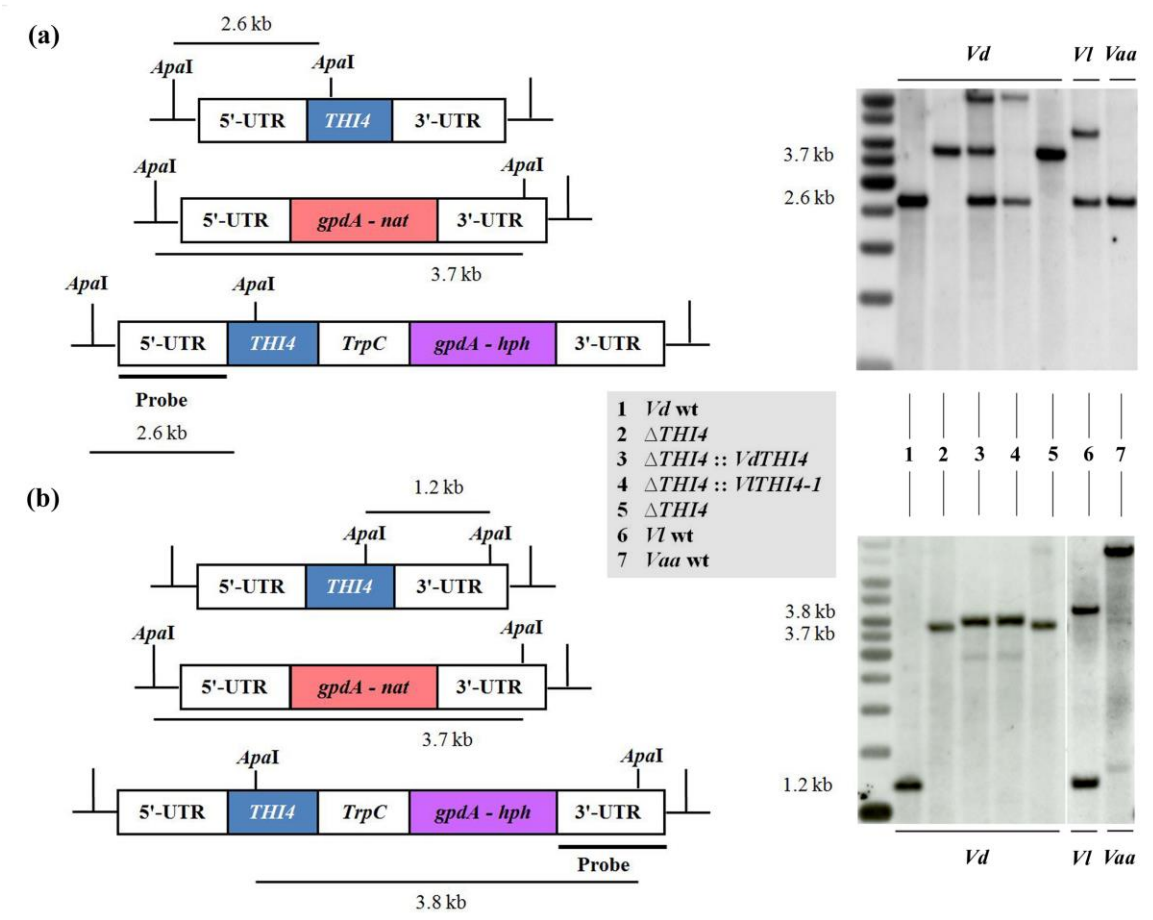

Figure 8: **Southern hybridization of *THI4 V. dahliae* wt, Δ*THI4*, Δ*THI4* :: *VdTHI4* and Δ*THI4* :: *VlTHI4-1*, *Vl* wt and *Vaa* wt. (a)** 5'-probe: Knockout cassette was integrated homologously into the locus. Complementation cassettes were integrated into the endogenous locus and ectopically (2 and 3 bands). *V. longisporum* and *V. albo-atrum THI4* show same signals like *V. dahliae* wt. **(b)** 3'-probe: The complementation cassettes integrated in the locus and differ in size from the knockout cassette. All digestions of deletion and complementation strains were performed with *Apa*I.

Figure 8 shows Southern hybridizations of the transgenic fungi with probes of 5'- (Figure 8 a) and 3'- flanking regions (Figure 8 b). The signals for locus integrated *THI4* knockout cassette in *V. dahliae* (3.7 kb) show that the complementation cassette was integrated as well into the locus (same 2.6 kb signal like *Vd* wild type) as ectopically. The difference of the signal size

between complementation cassettes to the knockout cassette is shown in Figure 8 b. For heterologous complementation, the *V. dahliae* like *V. longisporum* isogene *VlTHI4-1* was integrated into the *V. dahliae* genome. This gene was found to be highly expressed in transcriptomical analyses in contrast to the *V. albo-atrum* like *VlTHI4-2* isogene which, was found to be low expressed.

The allodiploid *V. longisporum* wild type strain reveals *THI4* signals for both isogenes. With Southern hybridization using the 5'- and 3'-flanking region as probe it was shown that one signal matches to both, *V. dahliae* wild type and *V. albo-atrum* wild type signal size. The secong signal of *V. longisporum THI4* does not match to the *V. dahliae* or the *V. albo-atrum* signal of the gene. This is caused by sequence differences in the flanking regions of the isogenes. The *V. albo-atrum* wild type shows the same *THI4* signal as in *V. dahliae* wild type. This high sequence identity of 99% in the deduced *Verticillium Thi4* sequence is shown in Figure 6.

Deleting *VdTHI4* leads to viable mutants, which grow wild type like on thiamine containing complex media (pectin and casein rich simulated-xylem-medium (SXM) or potato dextrose agar (PDA)) in a spore amount of $5*10^6$ per plate (Figure 9). Likewise, no growth difference between Δ*THI4* strain and *Vd* wild type strain was detectable on different carbon sources (galactose, glucose, raffinose, mannose, fructose, cellulose and xylan) (data not shown).To complete the phenotypic analyses, the strains with reintroduced gene in the knockout were also tested in this growth assays and showed wild type-like growth likewise (Figure 9).

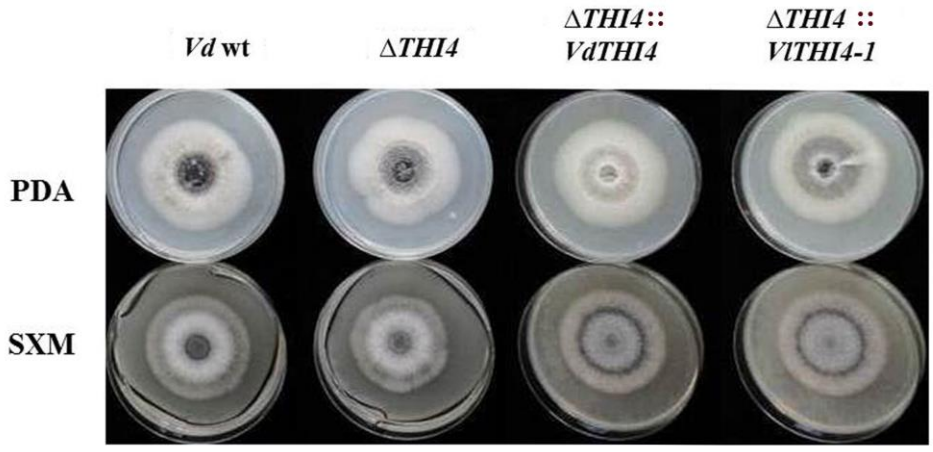

Figure 9: ***Vd*Δ*THI4*, Δ*THI4* :: *VdTHI4* and Δ*THI4* :: *VlTHI4-1* strains show wild type-like phenotype.** The *Vd*Δ*THI4* mutant shows no growth reduction or melanization defects on potato dextrose agar (PDA) and on simulated xylem medium (SXM) after 14 days incubation in light at 25°C using a spore inoculum of $5*10^6$ spores.

In order to screen for growth defects caused by the absence of thiamine, the Δ*THI4* strain was tested on thiamine free minimal medium (Czapek-Dox medium (CDM)) with low spore inoculum (10^4 to 10^1 spores). In comparison to the *Vd* wild type and to the complementation strains, the *Vd*Δ*THI4* mutant showed significant reduced growth in less spore amounts on CDM or on complex potato dextrose agar (PDA) according to Students t-test (Figure 10).

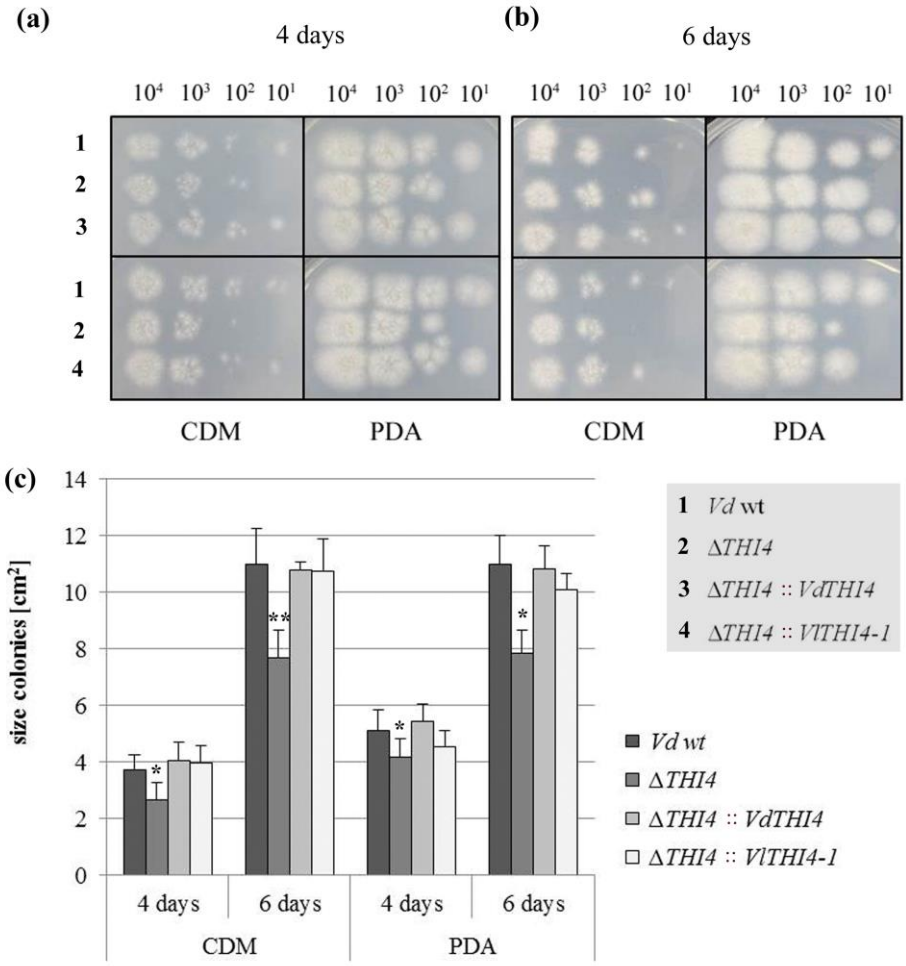

Figure 10: **Growth rate of *Vd*Δ*THI4* deletion strain in comparison to wild type *V. dahliae ex planta* and without supplemented thiamine visualizes a reduced growth phenotype using small spore inoculum. (a, b)** Δ*THI4* mutant shows significant reduced growth in low spore amounts on minimal (CDM) and complex (PDA) medium without thiamine supplementation. **(c)** Similar amounts of spores of *V. dahliae* wild type (*Vd* wt), *Vd*Δ*THI4* deletion strain (Δ*THI4*), and complemented deletions strains (Δ*THI4* :: *VdTHI4* and Δ*THI4* :: *VlTHI4-1)* incubated on minimal (CDM) or complex (PDA) media without thiamine supplementation. Colony sizes were measured after 4 or 6 days at 25°C. Reduced growth of the Δ*THI4* mutant strain (n=3) on CDM minimal medium in comparison to wild type corresponds to a P-value of 0.05 (*) after 4 days and 0.01 (**) after 6 days.

To reveal that VdThi4 is involved in the essential thiamine pathway, a complementation of the growth defect on thiamine free medium should be visible on thiamine supplemented plates. For *F. oxysporum* an auxotrophic phenotype on thiamine-free minimal medium in less amounts of plated spores is known that can be complemented by supplementation with 0.8 µg/ml thiamine (Ruiz-Roldan *et al.*, 2008). Thiamine supplementation of 0.2 µg/ml up to 2.0 µg/ml could restore growth defect of the *Vd*Δ*THI4* deletion strain (Figure 11 a, b), supporting a role of *Verticillium* Thi4 in thiamine biosynthesis. This is further strengthed when transcription for thiamine uptake was monitored. Besides synthesis of thiamine, the acquisition of exogenously available thiamine occurs in *S. cerevisiae* by the plasma membrane thiamine carrier Thi7 (Thi10) (Enjo *et al.*, 1997; Singleton, 1997). A bioinformatic screen by BLAST analysis indicated that the *S. cerevisiae* Thi7 transporter ortholog VDAG_03620.1 is the only ortholog with a putative thiamine carrier function in *Verticillium*. Real-time PCR analysis revealed that in *Verticillium dahliae* wild type strain, which is able to synthesize thiamine, VDAG_03620.1 is not expressed when supplementing no or 0.8 µg/ml thiamine (Figure 11 c). However, in the Δ*THI4* strain the transporter is four times higher expressed than in *Vd* wild type strain with and without thiamine. Expression is even more pronounced (>20 fold) when the *THI4* deletion strain is supplemented with 0.8 µg/ml thiamine.

Complementation of the *VdTHI4* knockout was performed to exclude deletion-derived genetic side effects. Integration of the complementation cassette ectopically or at the endogenous locus restored the mutant growth defect (Figure 10 and Figure 11).

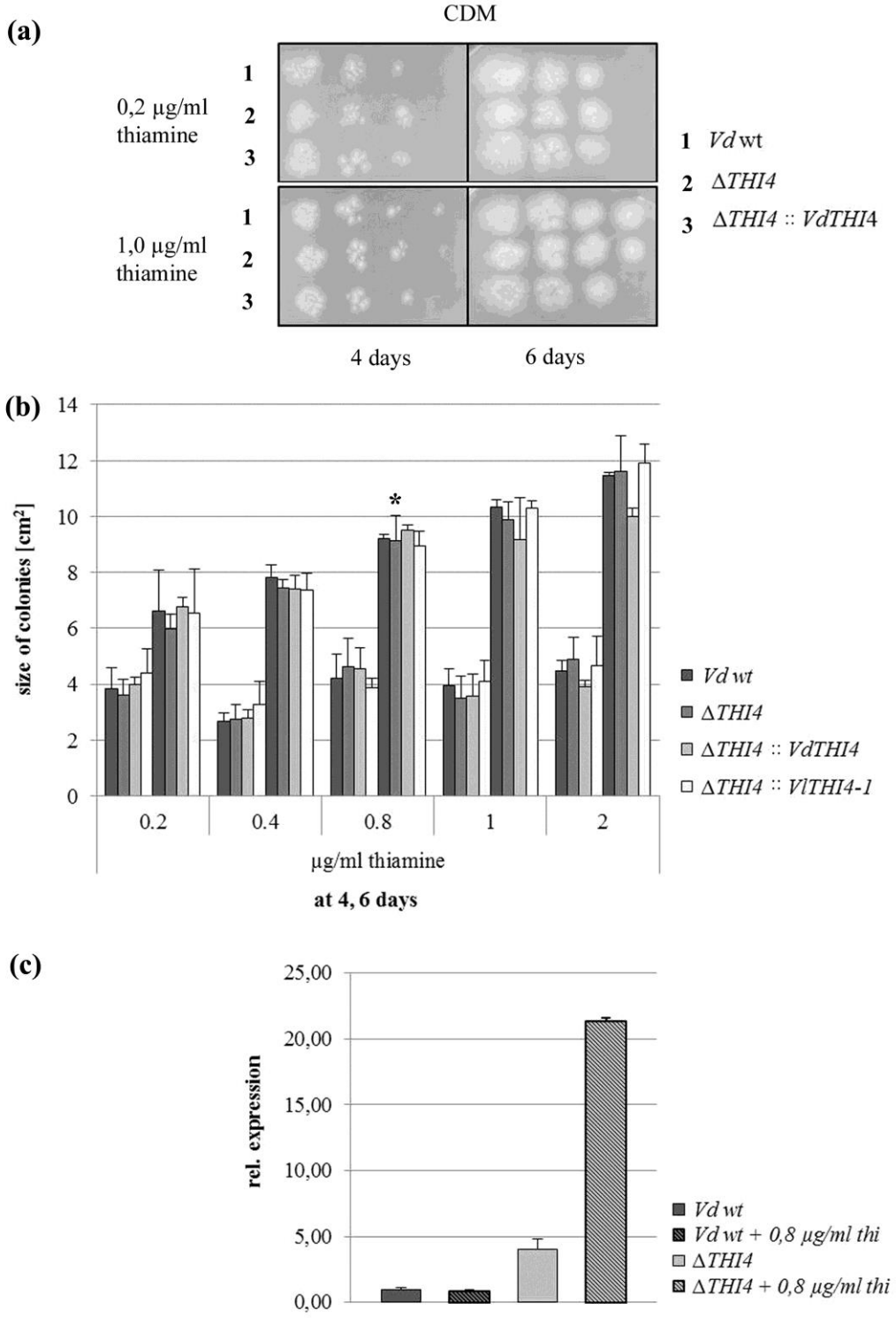

Figure 11: ***VdΔTHI4* is involved in thiamine pathway. (a)** Reduced growth of Δ*THI4* on minimal CDM medium is complemented by supplementation of 0.2 to 2.0 µg/ml thiamine. **(b)** Quantification of colonies sizes of *Vd* wt, Δ*THI4*, Δ*THI4* :: *VdTHI4* and Δ*THI4* :: *VlTHI4*-1 on thiamine supplemented CDM medium (0.2 – 2.0 µg/ml) after 4 and 6 days. No significant growth difference is detectable on thiamine supplemented plates of *Vd* wt and Δ*THI4* anymore. The growth experiment was repeated three times. Plates were incubated for 4 to 6 days at 25°C. **(c)** Expression level of thiamine transporter VDAG_03620.1 in *VdΔTHI4* and *Vd* wt strain in thiamine free and thiamine supplemented CDM medium. Relative gene expression is measured versus H2A after 7 days of growth, n=3. VDAG_03620.1 transporter is not expressed in *Vd* wt with and without thiamine (first two columns). The *VdΔTHI4* strain shows four times increased expression of the thiamine transporter VDAG_03620.1 in thiamine free CDM medium (third column) and high expression (more than 20 times) in thiamine supplemented CDM (fourth column).

3.1.2 *Verticillium* Thi4p is localized in mitochondria

The *S. cerevisiae* Thi4p, which includes a mitochondrial target site, was predicted by sequence to be localized in the mitochondria (Machado *et al.*, 1996), but so far only a cytosolic localization pattern has been shown (Mojzita & Hohmann, 2006). A sGfp (synthetic green fluorescent protein) was fused C-terminally to VdThi4 to visualize the localization of the protein in the plant pathogen by fluorescence microscopy. The cassette included the native promoter of *THI4* (Figure 12). It was integrated into the *THI4* locus in the genome of *V. dahliae* (Figure 12) by protoplastation, resulting in a phenotype described below.

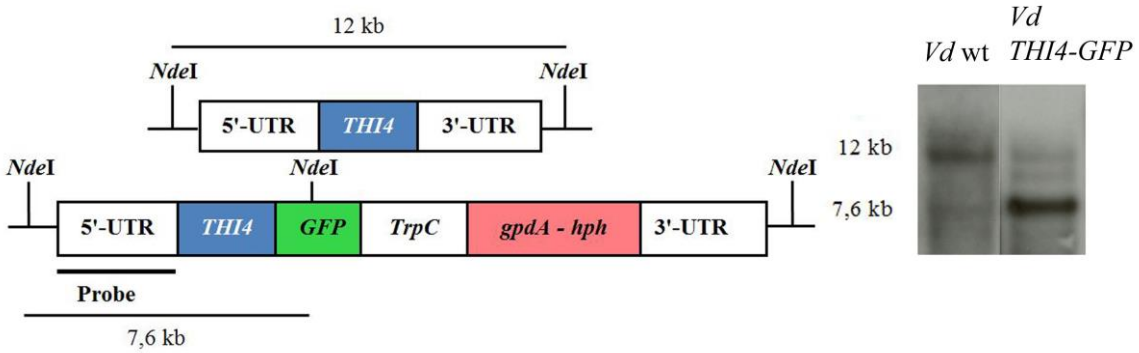

Figure 12: **Restriction map and Southern hybridization of *THI4* - *GFP* strain.** *GFP* is under the native promotor of *V. dahliae THI4*. Homologous insertion of the cassette into the locus was achieved via protoplastation transformation method. Digestion with *Nde*I was performed to verify the endogenous integration.

The N-terminal region of the *V. dahliae* Thi4 sequence includes positively charged amino acids, which are a typical feature of mitochondrial target sites. *V. dahliae* Thi4 localization was predicted by YLoc+ (Briesemeister *et al.*, 2010) to be partially in the mitochondria or in the nucleus.

Fluorescence microscopy of the Gfp-tagged *V. dahliae* Thi4 strain revealed the localization in the mitochondria (Figure 13 a). This was visualized by the green Thi4-Gfp signal that merges with the red signal of the MitoTracker® stained mitochondria in yellow color. As a control the stained mitochondria were visualized as red dots in the *V. dahliae* Gfp control strain with Gfp stained cytosol (Figure 13 b).

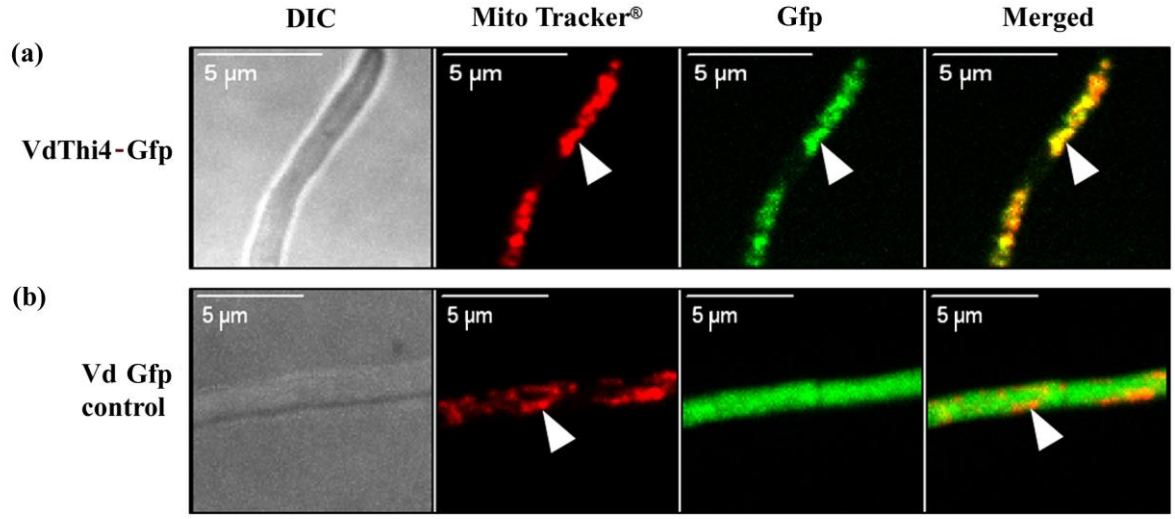

Figure 13: Mitochondrial localization of C-terminal Gfp-tagged Thi4 in *Verticillium dahliae*. Localization of C-terminal Gfp-tagged VdThi4 was detected by fluorescence microscopy. The Gfp signal is shown in green; mitochondria were stained with 50 nM MitoTracker® and are visible in red (white arrow). **(a)** The VdThi4 - Gfp strain visualizes the localization of *V. dahliae* Thi4 in the mitochondria. The green Gfp signals of VdThi4 - Gfp merges with the stained mitochondria red signals, visualized in yellow color. **(b)** *V.dahliae* Gfp control strain with Gfp fluorescent cytosol and stained mitochondria. Liquid cultures were grown for 5 days at 25°C.

3.1.3 DNA damage repair and oxidative stress response is affected by *Verticillium* Thi4

Verticillium Thi4 was shown to be involved in thiamine pathway (Figure 11). Homologues of the gene in other organisms are important for more than their role in the thiamine pathway. Yeast Thi4p for example is proposed to play a dual role. Besides its role in thiamine biosynthesis it is involved in maintenance of mitochondrial genome stability (Machado *et al.*, 1997). In *V. dahliae* it was shown that Thi4 is localized in the mitochondria (Figure 13), based on this fact experiments for a likewise involvement in mitochondrial genome stability were performed to estimate a further function of the protein. The repair of UV damaged DNA was estimated by survival experiments after UV-B light treatment. 1000 cells per plate were inoculated on minimal medium and treated with UV-light. Subsequently the survival rate was estimated by counting fungal colonies (Figure 14).

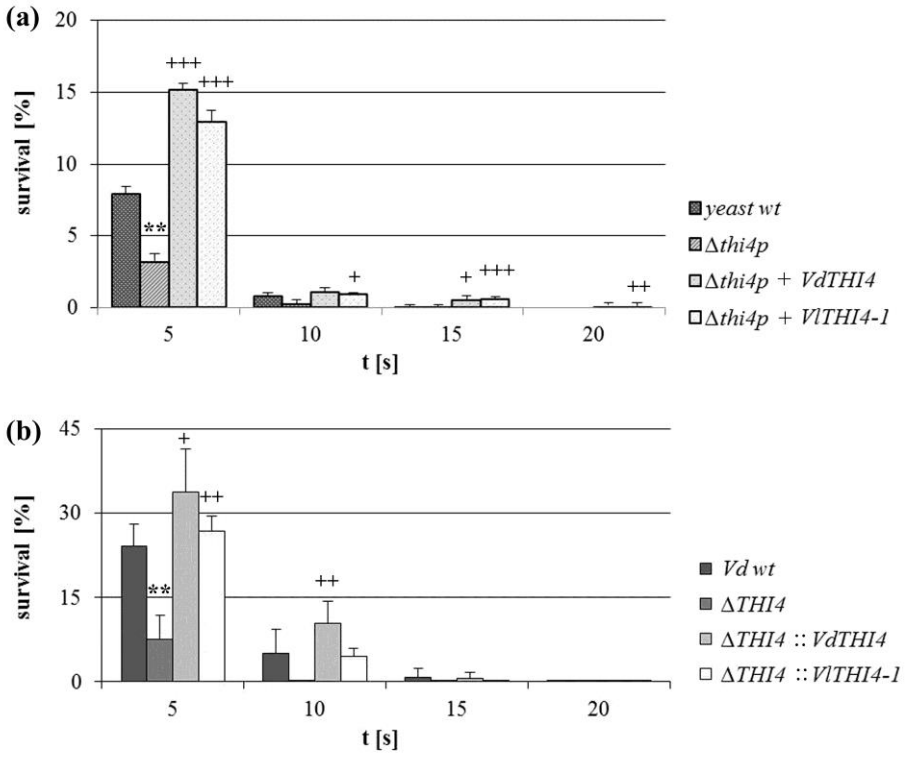

Figure 14: **UV-illumination assay.** Survival rate in percent of Yeast and *Verticillium* growing colonies after treatment with UV-light (302 nm) for 5, 10, 15 and 20 s. 3 plates per condition were used, 0 s accords to 100% **(a)** More colonies (12-15%) of yeast Δ*thi4* strain complemented with *Verticillium* DNA were growing compared to Δ*thi4* strain (3%). Growth difference is highly significant at 5 sec time point. *Verticillium* DNA containing yeast Δ*thi4* mutants growing better after UV-treatment than wild type yeast strain BY4741. Colonies were counted after 3 days incubation at 30°C. (n=3) **(b)** Growing *V. dahliae* colonies after treatment with UV-light (302 nm) for 5, 10, 15 and 20 s. More colonies of Δ*THI4* complementation strains were growing compared to Δ*THI4* mutant. The growth difference is significant at 5 s time point. Colonies were counted after 4 days incubation at 25°C (n=3). P-value 0.001 = highly significant *** or +++, 0.01 = significant ** or ++ and 0.05 = less significant * or + (significance: * to *Vd* wt; + to Δ*THI4*).

Survival after UV-treatment, affected by the existence or absence of *Vd* or *VlTHI4*, was tested in *S. cerevisiae* and *V. dahliae*. The tests revealed that *Verticillium THI4* compensates the lethal effect caused by UV-light in the *Vd*Δ*THI4* and the yeast Δ*thi4* strains.

Only 3% of the UV exposed colonies of the yeast Δ*thi4* strain survived (Figure 14 a) after 5 s of treatment (0 s UV-exposure accords to 100% growth). In contrast, 12 to 15% colonies of the *Verticillium THI4* complemented strains were surviving under these conditions. The effect on UV-light treated *V. dahliae* strains was comparable to yeast wild tpye. 24% of the *Vd* wild type colonies were surviving in comparison to mutant strains (7% surviving colonies) and the complemented strains (26-33% surviving colonies) (Figure 14 b). The colonies on plate were counted after four days but plates were incubated up to seven days. By this it was excluded that the growth difference was an effect caused by slower growing of the *THI4* deletion strain.

Thiamine plays an important role in oxidative stress response (Ahn *et al.*, 2005; Rapala-Kozik *et al.*, 2008; Rapala-Kozik *et al.*, 2012; Tunc-Ozdemir *et al.*, 2009). In previous studies on cellular lines it was shown that oxidative stress can lead to the degradation of mtDNA and the inhibition of base excision repair (Shokolenko *et al.*, 2009). In order to screen for oxidative stress-response of the Δ*THI4* mutant, growth tests on oxidative stress inducing agents were performed (Figure 15). In the cell oxidative stress always leads to stress in the mitochondria likewise, where *Verticillium* Thi4 is localized (Figure 13).

For the *F. oxysporum* homolog Δ*sti35* mutant it was shown, that it has a reduced growth on 0.001% menadione containing plates (Ruiz-Roldan *et al.*, 2008). A similar growth defect was monitored for *Vd*Δ*THI4* mutant strains in comparison to *V. dahliae* wild type during menadione-mediated oxidative stress (Figure 15 marked in red).

Furthermore, the antibiotic 2,4-Diacetylphloroglucinol (2,4-DAPG) produced by *Pseudomonas fluorescens* was tested in this study for putative inducing oxidative stress on the *Vd*Δ*THI4* strain. In *S. cerevisiae* it was shown that this affects multiple basic cellular processes, including membrane function, reactive oxygen regulation and cell homeostasis (Kwak *et al.*, 2011). We could reveal that the oxidative stress activating *P. fluorescens* antibiotic 2,4-DAPG affected fungal growth of both strains, the mutant and the wild type in same extent (Figure 15 marked in red). No growth difference or defect occurs on complete medium for both oxidative activating reagents.

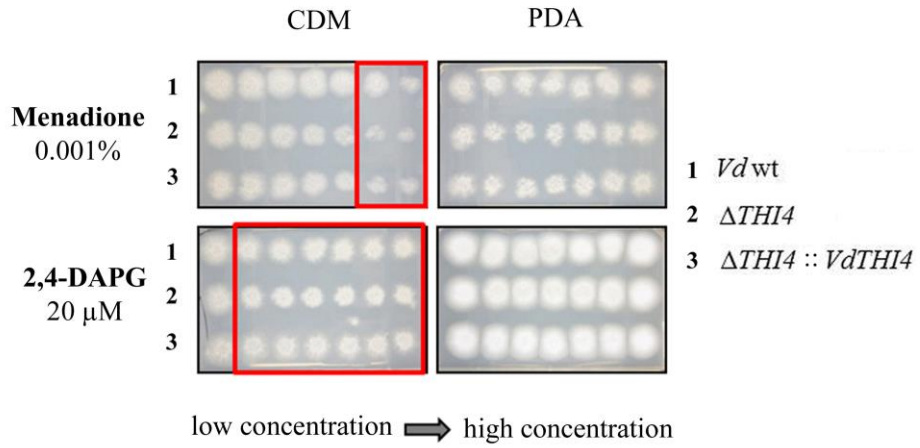

Figure 15: **Oxidative stress tests on gradient plates.** Under oxidative stress conditions (0.001% menadione) the deletion strain *Vd*Δ*THI4* exhibits reduced growth in comparison to *Vd* wt on CDM agar (indicated by red rectangle). The stress inducing antibiotic 2,4-DAPG induces growth reduction of both, *Vd* wt and *Vd*Δ*THI4* mutant strain on synthetic CDM medium (indicated by red rectangle). The stressors menadione and 2,4-DAPG induced no growth reduction phenotype on PDA medium. The experiments were performed with two different *Vd*Δ*THI4* transformants with the same effect. Gradient plates were used with low concentration (0%, µg left) and high concentration (0,001%, 20µg right). Spore amount: 10^4 spores. Plates were incubated at 25°C for 7 days.

The response of the fungus to reactive oxygen species is important for the plant-pathogen interaction. Hence, testing the Thi4 lacking strain with reduced tolerance to DNA damage agents (UV or menadione) in a plant infection assay *in vivo* inside the plant in the xylem-sap was the following experiment in this study.

3.1.4 *Verticillium* Thi4 is involved in plant pathogenicity

Verticillium is a plant pathogenic fungus with a not completely known infection process and growth behavior inside the host. To investigate the importance of the putative thiazole synthetic protein VdThi4 for the fungus infection of the plant or for pathogenic abilities, a plant infection assay was performed. Hereby three possible events can occur. First, the fungus cannot enter through the roots, so is not infecting the plants. The second possibility is that the fungus infects the plant by entering through the root cortex, but is not pathogenic anymore and causes no stunting symptoms. And the third possibility is a not affected infection and wild type like pathogenic phenotype on the host plants. These effects can be influenced by the uptake of the extracellular thiamine from the xylem-sap. Xylem-sap induces catalase peroxidase in *V. longisporum* (Singh *et al.*, 2012), suggesting that the response of the fungus to reactive oxygen species is important for the interaction between plant and fungus. In contrast, knockout strains of the homologous *F. oxysporum sti35* strain did not reduce pathogenicity to tomato or cucumber plants (Ruiz-Roldan *et al.*, 2008; Thanonkeo *et al.*, 2000). It is interesting to investigate, if lacking VdThi4 affects the pathogenicity on host plants.

Seven days after the infection of *S. lycopersicum* plants with *Verticillium* no obvious difference in size between non-infected mock plants, and the *THI4* deletion or complementation strains infected plants, was detectable (Figure 16 a). A difference became visible after 14 days post infection (dpi) and increased by time. At 28 dpi, the complementation strains infected plants showed a stunted phenotype like the *V. dahliae* wild type infected plants (Figure 16 a, b). These plants show stunting symptoms with very small stems and small leaves. In contrast to that, the *THI4* deletion strain infected plants show no stunting symptoms as also observed for non-infected plants, but qPCR analysis demonstrated fungal presence in the infected plants in a quarter of the amount of *Vd* wild type plants (Figure 16 c). The phenotype of those plants impairs a loss of pathogenic function of the strain.

To verify invasion of *V. dahliae* into infected plants, outgrowing assays from stem sections of infected plant material were performed. All strains (wild type, knockout and complementation strains) were able to colonize the infected plants (Figure 16 b). From non-infected mock stems no fungus was growing out. Fungus grew out of the *Vd*Δ*THI4* infected material.The fungus colonized the host without symptoms, because the plants show a healthy phenotype with stem heights nearly similar to the non-infected plants. The fungal phenotypes look like *V. dahliae* wild type in hyphal growing and melanization. The outgrowing of the fungus from the infected plant material occurs slowly and the plates were incubated for 14 days.

In order to estimate if the deletion strain enters the hosts like *V. dahliae* wild type or if the fungus is not able to enter the plants, the amount of fungal DNA from infected plants was quantified by real-time PCR using internal transcribed spacer ITS1 rDNA primers of *V. dahliae* in a defined amount of plant DNA (25 ng) from infected plants (Figure 16 c). Infected plant material of *V. dahliae* wild type or the complemented strain revealed significantly more fungal DNA than *Vd*Δ*THI4* infected material. With 0.1 ng in 25 ng DNA in the *Vd*Δ*THI4* deletion strain compared to 0.4 ng in *V. dahliae* wild type, the amount is reduced to one quater. In plants infected with complemented strains, the yield of fungal DNA is lower than in *V. dahliae* wild type infected. Except the roots of Δ*THI4* :: *VlTHI4-1* infected *S. lycopersicum*, where the measured fungal DNA amount appropriates with 0.4 ng to *Vd* wild type.

For both, the plant height and the measured fungal amount, no differences are visible between the *V. dahliae* complemented or the *V. longisporum* homologous complemented strains. Both behave like the *V. dahliae* wild type. Measuring the fungal amount of the roots is a hint for fungal infection but could be affected by fungal adhering outside to the epidermis of the root cells.

Summing up the results of the plant infection assay, the *V. dahliae THI4* deletion strain still infects *S. lycopersicum* plants. The infected plants showed phenotypes approximately like the non-infected plants with clearly reduced symptoms of infection, like stunting. The data support that *Verticillium* Thi4 is not only required for thiamine biosynthesis and oxidative stress response, but also for successful and efficient infection of tomato host plants and to induce pathogenicity.

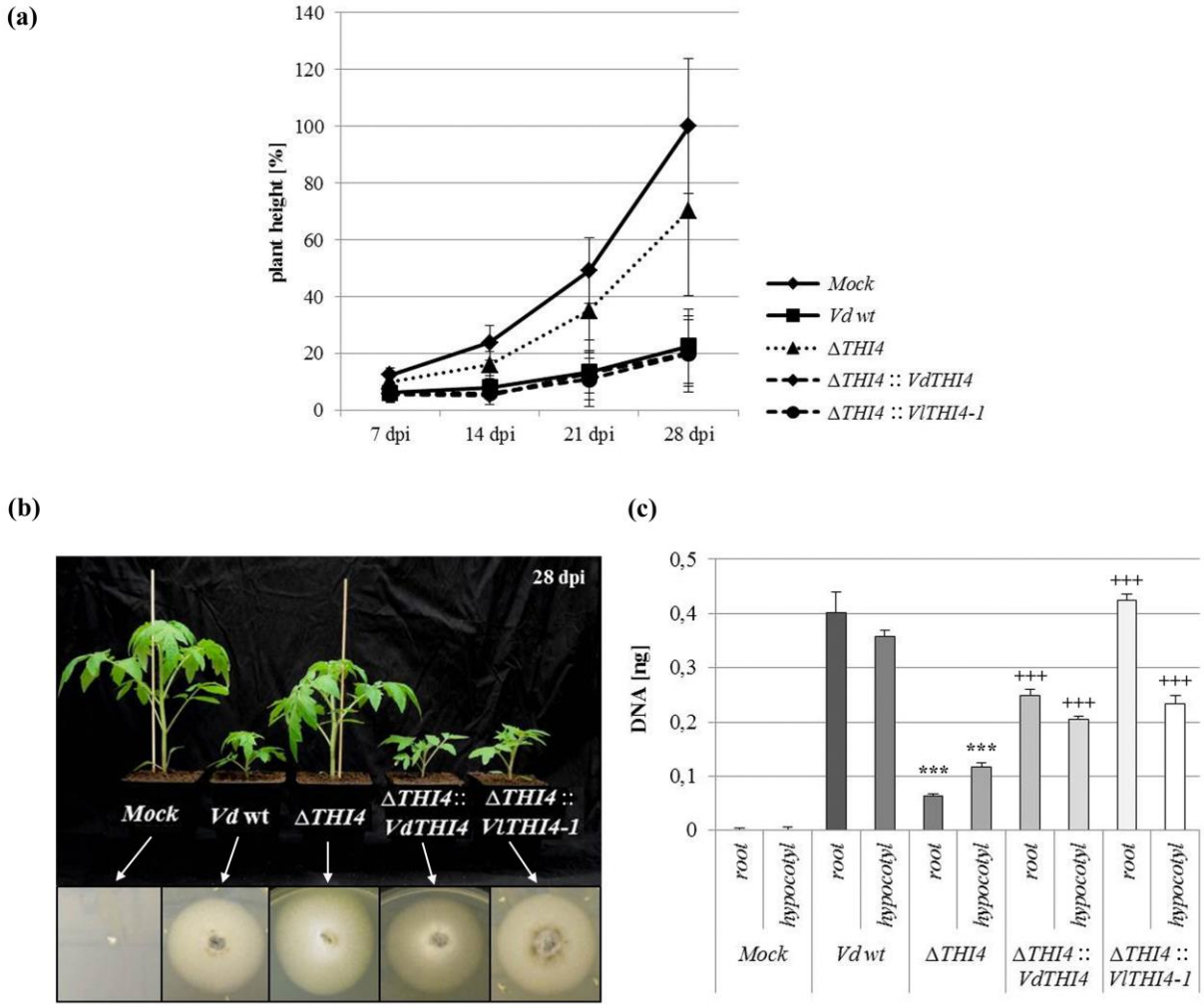

Figure 16: **Plant infection assay. (a, b upper part)** Growth of *S. lycopersicum* plants infected with *Vd* wt, Δ*THI4*, Δ*THI4* :: *VdTHI4* and Δ*THI4* :: *VlTHI4-1* for 28 days. 15 plants were used for each infection condition. Plants were infected by root dipping for 35 min with $1*10^6$ spores/ml and additional watering of the plants with 1.5 ml spores (mock control was treated with water). Growth occurs under long-day-conditions (16 h light / 8 h dark) at 22°C and plant heights were measured after 7, 14, 21 and 28 dpi. Plants infected with deletion strain Δ*THI4* grew like the non-infected mock plants. Complementation strains infected plants grew like wild type infected plants. All results are highly significant (***, +++) with a student's-test P-value of > 0.001. Infection assay was tested n=2 with two mutants. **(b lower part)** *Vd* grew out of stem pieces on PDA plates containing chloramphenicol (35 mg/ml). From both, Δ*THI4* deletion and complementation infected plant material; *Vd* grew out of the plant pieces identical to *V. dahliae* wild type infection. Plates were incubated for 14 days at 25°C. **(c)** Quantification of fungal DNA in 25 ng extracted plant DNA of infected plants after 28 dpi. PCR was performed with fungal specific ITS1 OLG70/71 primers (Eynck *et al.*, 2007). *Vd*Δ*THI4* strain infected plants contain four times less DNA than wt infected plants. Complemented strains infected plants have double up to four times DNA amount compared to deletion strain. All results are highly significant (***, +++) with a P-value of 0.001 (P-value calculations: 1. * = calculation in comparison to wt and 2. + = calculation in comparison to Δ*THI4*) n = 5.

3.2 Secreted *Verticillium dahliae* Pa14_2 protein is involved in infection process

A PA14_2 domain containing protein was identified in the exoproteome of *Verticillium longisporum* 43. This Pa14_2 called, putative secreted protein was analyzed by a knockout in a *Verticillium dahliae* strain. In the transcriptome, the transcript was detected to be needed in small amounts by the fungus for growth under different conditions. It is same less expressed in fungal *in situ* cultivation in xylem-sap of *Brassica napus*, and in *in-vitro* cultivation in SXM.

The PA14_2 domain was found in fungal adhesins, and it is related to the lectin-like ligand-binding PA14 domain of fungal adhesins (Linder & Gustafsson, 2008; Rigden *et al.*, 2004) like the *S. cerevisiae FLO1, FLO5, FLO9 and FLO10* genes (Kobayashi *et al.*, 1998; Rigden *et al.*, 2004; Zupancic *et al.*, 2008). The VdPA14_2 gene was chosen for analysis in this study, by the reason that originally the aim was to identify and characterize adhesive activities of *Verticillium* during the infection process of the host plants. Hence, putative adhesive abilities of *V. dahliae* and *V. longisporum* PA14_2 were screened in the non-adhesive *S. cerevisiae* Δ*flo8* strain for complementation of the adhesion. Lacking the transcription factor Flo8, the yeast looses the ability to adhere to surfaces or to make focculation. This could be complemented heterologous by genes encoding for proteins causing either directly adhesion or flocculation (like *FLO1*, *FLO5*, *FLO9*, *FLO10*). Or by genes, which replace the transcription factor that enables the yeast to produce its own adhesive proteins. However, no adhesion or flocculation in the yeast Δ*flo8* strain, caused by the *Verticillium PA14_2* genes, could be observed (data not shown). During this study it points out that VdPa14_2 is *Verticillium* specific and involved in other cellular processes.

BLAST analysis revealed that the protein is not well conserved and specific for *Verticillium* except the functional domain, which shows similarity of 38% to hypothetical proteins in the phytopathogenic fungi *Colloetrichium gloeospoioides Nara* and *Gaeumannomyces graminis var. Tritici*.

SignalP predicts that the *Verticillium* Pa14_2 has a signal peptide cleavage site between the amino acids 16 and 17 (Figure 17 marked in red), suggesting that the protein can be secreted. Furthermore, sequence analyses revealed an N-terminal insertion (marked in green) and the GLEYA sequence (marked in yellow), which is not included in the PA14_2 domain. The PA14_2 domain itself (marked with blue background) is C-terminally located in the protein. By performing an alignment of the deduced amino acid sequence (Figure 17) and Southern

hybridization (Figure 22) it was discovered that only one isogene exists in *V. longisporum* 43 named *VlPA14_2-1*.

Figure 17: **Alignment of deduced amino acid *Verticillium* Pa14_2 sequence.** *V. dahliae* VdPa14_2 (VDAG_03374.1 (BROAD) modified after resequencing)) and *V. albo-atrum* VaaPa14_2 (VDBG_06221.1 (BROAD) modified after resequencing)) were aligned with *V. longisporum* VlPa14_2-1. Sequences are with 99% identity highly similar. The sequences contain N-terminally a signal peptide cleavage site (red, red arrow). The sequencing analysis revealed that the *Verticillium* Pa14_2 contains N-terminal a sequence insertion (green). Within the protein the PA14_2 domain is C-terminally localized (blue background). The GLEYA domain (yellow) is not included in the PA14-like PA14_2 domain. Analysis performed with ClustalW2 (http://www.ebi.ac.uk/Tools/msa/clustalw2/).

3.2.1 The *VdPA14_2* knockout is deficient in black colored microsclerotia formation

In order to investigate the function of *V. dahliae PA14_2*, a knockout was constructed to investigate its role *ex planta* by different growth tests before the strain was tested *in planta* for pathogenicity on *Solanum lycopersicum* plants.

Screening for a *VdPA14_2* mutant, 44 transformants in total, from ATMT (25) and protoplastation transformation (19) were tested, to find two positive clones only by the protoplastation based method. One of those clones was used for further analyses. The complementation of *VdPA14_2* deletion was also performed via protoplastation based

transformation method. For homologous and heterologous integration 17 respectively 22 transformants from both, one transformation, were testet, and 10 respectively 5 positive clones were found.

Southern hybridizations with probes of 5'- and 3'-prime flanking regions (Figure 18 a and b) showed signals for the locus integrated *PA14_2* knockout cassette in *V. dahliae* as well as the locus and ectopically inserted complementation cassettes (two signals). The difference of the signal size between the complementation-cassettes (3.5 kb) and *Vd* wild type (0.9 kb and 4.6 kb) is visualized in Figure 18 b to confirm the integration. *V. longisporum* shows only one signal for *PA14_2* with the same size (3.8 kb) like *Vd* wild type and *V. albo-atrum* wild type. Also the flanking regions are highly similar in their sequences (shown in Figure 6), resulting in this same restriction pattern.

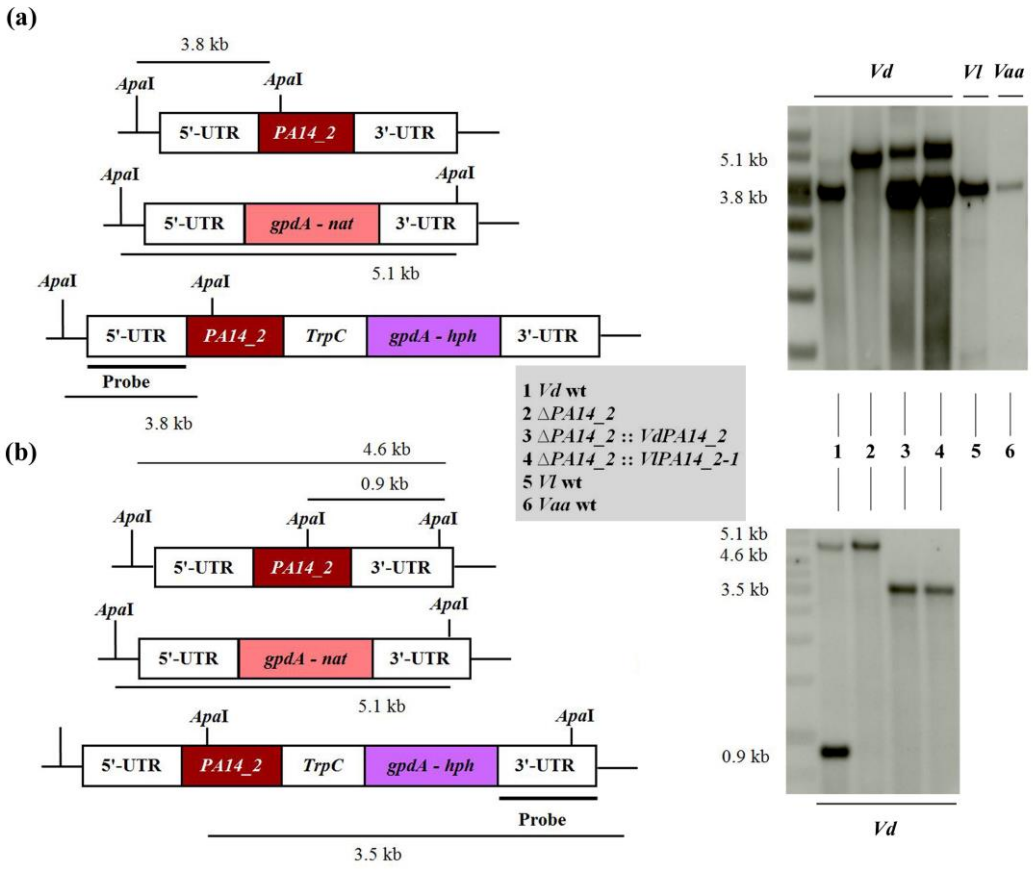

Figure 18: **Southern hybridization of *VdPA14_2* wt, Δ*PA14_2*, Δ*PA14_2* :: *VdPA14_2* and Δ*PA14_2* :: *VlPA14_-1l*, *Vl* wt and *Vaa* wt. (a)** 5'-probe: Knockout cassette is integrated into the endogenous locus. The complementation cassettes were integrated into the endogenous locus as well as ectopically (2 times, shown in lane 3 and 4). *V. longisporum* and *V. albo-atrum THI4* show bands of the same size as *V. dahliae* wt. Only one signal occurs for *V. longisporum* wt. **(b)** 3'-probe: The complementation cassettes differ in size from the knockout cassette. All digestions of deletion and complementation strains were performed with *Apa*I.

The deletion of the *V. dahliae PA14_2* leads to viable mutants, which show no growth deficiency in colony size compared to *V. dahliae* wt growing in low and in high spore inoculum on complex medium (potato dextrose agar (PDA)) and on minimal medium (Czapek-Dox medium (CDM)). Indeed, the *VdΔPA14_2* deletion strain is defective in melanization. No black color of the melanized hyphae could be observed even after 14 days (Figure 19). To complete the phenotypic analyses a homologous complementation of the knockout by *VdPA14_2* and heterologous complementation by *VlPA14_2-1* gene were performed. These strains with two integrated copies (one endogenous, one ectopically) of reintroduced *PA14_2* genes (see 2.4.2) show weak melanization again (Figure 19 red arrows) when growing on complex PDA medium. This implicates that the knockout of *VdPA14_2* is complemented only partially.

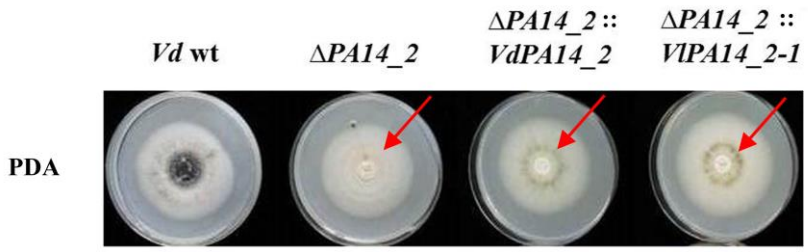

Figure 19: Phenotype of *Vd* wt, *VdΔPA14_2*, *ΔPA14_2* :: *VdPA14_2* and *ΔPA14_2* :: *VlPA14_2-1*. *VdΔPA14_2* mutant grows without black colored melanized hyphae on PDA plates. The *PA14_2* complemented strains melanize again (red arrow). The used spore amount is $5*10^6$, cultivation conditions: 14 days in light at 25°C.

Loss of the black melanin color in the *VdPA14_2* mutants could be a genetic side effect or a result of a function of the protein in melanin synthesis. Fungal melanin is produced by polyketide biosynthesis. The 1,8-dihydroxynaphthalene (DHN) melanin is the major color determinant and this type of melanin is widely distributed among ascomycetous fungi like *Verticillium* (Bell & Wheeler, 1986). DHN for melanin synthesis is made from 1,3,6,8-tetrahydroxynaphthalene (THN), which is assembled by a polyketide route (Fujii *et al.*, 2000; Fulton *et al.*, 1999; Takano *et al.*, 1995).

A defect in melanization production was detectable by qPCR expression patterns of the polyketide synthase 1 (*PKS1)* gene of *Verticillium* in the deletion strain.

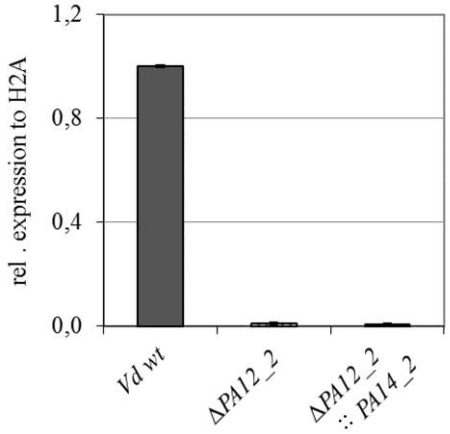

Figure 20: ***PKS1* expression is not detectable in Δ*PA14_2* mutant and in Δ*PA14_2* :: *VdPA14_2*.** In hyphae of 21 day old mutant and in complementation strains no *PKS1* expression is detectable by qPCR (n=3).

The analysis of 21 days old *VdΔPA14_2* strain hyphae reveals that the *PKS1* gene, which is essential for melanin biosynthesis, is not expressed (Figure 20). Interestingly, *PKS1* is not expressed in the not completely black colored complementation strains either.

The loss of back melanin in the *V. dahliae* Δ*PA14_2* deletion strain could complicate the growth of the fungus inside the soil during infection and inside the host. The infection through the roots will be analyzed in a plant infection assay. A deficient growing inside the host could lead to growth reduction or reduction in pathogenicity. When growing inside the host or in the soil the phytopathogenic fungus has access to different carbon sources in its natural environment. In a growth assay, some of potentially occurring carbon sources were tested if they could be utilized by the *VdPA14_2* deletion strain (Figure 21).

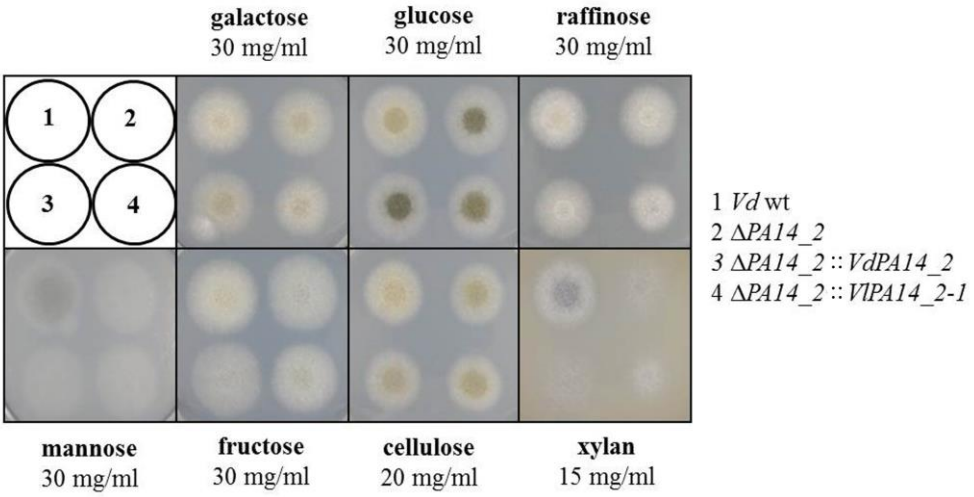

Figure 21: **Growth on different carbon sources of *Vd* wt, Δ*PA14_2*, Δ*PA14_2* :: *VdPA14_2 and* Δ*PA14_2* :: *VlPA14_2-1*.** On minimal CDM medium with different carbon sources the *VdΔPA14_2* mutant and complementation strains show different colored phenotype on glucose, mannose, cellulose and xylan compared to *Vd* wt. *VdΔPA14_2* :: *VlPA14_2-1* heterologous complemented strain grows less on fructose and raffinose. Used spore amount was $5*10^4$ spores and incubation time was 7 days at 25°C (n=3).

The phenotypic growth analyses with different carbon sources (galactose, glucose, raffinose, mannose, fructose, cellulose, lignin and xylan) (Figure 21) revealed growth phenotypes of the *Pa14_2* deletion strain that differ from *Vd* wt in colony color. On glucose, mannose, cellulose and xylan containing media, the *PA14_2* knockout strain and the complementation strains (with the two gene copies) have the same colony color, which differ from *Vd* wild type. This color difference was also shown for black melanin (Figure 19) and confirms the partial complementation.

3.2.2 *Verticillium* Pa14_2 is localized at the fungal membrane

The VdPa14_2 protein deduced sequence contains a peptide cleavage site and is predicted to be secreted, but does not contain a GPI anchor signal. It was shown that the GLEYA domain (PA14_2 domain) containing family of adhesins does not appear to be dependent on C-terminal GPI (glycosyl phosphatidyl inositol) anchors for their attachment to the cell wall. In addition, the C-terminal location of their ligand-binding domains would suggest an alternative form of cell wall attachment (Linder & Gustafsson, 2008). A *sGfp* (synthetic green fluorescent protein) was fused C-terminally to Pa14_2 to analyze the localization pattern of the protein in the plant pathogen by fluorescence microscopy.

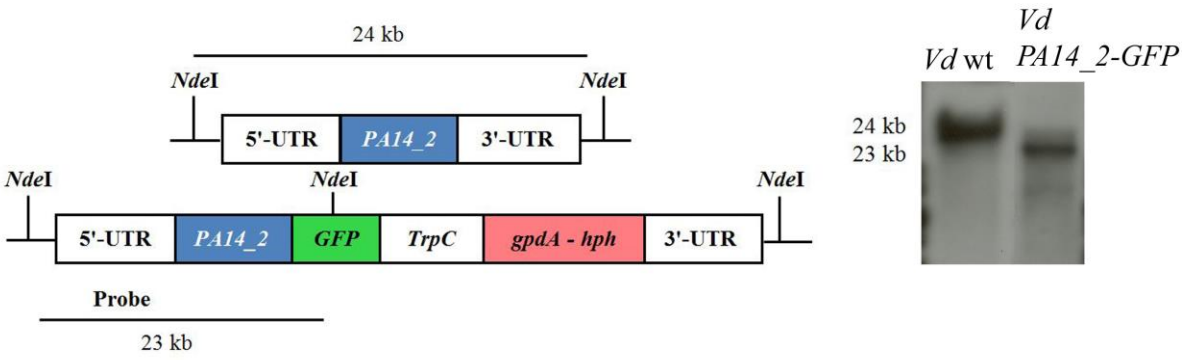

Figure 22: **Restriction map and Southern hybridization of *PA14_2* - *GFP* strain.** GFP is under the native promotor of *V. dahliae PA14_2*. Homologous insertion of the cassette into the locus was performed via protoplastation based transformation method. Restriction was performed with *Nde*I enzyme.

The *VdPA14_2 - GFP* cassette including the native promoter of *PA14_2* was integrated into the genome of *V. dahliae* by protoplastation (Figure 22). Fluorescence microscopy analysis of the Gfp-tagged Pa14_2 revealed a localisation of the protein at the fungal membrane (Figure 23 a). A co-localization between the green fluorescent Pa14_2 signal and the red signal of the plasma membrane stained with FM®4-64 was observed and visualized in yellow color.

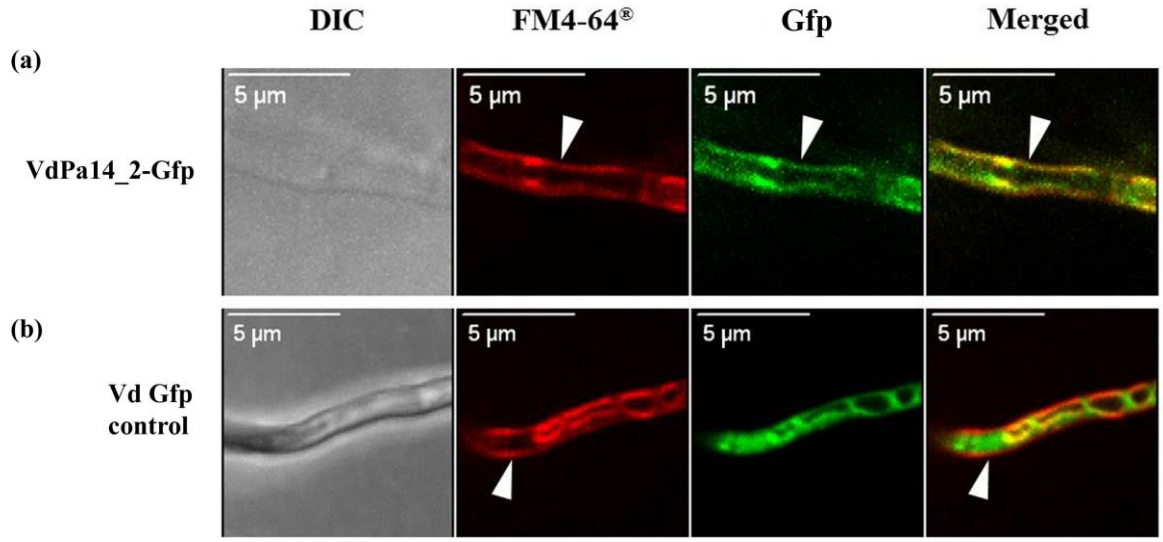

Figure 23: **Plasma membrane localization of C-terminal Gfp-tagged Pa14_2 in *Verticillium dahliae*.** Localization of C-terminal Gfp-tagged Pa14_2 was detected by fluorescence microscopy. The Gfp signal is shown in green; plasma membrane was stained with 1.25 µM FM®4-64 and is visible in red. **(a)** The VdPa14_2-Gfp strain visualizes the localization of *V. dahliae* Pa14_2 at the fungal plasma membrane. The green Gfp signals of VdPa14_2 - Gfp merges with the red stained plasma membrane signals, visualized in yellow color. **(b)** *V.dahliae* Gfp control strain with Gfp fluorescent cytosol and stained plasma membrane. Liquid cultures were grown for 5 days at 25°C.

3.2.3 *Verticillium* Pa14_2 increases oxidative stress in the cell

The membrane bound protein Pa14_2 was shown to affect the production of black colored melanin in *V. dahliae* (Figure 19). Additionally, a loss of function of this protein mediates changes in the plasma membrane and could result in effects on stress inducing media. For functional analyses of the Pa14_2 protein, the deletion strain was tested for response to oxidative stress induced by 0.001% menadione (Figure 24), and for cell wall stress induced by 0.01% SDS.

The experiment reveals *PA14_2* mutant to show better colony growth than *Vd* wt (marked in red) on 0.001% oxidative stress inducing menadione containing minimal CDM and complete

PDB medium containing after 7 days. In contrast, all strains were equally unable to grow on concentrations of 0.01% SDS in CDM medium, but on PDB all strains grew without deficiencies (data not shown). These findings point out that for the black colored melanin formation required Pa14_2 increases oxidative stress in the cell.

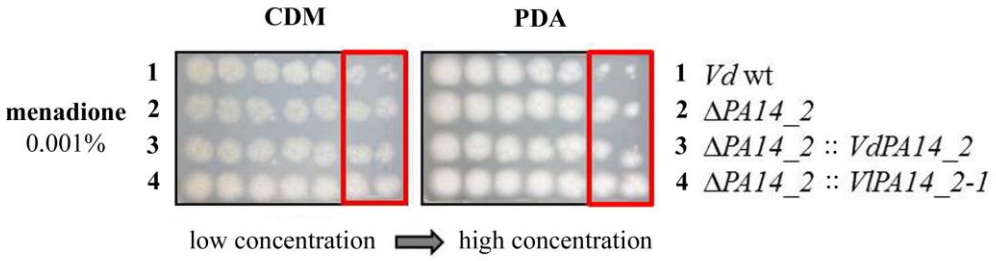

Figure 24: **Stress tests for oxidative and cell wall stress on gradient plates.** Under oxidative stress conditions (0.001% menadione) the *Vd* wt exhibits reduced growth in comparison to *VdPA14_2* deletion strain on CDM and PDA agar (red rectangle). Tests were performed n=2 with the same effect. Gradient plates were used with low concentration (left) and high concentration (right). Spore amount of 10^4 spores. Plates were incubated at 25°C for 7 days.

3.2.4 *Verticillium* Pa14_2 is involved in the infection process of the host

The infection process of the plant vascular pathogen *Verticillium* is not completely known until now. To investigate if the membrane bound VdPa14_2 protein plays a role in the infection process on the plant or for pathogenic abilities; a plant infection assay was performed on *Solanum lycopersicum* plants. There were three possibilities if and why infection by the knockout strain could occur, like it was described for the *VdTHI4* deletion strain infection assay (3.1.4).

Seven days after the infection of *S. lycopersicum* plants with *Verticillium* no obvious differences in growth height between non-infected, called mock, plants and *PA14_2* deletion or complementation infected plants were detectable (Figure 25 a). The difference became visible after 14 dpi and increased by time. At 28 dpi the complementation strains infected plants were as small as the *Vd* wild type infected hosts (Figure 25 b). These plants show stunting symptoms with very small stems and small leaves. In contrast to them, the *VdΔPA14_2* strain infected ones have growth heights like the non-infected mock plants. (Figure 25 a, b). Phenotype of those plants reveals a loss of pathogenic function of the strain.

Outgrowing assays on plates of the fungus from stem sections of infected plant material were performed to verify invasion of *V. dahliae* into plants (Figure 25 b). The assay revealed that not all fungal strains were able to colonize plants. The *VdΔPA14_2* strain was not growing out of the plant material. In contrast, *Vd* wild type, and both complemented strains, *VdΔPA14_2* :: *Vd PA14_2* as well as *VdΔPA14_2* :: *VlPA14_2-1*, grew out of the infected plant material. Their fungal phenotypes look like *V. dahliae* wild type in growing of hyphae and melanization. Fungal outgrowth from the infected plants occurs very slowly and the plates were incubated for 14 days.

As a second control to estimate if the deletion strain enters in small amounts, or if it is not able to enter the plants, the amount of fungal DNA from infected plants was quantified by real-time PCR using internal transcribed spacer ITS1 rDNA primers of *V. dahliae* in a defined amount of plant DNA (25 ng) from infected plants (Figure 25 c). In qPCR analysis, fungal presence of *Vd* wild type and the complementation strains was detectable. The *VdΔPA14_2* strain could only be detected in significantly low amount inside the hypocotyl and in nearly no amount in the root in the infected plant material. With 0.05 ng amount of detectable *VdΔPA14_2* DNA in 25 ng extracted DNA compared to 0.4 ng of *Vd* wild type, the amount is eight times less. Furthermore, it is four times less than the amount of DNA (up 0.2 ng in 25 ng DNA) measured in the complementated strains.

Summing up the results of the plant infection assay, the *V. dahliae* Δ*PA14_2* deletion strain is reduced in the capability of entering the *S. lycopersicum* plants. The infected plants showed phenotypes approximately like the non-infected plants with clearly reduced symptoms of infection, like stunting. Consistent with these symptoms, the quantification of fungal DNA and the outgrowth experiment suggests, the deletion strain is impaired in colonizing the plants.

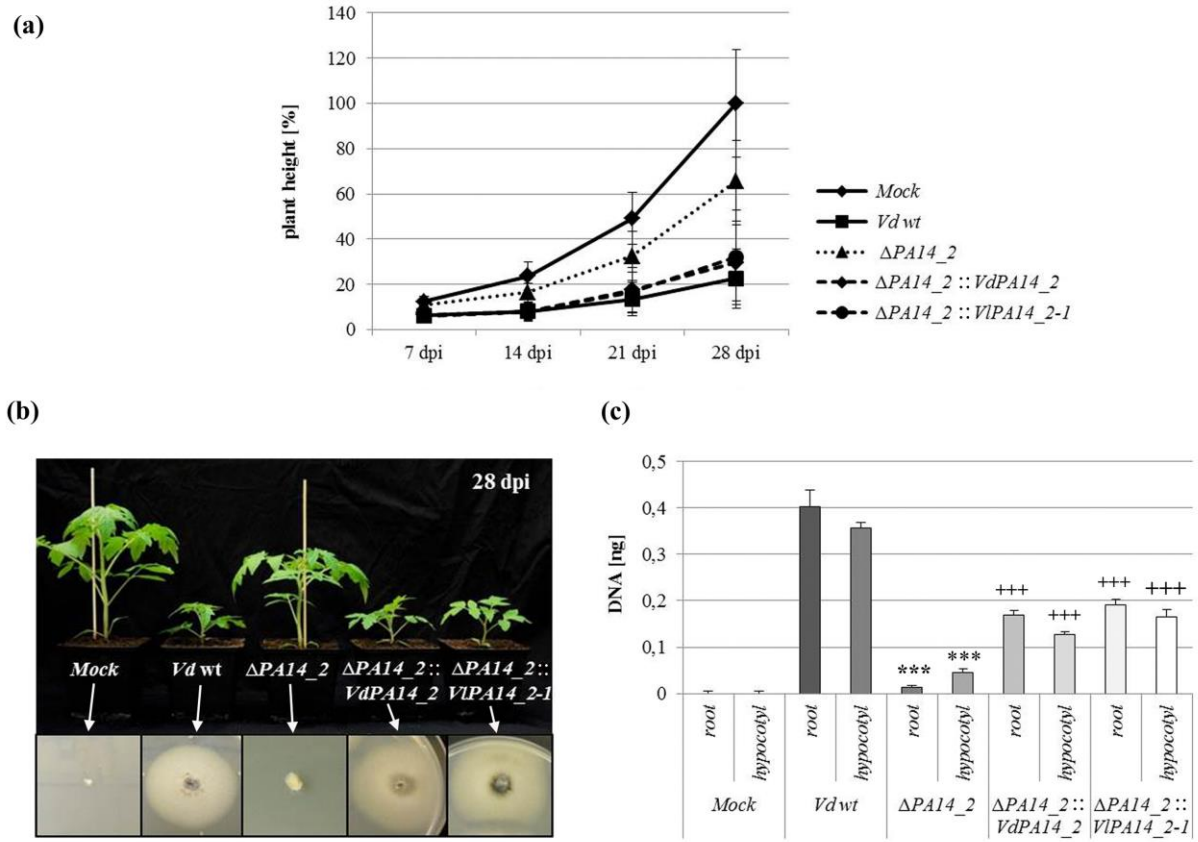

Figure 25: **Plant infection assay. (a, b upper part)** Growth of *S. lycopersicum* plants infected with *Vd* wt, Δ*PA14_2*, Δ*PA14_2* :: *VdPA14_2* and Δ*PA14_2* :: *VlPA14_2-1* for 28 days. 15 plants were used for each infection condition. Plants were infected by root dipping for 35 min with $1*10^6$ spores/ml and additional watering the plants with 1.5 ml spores (mock control was treated with water). Growth occurs under long-day-conditions (16 h light / 8 h dark) at 22°C and plants were measured after 7, 14, 21 and 28 dpi. Plants infected with deletion strain Δ*PA14_2* grew like the non-infected mock plants. Complementation strains infected grew like wild type infected plants. All results are highly significant with a student's-test P-value of > 0.001. Infection assay was tested n=2. **(b lower part)** *Vd* grew out of stem pieces on PDA plates containing chloramphenicol (35 mg/ml) *PA14_2* deletion strain showed no colonization of the plants. From both Δ*PA14_2* complementation strains infected plants, *Vd* grew out of the plant pieces identical to *V. dahliae* wild type infection. Plates were incubated for 14 days at 25°C. **(c)** Quantification of fungal DNA in 25 ng extracted plant DNA of infected plants after 28 dpi. PCR performed with fungal specific ITS1 OLG70/71 primers (Eynck *et al.*, 2007). *Vd* Δ*PA14_2* strain infected plants contain nearly no DNA. Plants infected by complemented strains have less than half of DNA amount compared to *Vd* wt strain. Results are highly significant (significance: * to *Vd* wt; + to Δ*PA14_2*). n = 5.

3.3 Transcriptomic analysis of *in situ* and *in vitro* expressed transcripts of *Verticillium longisporum* 43

Global approach experiments were performed to investigate transcriptomic, metabolomic and proteomic processes of *Verticillium longisporum* 43. The transcriptomic approach is part of this study. *In situ* cultivation of the fungus was performed in *B. napus* xylem-sap and *in vitro* cultivation in SXM (see 2.12). For comparability, the samples for all three different approaches were taken from the same flasks and analyzed by different persons. For the transcriptomic approach two biological replicates (samples 2 and 4) with two technical replicates (samples 3 and 1) of xylem-sap growing fungus (Figure 26 a) were analyzed by RNAseq (2.13.1). One biological replicate with four technical replicates of SXM cultured fungus was analyzed.

The sequenced short transcript reads from cDNA by deep sequencing (RNAseq) were mapped on the genome of *Verticillium longisporum* 43 to reveal the predicted ORFs of the fungus and were annotated based on the *V. dahliae* and *V. albo-atrum* genomes. To analyze the data, reads per kilo base per million of mapped reads (RPKM) were calculated (see 2.13.2) and filtered by MarVis tool and clustered in a 1D-self organizing map (see 2.13.3). The extracted data were used for further analyzes of the core-regulated and the specific up-regulated transcripts. This approach revealed that the transcriptomic dataset of *V. longisporum* includes 21,192 candidates in total to be expressed in xylem-sap (*in-situ*) and SXM (*in-vitro*).

Table 10: Number of RNA-seq mappable reads on the genome of *V. longisporum* 43

mappable reads			
xylem-sap		SXM	
1	20,514,187	1	15,668,005
2	17,649,324	2	31,368,400
3	12,051,997	3	28,298,234
4	9,378,664	4	24,096,142

In general about 1000 reads or more were mappable for one gene in the transcriptome of *V. longisporum* 43, which includes more then 20.000 candidates to be expressed. For the librarys 3 and 4 of xylem-sap and 1 of SXM the mappable reads were little less.

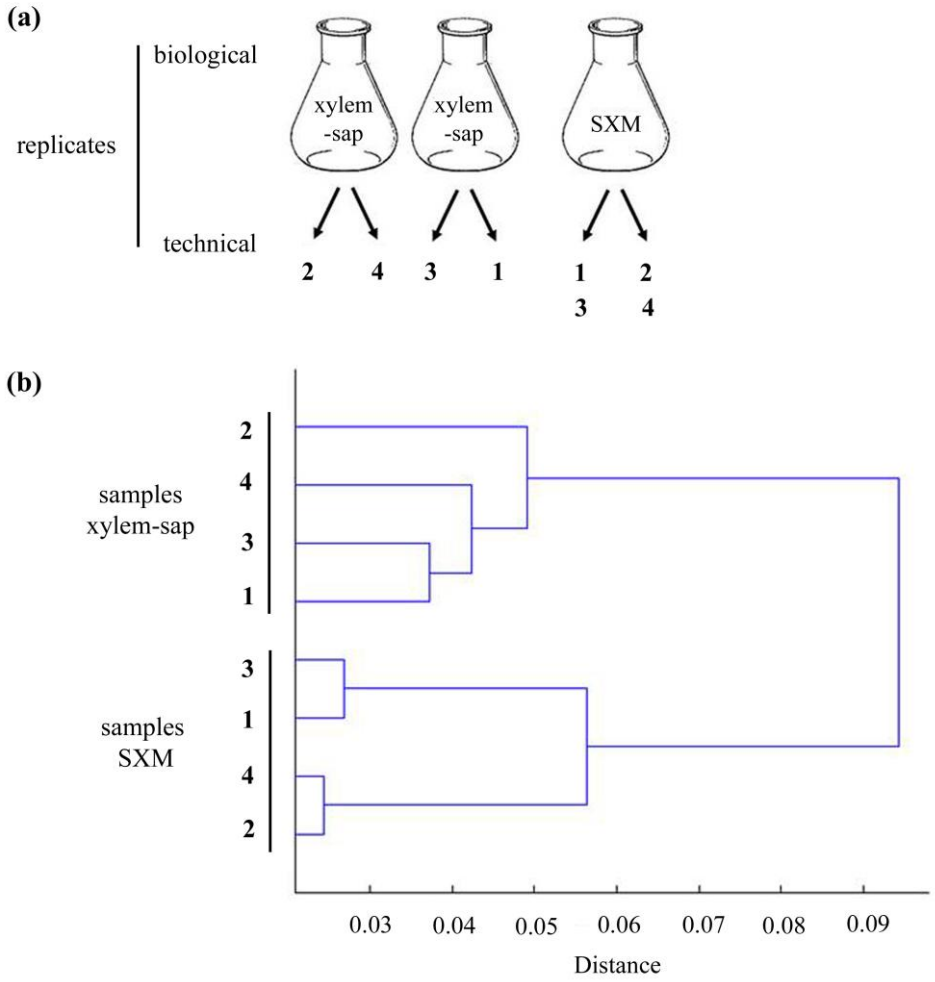

Figure 26: **Experimental setup and HCA dendrogram of specific up-regulated transcripts of *Verticillium longisporum* 43 global approach RPKM data sets. (a)** Experimental setup of the global experimental approach. **(b)** HCA (hierarchical cluster analysis) of *Verticillium longisporum* 43 technical replicates from xylem-sap and SXM medium. For xylem-sap two biological replicates with two technical replicates each, for SXM one biological replicate, with two technical replicates of two preparations each were used for clustering. Clustering performed by MarVis tool (http://marvis.gobics.de, (Kaever *et al.*, 2009)). SXM transcripts of the technical replicates from two preparations are highly similar, replicates 1 and 2 of xylem-sap not.

The differences of transcriptomic profiles in the data set of xylem-sap and SXM specific up-regulated transcripts is highlighted by a HCA (hierarchical cluster analysis) (Figure 26 b). This reveals the RNAseq datasets of *V. longisporum* samples from the different conditions are more similar within the biological and technical replicates than to the other cultivation condition.

3.3.1 Core regulated transcripts of *V. longisporum* in *in situ* (xylem-sap) and *in vitro* (SXM) cultivation

The first part of the chapter will be focused on the group of same-regulated transcripts of *V. longisporum* 43 during *in situ* and *in vitro* cultivation. 38% of all transcripts are genes with unchanged abundance. These 8,121 genes were expressed but not regulated with regard to cultivation in xylem-sap and SXM and are the core set of expressed transcripts. In Figure 27, the 1-D self organizing map visualizes the clustering of all transcripts. The analyzed similary regulated 8,121 core-regulated transcripts were marked with a red rectangle.

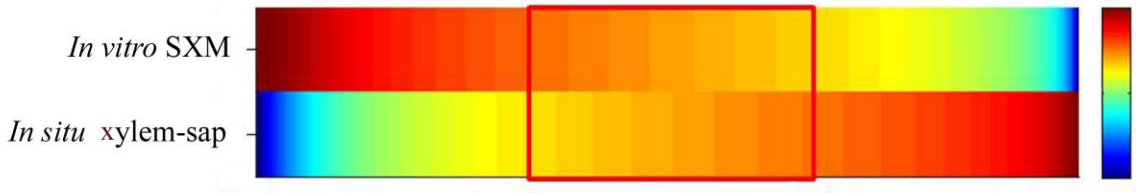

Figure 27: ***Verticillium longisporum* 43 transcripts up-regulated in xylem-sap and in SXM.** MarVis cluster (1-D self organiszing map) of all 21,192 transcripts that are regulated in SXM and xylem-sap. Up-regulated transcripts are shown in red (1) left: SXM, right: xylem-sap. Not regulated tanscripts are shown in blue (0), left: xylem-sap, right: SXM. Transcripts that are up-regulated under both conditions and being described in this chapter, are marked with a red rectangle (http://marvis.gobics.de, (Kaever *et al.*, 2009)).

For these core-regulated transcripts the cellular localization, functional categorization and domain function of the transcripts encoded proteins will be analyzed. Exel sheets of the data were attached on CD.

3.3.1.1 Cellular localization of core transcripts

To analyze the putative localization of those transcripts, the prediction tools WoLF PSORT (Horton *et al.*, 2007) and YLoc+ (Briesemeister *et al.*, 2010) were used (Figure 28).

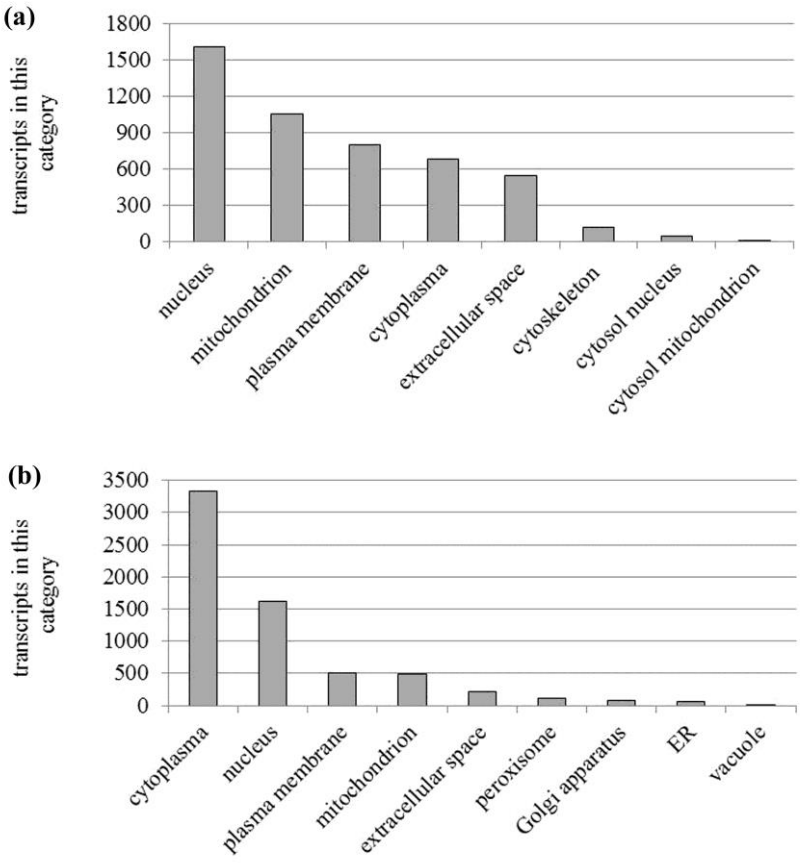

Figure 28: **Cellular localization of core set transcripts predicted by WoLF PSORT and YLoc+. (a)** WoLF PSORT (Horton *et al.*, 2007) analysis reveals most of the predicted proteins to be localized in the nucleus. In the mitochondria, plasma membrane, cytoplasm and extracellular also many proteins seem to be localized. **(b)** YLoc+ (Briesemeister *et al.*, 2010) analysis reveals about half of the proteins to be in the cytoplasma. About one quarter is nuclear localized and less were plasma membrane, mitochondrial or secreted proteins.

The prediction results of the two programmes differ. YLoc+ assigned the cellular localization for much more transcripts then WoLF PSORT. Most of the 6,427 YLoc+ predicted proteins seem to be localized in the cytoplasm (3,324) or are nuclear proteins (1,627). In total 80% of the core regulated transcripts were assigned for localization by this tool. WoLF PSORT predicted a locally determination for 4,859 transcripts what is about 50% in total. Nuclear proteins are with 1,611 the biggest group. For cytoplama localization only 684 proteins were predicted what is a fractional amount of the YLoc+ assignment. Finally, both predictions revealed the core set of regulated transcripts to encode for proteins being localized nuclear, in the cytoplasm and at or in the plasma membrane.

3.3.1.2 Comparison of functional classes and predicted domains of the core transcriptome

To get more information of putative functions of the core-regulated transcripts encoded proteins either in xylem-sap or in SXM, the transcripts were sorted to functional categories using FunCat (http://mips.helmholtz-muenchen.de/proj/funcatDB/) and their domains were predicted usind InterproScan. Filtering and sorting for functional categorization was performed by using the "Hivi" tool (www.gobics.de) with a cutoff of 50% protein sequence identity to ensure a reasonable sorting into the functional groups. Proteins were predicted by comparison with the soil-borne plant pathogenic fungus *Fusarium graminearum*.

The predicted proteins were split up in 19 functional main groups. In these groups, 7,581 transcript encoded proteins were ordered to, what is about 93% of the same regulated transcripts. Most of the putative predicted proteins seem to be "metabolism" involved, where transcripts for synthesis as well as for degradation were assigned to. Putative proteins being involved in "cellular transport", "protein with binding function or co-factor requirement", "protein fate" and "transcription" were also detected in high numbers. Proteins with these functions are required for fungal growth *in situ* (xylem-sap) and *in vitro* (SXM) and seem to belong to the core set of proteins in *Verticillium longisporum.*

The main groups and the first 30 functional subcategories for the encoded proteins are analyzed (Table 11). By this it is possible to get a more detailed view of the 7,581 predicted functions for the core regulated transcripts in the *in situ* and the *in vitro* medium. In the table, main categories are written in italic and the subcategories not. For analyzing these data it has to be mentioned, that a putative protein could be sorted to more than one functional group. This is caused by the fact, that the proteins might have several functions.

Table 11: First 30 functional subcategories for xylem-sap (xyS) and SXM same regulated transcripts

Category with subcategories / genes in this category	xyS and SXM up
Metabolism	*1331*
amino acid metabolism	289
nitrogen, sulfur and selenium metabolism	114
nucleotide/nucleoside/nucleobase metabolism	181
phosphate metabolism	273
C-compound and carbohydrate metabolism	534
lipid, fatty acid and isoprenoid metabolism	307
metabolism of vitamins, co-factors, and prosthetic groups	136
secondary metabolism	190
Cellular transport, transport facilitation and transport routes	*792*
transported compounds (substrates)	454
transport facilities	249
transport routes	548
Protein with binding function or co-factor requirement (structural or catalytic)	*843*
protein binding	220
nucleic acid binding	292
nucleotide/nucleoside/nucleobase binding	312
Protein fate (folding, modification, destination)	*762*
protein targeting, sorting and translocation	209
protein modification	389
assembly of protein complexes	155
protein/peptide degradation	198
Transcription	*657*
RNA synthesis	462
RNA processing	278
Cell cycle and DNA processing	*594*
DNA processing	299
cell cycle	420
Biogenesis of cellular components	*428*
cell wall	122
Protein synthesis	*415*
translation	174
Cell rescue, defense and virulence	*375*
stress response	218
Interaction with the environment	*275*
cellular sensing and response to external stimulus	159
Energy	*272*

Table 11 continued

Category with subcategories / genes in this category	xyS and SXM up
Cellular communication/signal transduction mechanism	*250*
cellular signalling	209
Cell type differentiation	*216*
fungal/microorganismic cell type differentiation	209
Cell fate	*160*
cell growth / morphogenesis	142
Regulation of metabolism and protein function	*157*
regulation of protein activity	139
Development (systemic)	*39*
Systemic interaction with the environment	*10*
Transposable elements, viral and plasmid proteins	*3*
Organ differentiation	*2*
	7581

As expected, the core transcription reveals all essential functions of living cells. The four subgroups of "C-compound and carbohydrate metabolism", "RNA synthesis", "transported compounds (substrates)" and "transport routes" are with over 400 predicted proteins the fourth highest up-regulated subcategories of core expressed transcripts in the xylem-sap and the pectin rich SXM medium. With a number of 534 (14% of the over 7,500 assigned proteins of core regulated transcripts), most encoded proteins are involved in "C-compound and carbohydrate metabolism" and many of them are putative CAZys (carbohydrate-active enzymes) that are also predicted by direct Pfam domain analysis of the dataset. The high number of core regulated putative CAZy proteins highlighted the importance of those enzymes for the fungus. Furthermore, transcripts coding for "RNA synthesis" proteins (main group of "transcription"), like the probable RPO31- DNA-directed RNA polymerase III, 160 KD subunit, being encoded by vl43-au16.g10116.t1 are highly up-regulated. Pfam analysis assisted the importance of those proteins. Here, especially ribosomal domains were detected in highest numbers. Also transcription factors were found by Pfam analysis to be represented in high amounts. The *CPC1* genes (vl43-au16.g19783.t1 and vl43-au16.g20638.t1) of the transcription factor, which is the activator of the cross-pathway control system of amino acid biosynthesis, and is relevant for *Verticillium* pathogenicity (Sasse *et al.*, 2008; Timpner *et al.*, 2013), were found to be core regulated. The genes were both found to be expressed in a higher level over 130 RPKM but could not be assigned to a functional group.

Transcription factors were found as well in the subgroup “nucleic acid binding” of the main category of “protein with binding functions”. For these binding proteins also the Pfam analysis detects lots of domains what is also the case for transporter domains especially sugar transporters that are needed by the fungus. Transport plays also an important role for *Verticillium longisporum* 43. In “transported compounds (substrates)” and “transport routes”. Transcripts of this functional group were found in high numbers to be core-regulated. Summing up, beside proteins with functions as ribosomal proteins, CAZys, transcription factors, binding proteins and transport proteins, the Pfam analysis and the analysis by categorization revealed lots of enzymes especially peptidases and kinases. That emphasized the importance of these proteins for the fungus.

Beside *CPC1*, the pathogenicity relevant *PA14_2* gene (vl43-au16.g5346.t1), which is characterized in this study, was found to be core-regulated. With RPKM values around 2 it was found to be less expressed. Unfortionately also the *PA14_2* gene could not be assigned to a functional category by the *F. graminearum* comparison using the “Hivi” tool.

3.3.2 Specific regulated transcripts of *V. longisporum* in *in situ* (xylem-sap) and *in vitro* (SXM) cultivation

The medium specific up-regulated transcripts from *in situ* medium xylem-sap and from *in vitro* medium are interesting to analyze. In this approach it can be proven if the simulated Xylem medium reflects the contitions of natural xylem-sap or not. The clustering of those medium specific up-regulated data is shown in Figure 29. To analyze medium specific up-regulated transcripts encoded proteins cellular localization, functional categorization and domain function of the will be analyzed like it was performed for the core regulated transcripts. Exel sheets of the data were attached on CD.

In this second part of this chapter the focus will be on the 7% transcripts that are up-regulated in the *in situ* medium xylem-sap (1,506 transcripts) and the 8% that are up-regulated in the pectin rich *in vitro* medium SXM (1,804 transcripts). These specific up-regulated transcripts are about 15%, of the whole *V. longisporum* transcriptomic dataset including 21,192 transcripts.

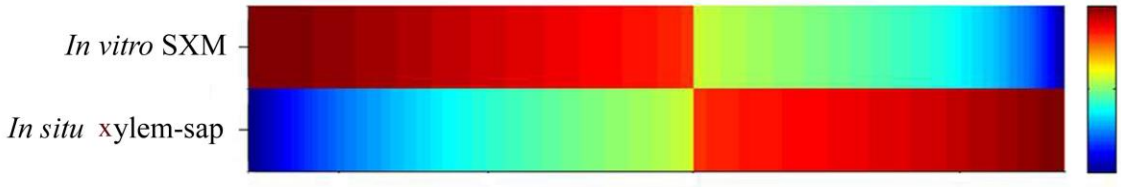

Figure 29: ***Verticillium longisporum* 43 transcripts specific up-regulated in xylem-sap and SXM.** MarVis cluster (1-D self organizing map) of the transcripts that are specific up-regulated in SXM or xylem-sap and are analyzed in this chapter. Clusters of up-regulated transcripts are shown in red (1) left: SXM, right: xylem-sap. Not up-regulated clusters are shown in blue (0) left: xylem-sap, right: SXM. (http://marvis.gobics.de, (Kaever *et al.*, 2009)).

3.3.2.1 Cellular localization of specific regulated transcripts

To analyze the putative localization of predicted proteins from specific up-regulated transcripts in *in situ* (xylem-sap) and *in vitro* (SXM) cultivation, the prediction tools WoLF PSORT (Horton *et al.*, 2007) and YLoc+ (Briesemeister *et al.*, 2010) were used (Figure 30 a and b). Whereas the xylem-sap analysis of WoLF PSORT revealed most putative proteins to be localized in the nucleus, in the pectin rich SXM most transcripts encode for proteins, which are localized in the extracellular space. In contrast, unsing the YLoc+ tool most predicted proteins of the specific up-regulated transcripts of both conditions were localized in the cytoplasm. In addition, many extracellular space and plasma membrane as well as nuclear localized proteins were predicted.

Using the two algorithms for prediction, the total number of proteins being localized to a specific compartment differs a lot, as it was mentioned, for the core regulated transcripts (3.3.1.1). The WoLF PSORT algorithm could predict localization for encoded proteins of in total 1,191 of the 1,804 specific up-regulated transcripts in the *in vitro* medium. Here most predicted proteins were assigned for extracellular localization. Most proteins of the 913 assigned proteins of the *in situ* cultivation of the total 1,506 transcripts were nuclear localized. Using YLoc+ as a tool for predicting cellular localization the numbers of assignments differ. For xylem-sap 1,157 up-regulated transcripts could be predicted for their protein localization and for SXM 1,349. For both media most putative proteins were predicted to be localized in the cytoplasm. In general, lots of the transcript encoded proteins of both cultivation conditions could be assigned by YLoc+ and their number is nearly equal.

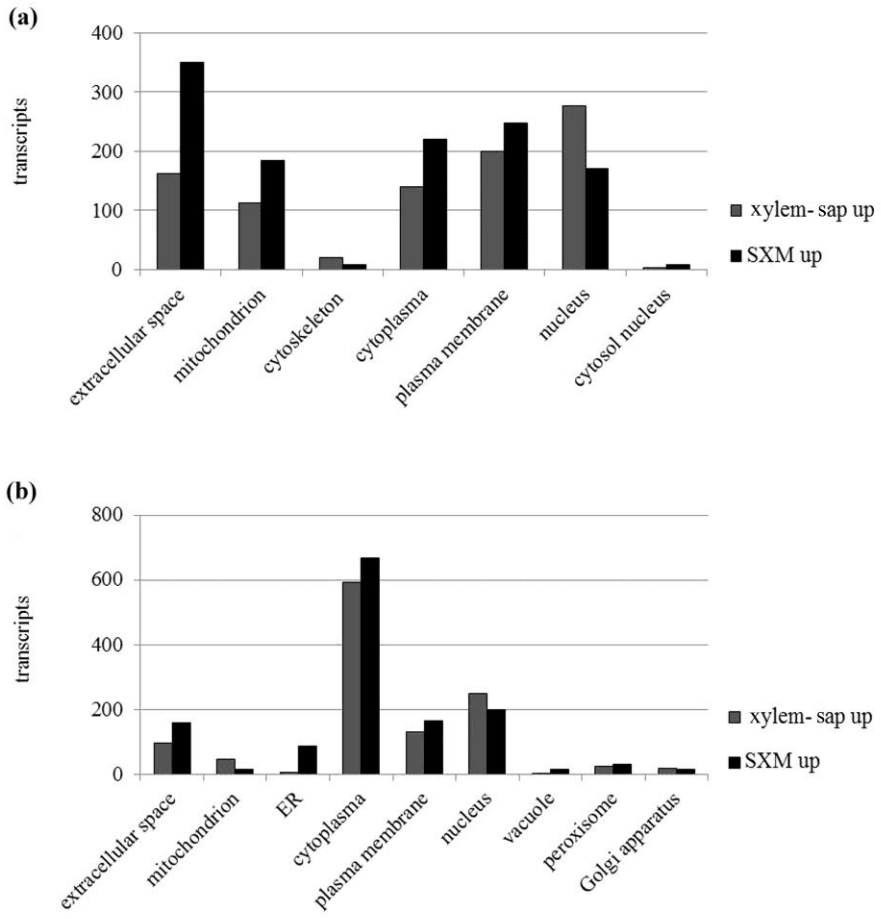

Figure 30: **Cellular localization of predicted proteins from specific xylem-sap or SXM up-regulated transcripts predicted by WoLF PSORT and YLoc+. (a)** WoLF PSORT (Horton *et al.*, 2007) analysis reveals most transcript encoded proteins of xylem-sap predicted to be localized in the nucleus (more than in SXM). For SXM most proteins seem to be localized extracellular. Few proteins are localized in the cytoskeleton or the cytosol of the nucleus. **(b)** YLOC+ (Briesemeister *et al.*, 2010) analysis reveals most transcripts encoded proteins of xylem-sap or SXM to be localized in the cytoplasma. Extracellular, in the membrane or in the nucleus fewer proteins are predicted to be localized. A higher amount of xylem-sap specific proteins seem to be nuclear localized compared to SXM.

The two algorithms used, predict different localization patterns. The analysis with WoLF PSORT reveals most transcript encoded proteins of xylem-sap predicted to be localized in the nucleus (more than in SXM). In SXM most proteins seem to be localized extracellular. Few proteins are localized in the cytoskeleton or the cytosol of the nucleus. In contranst, the YLOC+ analysis reveals most transcripts encoded proteins of xylem-sap or SXM to be localized in the cytoplasma. However, fewer proteins are predicted to be localized extracellular, in the membrane or in the nucleus. A higher amount of xylem-sap specific proteins seem to be nuclear localized compared to SXM. Finally, both tools assigned more nuclear transcripts to be expressed in xylem-sap compared to SXM. Furthermore, more transcripts for cytoplasma proteins seem to be expressed in the *in vitro* cultivated samples than under *in situ* conditions.

3.3.2.2 Comparison of xylem-sap and SXM specific up-regulated transcripts

To get more information of putative functions of the transcript encoded proteins the transcripts were assigned into functional categories like it is described in 3.3.1.2. The results are shown in Figure 31. When comparing the numbers of transcripts in the groups it is important to know that transcripts could be sorted in more than one functional category.

The predicted proteins were split up in the same 19 functional main groups like it was shown for the core regulated ones. Not all of the 1,506 xylem-sap and 1,804 SXM transcripts, being predicted to be specifically up-regulated, could be annotated and by that assigned to code for a protein. With 1,440 specific up-regulated transcripts being sorted into main functional categories, in the *in vitro* SXM medium and 913 in the *in situ* xylem-sap, a huge amount of the specific up-regulated transcripts have been predicted for their functions by annotation. The appendix 6.2 contains an overview of the functional main categories comparison of specific up-regulated and core-regulated transcripts.

The functional categorization reveals that the encoded proteins of the medium specific up-regulated transcripts generally belong to the same functional groups. Furthermore, the order of functional categories with assigned putative proteins sorted to is nearly equal. In both media, most specific up-regulated transcripts were assigned to the functional categories of "metabolism" with proteins for synthesis and degradation, "cellular transport", "proteins with binding function" containing also transcription factors and "protein fate" containing proteins for folding, modification, destination.

Figure 31 visualizes the main functional categories of the putative proteins from the specific up-regulated transcripts. A more detailed overview is shown in Table 12, (like Table 11 for the core-regulated transcripts) where functional subcategories were also listed.

Like it was mentioned for the core regulated transcripts, a putative protein could be sorted to more than one functional group. This is caused by the fact, that the proteins might have several functions. Putative proteins were assigned by comparison with the genome of *Fusarium graminearum*.

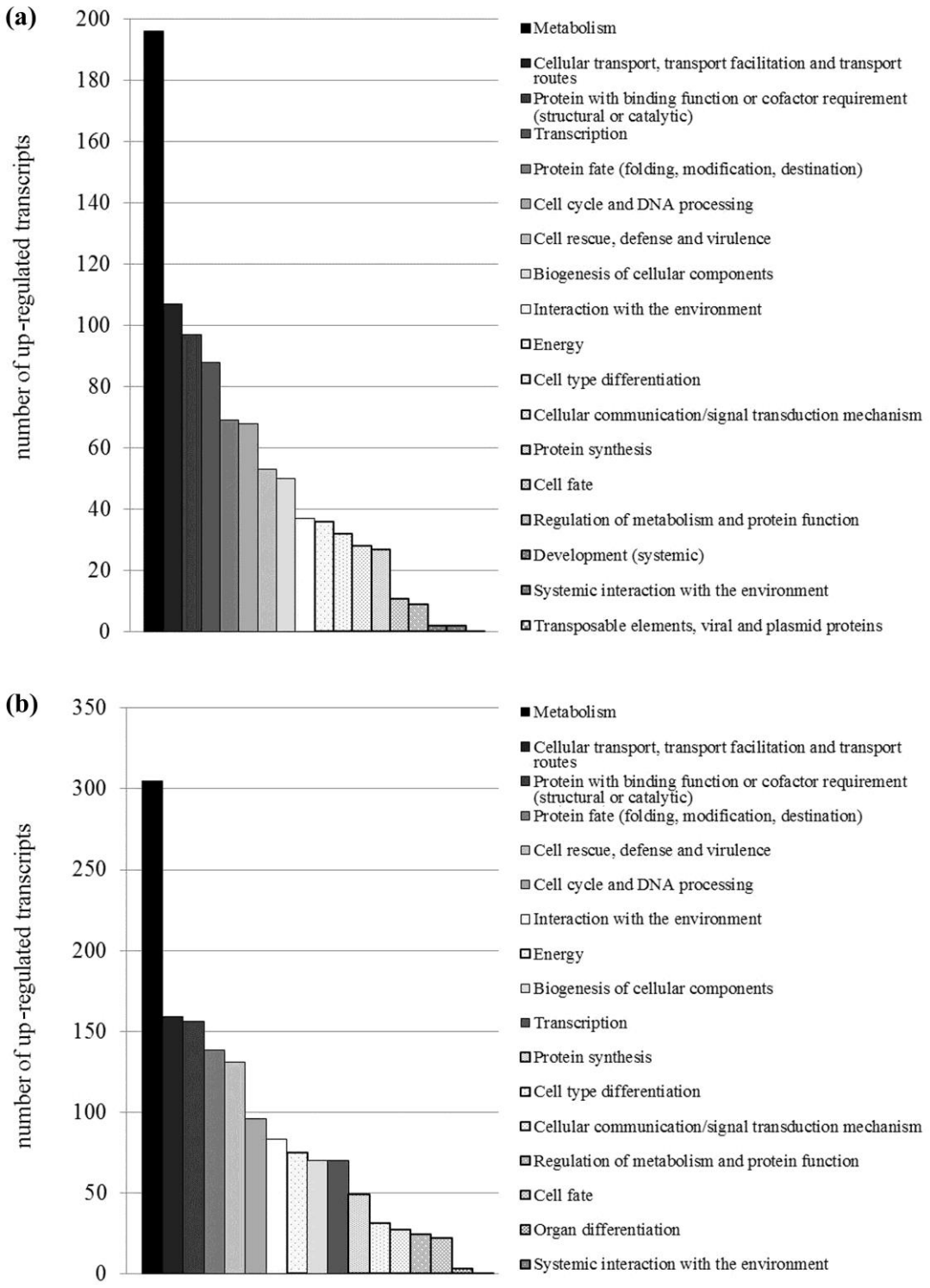

Figure 31: **Functional categories of predicted proteins specifically up-regulated in xylem-sap and SXM. (a xylem-sap and b SXM**) In xylem-sap and SXM most of the specific transcripts encode for cellular metabolism proteins, lots of them encode for cellular transport proteins and proteins with binding function. **(a)** In xylem-sap, many predicted proteins belong to the group of transcription. Less of the specific *in situ* up-regulated transcripts encoded proteins were assigned to the group of cell fate, regulation of metabolism and protein function, development (systemic), systemic interaction with the environment and at least transposable elements. **(b)** In SXM fewer transcripts encode for proteins for the categories of cell fate, organ differentiation and at least systemic interaction with the environment. Functional categorization analysis was performed with FunCat (http://mips.helmholtz-muenchen.de/proj/funcatDB/) and by "Hivi" tool (www.gobics.de).

More transcripts of functional “transcription” proteins are specific for xylem-sap cultivation, than for SXM. It point out their importance for fungal growth under *in* situ conditions when comparing the 88 specific up-regulated transcripts, with the 70 of the *in* vitro cultivation in SXM. In xylem-sap “transcription” is the fourth highest category in contrast to SXM, where it is one of the categories with fewer transcripts sorted to. *In situ,* putative proteins for transcription like the probable DNA-directed RNA polymerase II largest chain, vl43-au16.g6931.t1, as well as proteins like the propable ATPase component of chromatin remodeling complex (ISW1), vl43-au16.g10476.t1, vl43-au16.g14496.t1, vl43-au16.g1875.t2 encode for, were detected. Also highly up regulated are proteins related to transcriptional regulator CHD1, vl43-au16.g2865.t1, vl43-au16.g2871.t2 and vl43-au16.g3663.t1.

The 196 predicted proteins of the xylem-sap specific transcripts for “metabolism” including synthesis as well as degrading coding proteins, are a fewer number of specific up-regulated transcripts than the 305 transcripts of SXM. It points out that during the *in vitro* cultivation one third more specific transcripts encoding for proteins of this functional group are up-regulated. Besides “metabolism”, a higher number of SXM specific predicted proteins with functions in “protein fate” (proteins for folding, modification and destination) like vl43-au16.g4895.t1, a probable 26S proteasome regulatory particle chain RPT5 as well as heat shock proteins like vl43-au16.g13076.t1, what is related to hsp70 protein, were found. Also transcripts with proteins coding for “cell rescue, defense and virulence”, where lots of enzymes are sorted to, were found. A DNA rescue protein, coded by vl43-au16.g5918.t3, that seems to be related to a UV-damaged DNA-binding protein, was also detected. The category of “energy”, where about the double amount of proteins from SXM cultivation compared to xylem-sap is sorted to, includes proteins like the probable acetyl-CoA synthetase, vl43-au16.g10882.t1, in SXM.

Finally, the analysis reveals much more encoded proteins of *in vitro* cultivation to be specific up-regulated than under *in situ* conditions. Especially with functions in “metabolism”, “protein fate”, “cell rescue, defense and virulence” and “cell cycle and DNA processing” as well as “energy” (groups were marked in balck in Table 12). Getting a deeper view into these groups their first 20 transcripts are shown in appendix 6.1.

To get a more detailed overview of the specific regulation *in situ* and *in vitro,* the main groups and 30 of the functional subcategories, where most of up-regulated transcripts are ordered to, are listed in Table 12 (main groups in italic).

Table 12: First 30 up-regulated KEGG functional subcategories for xylem-sap (xylS) and SXM different up-regulated transcripts

Category with subcategories / genes in this category	xylem-Sap vs. SXM	
	xylS up	SXM up
Metabolism	*196*	*305*
amino acid metabolism	41	77
nitrogen, sulfur and selenium metabolism	-	23
nucleotide/nucleoside/nucleobase metabolism	23	-
phosphate metabolism	25	43
C-compound and carbohydrate metabolism	94	160
lipid, fatty acid and isoprenoid metabolism	43	68
metabolism of vitamins, Co-factors, and prosthetic groups	18	24
secondary metabolism	28	49
extracellular metabolism	14	-
Cellular transport, transport facilitation and transport routes	*107*	*159*
transported compounds (substrates)	71	115
transport facilities	38	59
transport routes	72	89
Protein with binding function or Co-factor requirement (structural or catalytic)	*97*	*156*
protein binding	14	36
nucleic acid binding	32	37
metal binding	13	-
nucleotide/nucleoside/nucleobase binding	33	53
complex co-factor/cosubstrate/vitamine binding	-	32
Transcription	*88*	*70*
RNA synthesis	64	56
RNA processing	33	24
Protein fate (folding, modification, destination)	*69*	*138*
protein folding and stabilization	-	23
protein targeting, sorting and translocation	14	31
protein modification	36	69
protein/peptide degradation	17	66
Cell rescue, defense and virulence	*53*	*131*
stress response	20	82
disease, virulence and defense	21	35
detoxification	15	34
Cell cycle and DNA processing	*68*	*96*
DNA processing	33	55
cell cycle	44	60

Table 12 continued

Category with subcategories / genes in this category	xylem-Sap vs. SXM	
	xylS up	SXM up
Interaction with the environment	*37*	*83*
homeostasis	23	42
cellular sensing and response to external stimulus	18	44
Energy	*36*	*75*
fermentation	-	25
Biogenesis of cellular components	*50*	*70*
cell wall	16	27
nucleus	13	-
Cellular communication / signal transduction mechanism	*97*	-
cellular signalling	21	-
Cell type differentiation	-	*31*
fungal/microorganismic cell type differentiation	-	30
Protein synthesis	*27*	*49*
Cell fate	*11*	*22*
cell growth / morphogenesis	-	-
Regulation of metabolism and protein function	*9*	*24*
Development (systemic)	2	-
Systemic interaction with the environment	2	1
Organ differentiation	-	3
Transposable elements, viral and plasmid proteins	1	-
	913	1440

When investigating the first 30 subcategories with the highest numbers of specifically up regulated transcripts being expressed under *in situ* and *in vitro* cultivation, differences in sorting are detectable. In xylem-sap putative proteins of some functional subgroups are expressed medium specific (marked with a red rectangle). In these groups no putative protein of SXM was sorted to, because only lower numbers of them were expressed by that these categorys are not included in the 30 highest up-regulated categories. The identifier and functions of these xylem-sap predicted proteins are listed in appendix 6.2.

These groups are “nucleotide/nucleoside/nucleobase metabolism” with proteins like the probable ADP, ATP carrier protein (ADP/ATP translocase), coded by vl43-au16.g14375.t1. In “extracellular metabolism” binding proteins like a protein being related to an atochitin binding protein, encoded by vl43-au16.g15018.t1, were found. The category of “metal binding” contains transcripts like vl43-au16.g14578.t1, coding for a protein that is related to PHO36 – with a regulatory role in lipid and phosphate metabolism. “Cellular signaling”

includes enzymes like kinases and cyclases, as well as binding proteins like vl43-au16.g10660.t1, which is related to the hexamer-binding protein HEXBP. In "biogenesis of cellular components, subcategory nucleus", proteins like the probable ATPase component of chromatin remodeling complex (ISW1), coded by vl43-au16.g10476.t1 was detected, this transcript is also found in the group of "transcription".

Obvious transcripts of classes are enriched in high numbers in SXM medium (marked with a blue rectangle). Some of these groups do not contain putative encoded protein in xylem sap or only in low numbers. This is the case for "sulfur and selenium metabolism" that contains proteins like vl43-au16.g10131.t1, which is related to a flavin-containing monooxygenase. In "protein folding and stabilization" stress induced proteins and heat shock proteins were found. And the goup of "fungal/microorganismic cell type differentiation" includes transcripts like vl43-au16.g10931.t1, a probable hymA gene. Other categories include double amount of putative encoded proteins or more that implicates a higher necessary of synthezising proteins for surviving under *in vitro* cultivation.

3.3.2.3 Comparison of xylem-sap and SXM specific 20 highest up-regulated transcripts

For a detailed look, the first 20 up-regulated transcripts with specific expression pattern found in xylem-sap and in SXM are listed in Table 13 and Table 14.

Up-regulated transcripts for both, xylem-sap and SXM could be assigned to similar functional classes like peptidases as well as CAZys (putative carbohydrate-active enzymes). Under both conditions, two CAZys were found. These putative carbohydrate-active enzymes might be involved in synthesis and breakdown of complex carbohydrates and glycoconjugates. Different fungal transporters and secreted proteins were also found to be specific up-regulated under both cultivation conditions.

Furthermore, in xylem-sap two putative Rieske proteins were found to be highly expressed. Rieske proteins and Rieske ferredoxins (RFds) are small iron–sulfur proteins of <130-amino-acids that act as electron-transfer components. They contain the Rieske center, what is a [2Fe–2S] cluster, in which one of the iron atoms is coordinated by the $N^{\delta 1}$ atoms of two histidine side chains and the other by two cysteine S^{γ} ligands (Schmidt & Shaw, 2001).These proteins are membrane-bound components. For example the Rieske domain fused to a transmembrane helix is a part of the cytochrome bc_1 complexes (Bandeiras *et al.*, 2013). In addition, a putative proteinase R containing a S8 domain, which is predicted to be an intracellular peptidase and involved in ATP binding, mRNA synthesis, RNA processing, mRNA processing (splicing, 5'-, 3'-end processing), detoxification, ribosome biogenesis and translational control

was detected (Samal *et al.*, 1990). In the pectin rich SXM medium two peptidases were found. The M14 domain peptidase, containing a signal peptide and seems to be an extracellular peptidase, responsible for extracellular protein degradation, protein/peptide degradation and cell wall biogenesis. The second peptidase is predicted to be non-secreted and to be involved in the metabolism of tyrosine. The detection of different peptidases and CAZys matches to the proteomic analyses results, where these proteins were found likewise (data by Anika Kühn, not shown here).

Predicted proteins of the 20 hightest up-regulated transcripts in xylem-sap and SXM cultivated *Verticillium longisporum* 43 are non-secretory proteins in majority. The transcripts of the *in situ* medium include five transcripts with a secretion signal predicted by SignalP tool. For the pectin rich *in vitro* medium four transcripts are predicted to contain a secretion signal and three to have a signal anchor but no transmembrane domains.

It points out that the 20 highest up-regulated transcripts encode for peptidases and proteins with unknown function. Additionally carbohydrate metabolism is important for the fungus, because transcripts encoding for CAZys were identified to be highly expressed. The prediction reveals most of the highest expressed putative proteins not to be secreted.

Table 13: Xylem-sap up-regulated top 20 transcripts of *Vl*43

identifyer	predicted proteins	Pfam domain	secretion	GPI	NLS	category
au16.g14703.t1	choline monooxygenase	Rieske				
au16.g15180.t1	predicted protein		Sign. pept.	YES		
au16.g15547.t1	naphthalene 1;2-dioxygenase subunit alpha	Rieske				
au16.g3414.t1	dicarboxylic amino acid permease	AA_permease				
au16.g10435.t1	dicarboxylic amino acid permease	AA_permease				
au16.g8347.t1	predicted protein		Sign. pept.			
au16.g16985.t1	conserved hypothetical protein	NmrA				
au16.g12331.t1	proteinase R	Peptidase_S8				ATP binding, mRNA synthesis, RNA processing, mRNA processing (splicing, 5'-, 3'-end processing), detoxification, ribosome biogenesis, translational control,
au16.g14926.t1	cytochrome b-245 heavychain subunit beta	FAD_binding_8; NAD_binding_6; Ferric_reduct				oxygen and radical detoxification, superoxide metabolism, homeostasis of cations, cellular signalling,
au16.g7877.t1	DJ-1/PfpI family protein	DJ-1_PfpI				
au16.g19329.t1	beta-glucosidase	Glyco_hydro_3;Glyco_hydro_3_C				
au16.g7878.t1	conserved hypothetical protein	NmrA				
au16.g14096.t4	beta-glucosidase	Glyco_hydro_3; Glyco_hydro_3_C	Sign. pept.			sugar, glucoside, polyol and carboxylate catabolism
au16.g16264.t1	Zn(II)2Cys6 transcription factor	Fungal_trans				
au16.g13278.t1	secretory phospholipase A2	Phospholip_A2_3	Sign. pept.		YES	RNA binding, mRNA processing (splicing, 5'-, 3'-end processing), assembly of protein complexes
au16.g944.t1	reticulon-4-interacting protein	ADH_zinc_N				
au16.g5775.t1	predicted protein		Sign. pept.		YES	
au16.g2638.t1	SpvB domain-containing protein	TcdB_toxin_midC; TcdB_toxin_midN;SpvB				
au16.g8937.t1	polysaccharide deacetylase family protein	Chitin_bind_1; Polysacc_deac_1				extracellular aminosaccharide degradation, polysaccharide binding
au16.g17565.t2	SpvB domain-containing protein	TcdB_toxin_midC; TcdB_toxin_midN; SpvB				

Data analysed by SignalP V.3.0 and 4.0, WoLF PSORT, TargetP, YLoc+, Interpro Scan, PredGPI

Table 14: SXM up-regulated top 20 transcripts of *Vl*43

identifyer	predicted proteins	Pfam domain	secretion	GPI	NLS	category
au16.g1258.t1	polygalacturonase	Glyco_hydro_28	Sign. pept.			polysaccharide metabolism,
au16.g7849.t1	X-Pro dipeptidyl-peptidase protein	Peptidase_S15; FAA_hydrolase; PepX_C;DUF1969				metabolism of tyrosine
au16.g16520.t1	polygalacturonase	Glyco_hydro_28	Sign. pept.			
au16.g17247.t1	2-oxoglutarate-dependent ethylene/succinate-forming enzyme	2OG-FeII_Oxy				
au16.g10757.t1	2-oxoglutarate-dependent ethylene/succinate-forming enzyme	2OG-FeII_Oxy				
au16.g7848.t1	cupin domain-containing protein	Cupin_2				
au16.g7850.t1	aromatic ring-opening dioxygenase family protein	LigB				
au16.g16884.t1	No significant similarity found		Sign. anch.			
au16.g8722.t1	phosphate-repressible phosphate permease	PHO4				anion transport, phosphate transport, sodium driven symporter, homeostasis of cations, homeostasis of anions, homeostasis of phosphate,
au16.g1969.t1	No significant similarity found		Sign. anch.			
au16.g19129.t1	Na+/H+ antiporter 2	Na_H_Exchanger				
au16.g19616.t1	phosphate-repressible phosphate permease	PHO4				
au16.g8359.t1	multidrug resistance protein	ABC_membrane; ABC_tran				
au16.g12328.t1	carboxypeptidase A5	Peptidase_M14	Sign. pept.			extracellular protein degradation, protein/peptide degradation, cell wall biogenesis
au16.g1927.t1	phosphatidylethanolamine-binding protein					DNA repair
au16.g10876.t1	xylulose-5-phosphate phosphoketolase	XFP; XFP_C; XFP_N			YES	C-compound and carbohydrate metabolism, pentose-phosphate pathway, lactate fermentation, heterofermentative pathway and fermentaton of other saccharides
au16.g11423.t1	hypothetical protein VDAG_04534		Sign. pept.			
au16.g2960.t1	predicted protein		Sign. anch.		YES	
au16.g1007.t1	molybdenum co-factor sulfurase	Aminotran_5				
au16.g10131.t1	quinate permease	Sugar_tr				nitrogen, sulfur and selenium metabolism, C-compound and carbohydrate transport

Data analysed by SignalP V.3.0 and 4.0, WoLF PSORT, TargetP, YLoc+, Interpro Scan, PredGPI

3.3.2.4 Comparison of predicted domains in xylem-sap and SXM specific up-regulated transcripts

Analyzing the transcripts of the two different growth media by comparing the predicted domains is a second way of analysis than the upper described where the predicted annotations by *F. graminearum* were evaluated. In the Pfam analysis a protein could be assigned only into one functional group, what erases drawing conclusions of the transcriptomic up-regulations. This analysis was performed to simplify the functional comparison of predicted proteins in the two growth conditions.

A genome wide InterproScan for *V. longisporum* 43 revealed Pfam assignment to many ORFs. The first 20 most occurring domains of each medium are shown in Table 15.

Table 15: Domains predicted for xylem-sap up- and SXM up-regulated transcripts

PFAM		xylem -sap	PFAM		SXM
Zn_clus	Zn(2) Cys (6)	46	MFS_1	major facilitator superfamily	52
Fungal_trans	transcription factor	39	adh_short	short chain dehydrogenase	33
MFS_1	major facilitator superfamily	30	Sugar_tr	sugar transporter	33
Sugar_tr	sugar transporter	25	Aldo_ket_red	aldo-keto reductase	16
adh_short	short chain dehydrogenase	23	Zn_clus	Zn(2) Cys (6)	16
p450	cytochrome P450	21	WSC	WSC domain	14
Pkinase	protein kinase	20	AAA	ATPases Associated with diverse cellular Activities	13
ADH_zinc_N	zinc-binding dehydrogenase	16	ADH_zinc_N	zinc-binding dehydrogenase	13
Ank	ankyrin repeat	15	Peptidase_M28	peptidase M28	13
RRM_1	RNA recognition motif	13	Glyco_hydro_28	glycosyide hydolase family 28	12
AMP-binding	AMP binding enzyme	12	ADH_N	alcohol dehydrogenase	11
AA_permease	amino acid permease	11	Cation_ATPase_C	cation transporting ATPase	10
ADH_N	alcohol dehydrogenase	11	E1-E2_ATPase	proton ATPase	10
Glyco_hydro_3	glycosyide hydolase family 3	11	FAD_binding_4	FAD binding domain	10
HET	heterokaryon incompatibility protein	11	p450	cytochrome P450	10
Amino_oxidase	Flavin-containing amine oxidoreductase	10	PA	protease associated domain	10
Glyco_hydro_3_C	glycosyide hydolase family 3	10	Fungal_trans	transcription factor	9

Table 11 continued

PFAM		xylem -sap	PFAM		SXM
Helicase_C	helicase	10	NmrA	negative transcriptional regulator	9
ABC_tran	ABC transporters	9	Pectate_lyase	pectate lyase	9
Beta-lactamase	β-lactamase	9	Peptidase_M14	zinc carboxypeptidase	9
total		1257	total		1377

By this Pfam domain based analysis 1,257 domains were detected for the expressed transcripts in xylem-sap and 1,377 for SXM. Most predicted proteins of the specific up-regulated transcripts contain domains for Zinc-cluster transcription factors and other fungal transcription factors. Also protein kinases and CAZys (carbohydrate-active enzymes) are found to be domains in the up-regulated proteins encoded by the specific up-regulated transcripts. The specific up-regulated transcripts of the *in situ* cultivation reveal the fungus to express more CAZys and transcription factors than under *in vitro* conditions. In the pectin and casein rich SXM medium domains for pectinases, peptidases and CAZys were assigned in high amount. Furthermore, both media reveal a high number of sugar transporters. In Appendix 6.4 the detected Pfam domains were listed in direct comparison of the two media, ordered by the first 120 domains of xylem-sap specific up-regulated ones.

Finally, in both approaches, analyzing the transcriptomic data of *V. longisporum* grown in the *in situ* xylem-sap medium or the *in vitro* SXM medium by functional categorization by FunCat analysis (see 3.3.1 to 3.3.1.2 and 3.3.2 to 3.3.2.3), it was shown that putative encoded proteins of both media are sorted to the same functional main classes with different quantities. When analyzing the deeper level of subgroups, more distinctions become obvious, of the specific up-regulated transcripts. Under the 30 highest upregulated subgroups of xylem-sap specific transcripts are some categories, what are not found under the 30 highest upregulated subgroups of SXM specific dataset. Transcripts in these groups emerge in a lower number in SXM. However, in general, the analysis reveals much more encoded proteins of *in vitro* cultivation to be specific up-regulated than under *in situ* conditions.

For the specific up-regulated transcripts as well as for the core-set of transcripts, proteins with functions as CAZys, transcription factors and proteins for cellular transport were detected. These findings highlight the importance of those proteins for surviving under different conditions. However, not for all genes functions could be assigned. This is the case for *PA14_2*, also a core regulated and a pathogenicity relevant gene, which is characterized in this study, could also not been sorted to a functional group.

Overall, the specific up-regulated transcripts reveal a higher number of transcription factors and CAZys for fungal growth under *in situ* conditions than under *in vitro* cultivation. In that pectin and casein rich medium medium, peptidases and pectinases were specifically detected.

As an output of this first transcriptomic analysis, putative encoded proteins being expressed specific or core regulated were identified. Interestingly these various proteins belong to the same functional groups. They have functions in carbohydrate metabolism like CAZys, as fungal transcription factors (TFs) and in cellular transport. When growing inside the vascular system of the plant, the fungus seem to need more expressed transcription factors, protein kinases and CAZys comparing with the *in vitro* growth. The SXM medium does not reflect the xylem medium of *Brassica napus*. In this pectin and casein rich especially peptidases as well as pectinases were found in high numbers. The core-set of proteins contain beside the mentioned CAZys, fungal transcription factors transport proteins a high number of ribosomal proteins as well as peptidases, kinases and binding proteins, required for the fungal growth.These findings are shown in a model in Figure 32.

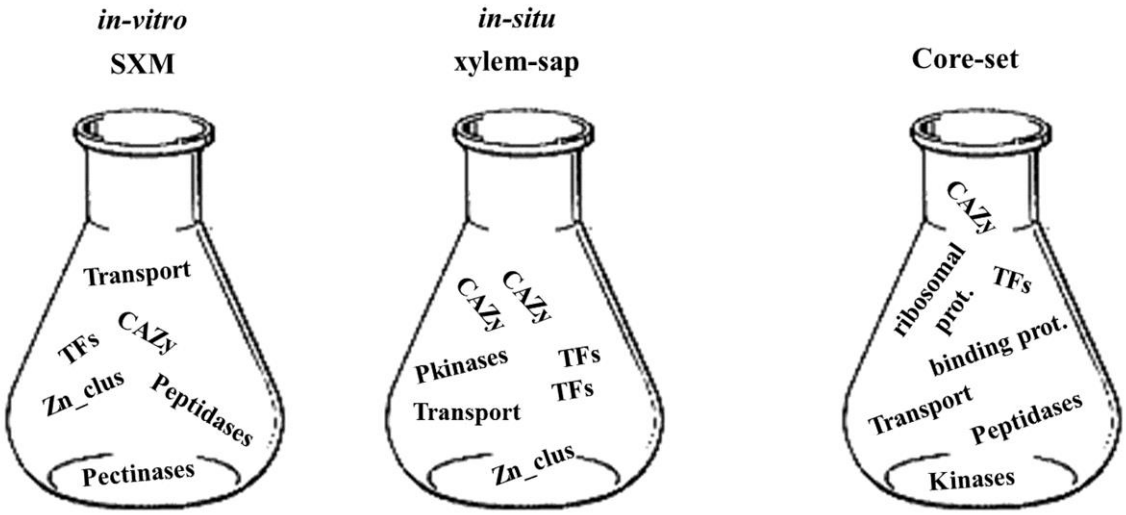

Figure 32: ***Verticillium longisporum* 43 transcriptome reveals SXM not to reflect xylem-sap conditions.** Transcripts of *V. longisporum* core-set and for the specific up-regulated ones, putatively encode for carbohydrate metabolism proteins like CAZys as well as for fungal transcription factors and transport proteins. Under *in situ* (xylem-sap) cultivation conditions more transcription factors and CAZys were detected, than under in *in vitro* (SXM) conditions. In this pectin and casein rich medium especially peptidases as well as pectinases were detected.The core-set includes besides CAZys, transcriptions factors and transporter especially ribosomal proteins, enzymes like peptidases and kinases as well as binding proteins.

4 Discussion

4.1 Thi4, the mitochondrial localized thiazole synthase in *Verticillium dahliae*

The investigation of central metabolic/biochemical pathways in the pathogenic fungus *Verticillium* is crucial to understand its lifestyle and mechanisms of infection. Thereby determined essential genes might be targets for antifungal strategies. It contributes to find a point of attack for stopping infections on plants.

In this study we detected that the *VdTHI4* gene of the thiamine (vitamine B1) pathway is required for plant disease in tomato, induced by the vascular plant pathogen *V. dahliae*. Gene deletion results in a viable strain with defects in hyphal growth (Figure 6 and Figure 9). By complementing the growth reduction on thiamine free minimal medium via thiamine supplementation, it was shown that Thi4 is involved in the thiamine pathway in *V. dahliae* (Figure 11). Similar findings has been reported for ortholog gene deletions of *Fusarium oxysporum* (Ruiz-Roldan *et al.*, 2008) or the plant *Arabidopsis thaliana* (Machado *et al.*, 1996). The protein function for Thi4 was originally described in *Saccharomyces cerevisiae* and the Thi4 family of proteins is required for the formation of the thiazole moiety of thiamine. Recent mass spectrometric protein analyses revealed that *S. cerevisiae* Thi4p acts as a co-substrate rather than an enzyme (Chatterjee *et al.*, 2011; Jurgenson *et al.*, 2009). Putatively VdThi4 is a pseudoenzyme with the ability to bind but without catalytically active functions, like it is known for pseudokinases and other pseudoenzymes (Leslie, 2013).

In the cell, thiamine is a co-factor for several enzymes involved in carbohydrate metabolism but it seems that the protein is not localized in all organisms in the same cell compartiment. The homolog *S. cerevisiae* Thi4p was predicted by sequence analyses to be localized in the mitochondria (Kumar *et al.*, 2002; Machado *et al.*, 1996), but it has been shown by GFP-tagging that it is localized in the cytosol (Mojzita & Hohmann, 2006). In contrast, the maize orthologous gene *thi1* has been shown to be localized in the membrane of chloroplasts (Belanger *et al.*, 1995). The Thi4 protein of *V. dahliae* was predicted by YLoc+ (Briesemeister *et al.*, 2010) to be localized in mitochondria or in the nucleus. Fusing *sGfp* C-terminally to VdThi4 in *Verticillium* and integrating it endogenously reveals a localization pattern in mitochondria by fluorescence microscopy.

The 53% overall sequence similarity between *Verticillium THI4* and *S. cerevisiae THI4* are not equally distributed. Especially the N-terminal regions of *Verticillium* Thi4 and yeast Thi4p protein sequences are not conserved. *S. cerevisiae* has an N-terminal sequence

suggestive of mitochondrial targeting sequences. In general, mitochondrial targeting sequences are positively charged and capable of forming an amphiphilic α-helical secondary structure (Bedwell *et al.*, 1989; Roise & Schatz, 1988). Although there are some negatively charged residues in the fungal N-terminal sequences, a protein could be mitochondrial localized, when they are displayed as helical wheels, and further the positively charged residues are clustered on one side of the protein (Belanger *et al.*, 1995). The N-terminal Thi4 sequence of *V. dahliae* resembles more the positively charged amphiphilic α-helical secondary structure, which is typical for mitochondrial target peptides, than the corresponding N-terminus in yeast. This might be an explanation why VdThi4 is localized in mitochondria in *Verticillium*, which is not the case for the Thi4p in yeast.

Biosynthesis of thiamine diphosphate (ThDP) involves the independent formation of the two moietys 2-methyl-4-amino-5-hydroxymethylpyrimidine (HMP) as well as 4-methyl-5-β-hydroxyethylthiazole (HET). Subsequent phosphorylation and condensation to thiamine monophosphate, is followed by its hydrolysis to free thiamine, and finally a pyrophosphorylation to the active form of thiamine, the thiamine diphosphate (ThDP) (Begley, 1996; White & Spenser, 1982). Most of the enzymes being involved in this whole pathway are discovered in *S. cerevisiae* and are highly conserved in *Verticillium dahliae*, *V. albo-atrum* and *V. longisporum*. They might be comparable in function in the plant pathogens what could be analyzed in further investigations.

Localization of *Verticillium* Thi4 leads to the hypothesis that the synthesis of the HET thiazole moiety occurs in the mitochondria (Figure 13). Afterwards, the HET has to be transported out of the mitochondria into the cytosol where it will be phosphorylated. In the cytosol the active form ThDP is then synthesized from HET and HMP. In contrast to these findings, the HET biosynthesis in *S. cerevisiae* by Thi4p was shown to occur inside the cytosol, where the protein is localized (Mojzita & Hohmann, 2006).

besides vitamine synthesis, the uptake of external thiamine through the plasma membrane was observed in *S. cerevisiae*, which occurs by the thiamine transporter Thi7p. Afterwards thiamine is converted to ThDP by Thi80p inside the cell (Enjo *et al.*, 1997; Singleton, 1997). In the thiamine synthesis deficient *V. dahliae* Δ*THI4* strain it was shown that the yeast Thi7p homologous transporter VDAG_03260.1 (VdThi7) is highly expressed without the presence of thiamine in the minimal CDM medium. Furthermore, the transporter is much higher expressed in thiamine supplemented minimal medium (Figure 11 c). By this the fungus could try to raise the amount of uptaken thiamine that might be converted in the cell to the essential thiamine diphosphate co-factor. This way of thiamine uptake would assure the appearance of

this essential protein in fungal cells. The *Verticillium* Δ*THI4* strain shows a phenotype with a growth defect, suggesting that in this strain another pathway must exist, in which thiamine diphosphate or thiamine is synthesized. Otherwise the fungus could not be able to grow without these essential proteins.

These findings lead to a model of a VdThi4 cellular function during thiamine biosynthesis, which is proposed in Figure 33.

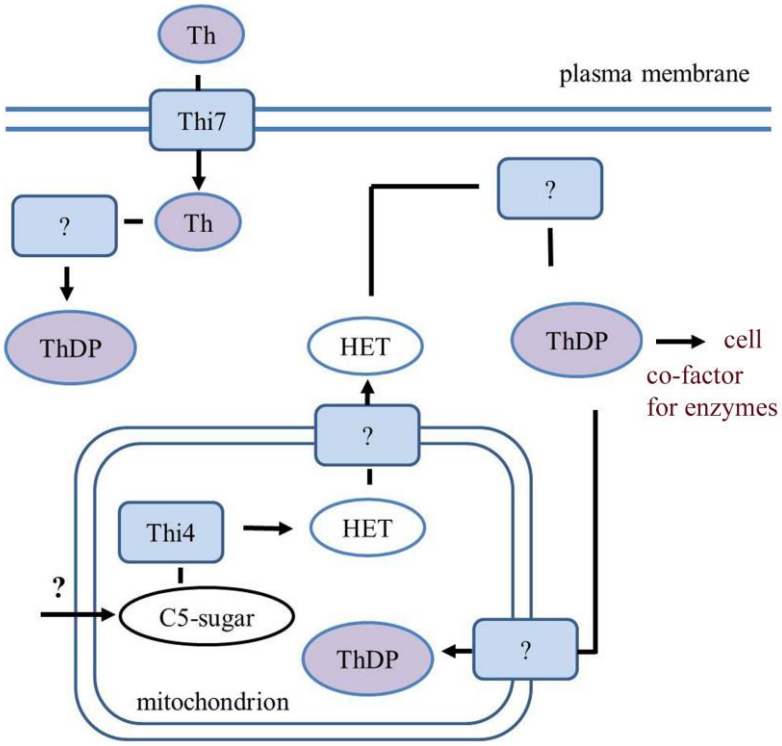

Figure 33: **Model of VdThi4 function in thiamine biosynthesis.** VdThi4 is involved in the synthesis of 4-methyl-5-β-hydroxyethylthiazole (HET), which occurs in the mitochondria and is then transported in the cytosol. There, thiamine diphosphate (ThDP) is synthesized and transported partially back into the mitochondria. The thiamine carrier Thi7 (VDAG_03260.1) transports extracellular thiamine inside the cell, which is there converted by an unknown mechanism to active thiamine diphosphate (ThDP). Enzymes are shown with blue color background, derivates with white and violet color background.

In yeast it was shown that synthesized thiamine diphosphate is transported by the ThDP transporter Tpc1 and the thiamine transporter Thi74 into the mitochondria, where it is involved in the TCA-cycle. In *V. dahliae* the synthesized HET would be transported out of the mitochondria for ThDP formation in the cytosol, which is then transported partially back into these compartments. Furthermore, ThDP is used functionally as a co-factor for several enzymes involved in glucose metabolism (carbohydrate metabolism). For example, it functions as a co-factor for enzymes that catalyze the decarboxylation of α-keto acids and some transfer reactions with aldehyde derivatives, such as the transketolase reaction in the

phosphogluconate pathway (Young, 1986). In the transcriptomic approach, *in situ* growth of *V. longisporum* reveals carbohydrate-active enzymes (CAZys) to be highly expressed (see 3.3). It could be proposed that the analyzed putative *V. dahliae* thiazole synthase VdThi4 and by this thiamine itself is important for the fungus. Proteomic approaches of *B. napus* xylem-sap revealed only low or even no amounts of thiamine. Furthermore, no thiamine was detected in the executed metabolomic approaches on xylem-sap. By this it could be proposed that *V. dahliae* has to synthesize its own thiamine because it occurs nearly no uptake from the xylem-sap.

4.1.1 Involvement of Thi4 in DNA repair mechanism and oxidative stress-response

From other members of the highly conserved thiamine synthase family it is known, that they have been associated with additional and apparently unrelated cellular functions besides their role in thiamine biosynthesis such as tolerance to DNA damage in *A. thaliana* (Machado *et al.*, 1996), maintenance of mitochondrial genome stability in *S. cerevisiae* after UV-light treatment (Machado *et al.*, 1997) or an appropriate oxidative stress response in *F. oxysporum* (Choi *et al.*, 1990; Ruiz-Roldan *et al.*, 2008). In plants, thiamine plays not only a role in oxidative or osmotic stress response, but also to protect against a pathogen attack (Ahn *et al.*, 2005; Rapala-Kozik *et al.*, 2008; Rapala-Kozik *et al.*, 2012; Tunc-Ozdemir *et al.*, 2009).

UV-light leads, amongst other defects, to damage in nuclear and mitochondrial DNA. In order to determine whether *Verticillium* Thi4 plays a role in DNA repair, the response of the *VdTHI4* deletion strain to treatment with DNA damaging agents was examined. The complementation of *S. cerevisiae* and *V. dahliae* UV-sensitive mutants by *V. dahliae* and *V. longisporum THI4* gene was observed and the possible involvement of this gene in DNA damage tolerance was investigated (see 3.1.3). *V. dahliae* Thi4 increases the survival of the fungus under UV-B light induced stress what implicates the involvement of the gene in DNA repair mechanism. In order to assure the function of *Verticillium* Thi4, the UV treatment was also performed with the *Vd*Δ*THI4* strain. The frequency of surviving mutants after UV treatment complemented by the *Verticillium THI4* gene was observed, too. These results are in agreement with further analyses on *S. cerevisiae THI4* (Machado *et al.*, 1997) and *A. thaliana* plant *thi1* genes (Machado *et al.*, 1996). It leads to the assumption that the *Verticillium* Thi4 protein might play a role in avoidance of the deleterious effects of mtDNA damage.

S. cerevisiae subjected to oxidative and osmotic stress showed an increased gene expression and enzymatic activity level of thiamine biosynthesis enzymes like Thi4p (Kowalska *et al.*,

2012). Other studies showed that oxidative stress can lead to the degradation of mtDNA and also the inhibition of base excision repair enhanced mtDNA degradation in response to oxidative damage (Shokolenko *et al.*, 2009). In this study the *VdTHI4* mutant shows a growth reduction upon oxidative stress induced by menadione. Finally, UV-light or oxidative stress causes DNA damage and the degradation of mtDNA because base excision repair is inhibited (Machado *et al.*, 1997; Shokolenko *et al.*, 2009). So, mitochondrial *Verticillium* Thi4 plays presumably a similar role in mtDNA damage tolerance.

4.1.2 Thiazole synthase mutant of *Verticillium dahliae* is impaired in pathogenicity

Verticillium and *Fusarium* are both soil borne plant pathogenic fungi, which can grow in the vascular tissue where the xylem-sap is the only source for nutrients. Even small amounts of thiamine are enough to compensate the lack of Thi4 for growth of *V. dahliae* (Figure 10) or *F. oxysporum* (Ruiz-Roldan *et al.*, 2008). In *V. dahliae* an uptake of external thiamine from the medium might occur by the highly expressed thiamine transporter Thi7 (VDAG_03260.1) (Figure 11 c).

Deletion of the *F. oxysporum* ortholog *sti*35 still results in plant disease on tomato and cucumber plants (Thanonkeo *et al.*, 2000) and suggests that the vitamine supply of the xylem-sap is sufficient for this fungus to grow. Furthermore, a putative fitness deficiency can be compensated when the fungus has entered and colonized the xylem vessels (Jonkers *et al.*, 2009). The plant infection assay on *Solanum lycopersicum* plants revealed that the *Verticillium THI4* deletion strain still enters the plants, but generates no stunting symptoms anymore (see 3.1.4), suggesting that thiamine supply might be not sufficient in the xylem-sap for efficient colonization in *Verticillium*. It was shown in this study that about 0.2 µg/ml thiamine are enough for *V. dahliae* and other studies in *F. oxysporum* revealed that 0.8 µg/ml are sufficient (Ruiz-Roldan *et al.*, 2008). One reason why *V. dahliae* Thi4 deletion strain revealed no stunting symptoms on the host plants, but *F. oxysporum* Δ*sti35* strains retained their pathogenicity, might be a difference in life style. *V. dahliae* stays for longer time in the lower parts of the plant before spreading all over the vascular tissue in contrast to *F. oxysporum* (Eynck *et al.*, 2007; Jonkers *et al.*, 2009). Metabolic and proteomic analysis revealed no thiamine source in the xylem-sap and suggest that *Verticillium* synthesizes its own thiamine in the lower parts of the plant prior to further plant colonization. The additional second function of the enzyme in stress protection might also contribute to the requirement of Thi4 for *Verticillium* to live inside the xylem-vessels and induce plant pathogenicity. In order to investigate differences between *VdTHI4* and *VlTHI4*, *VlTHI4-1*, which was highly

expressed shown by the transcriptomic approaches, was used for heterologous complementation of the *VdΔTHI4* disruption strain. The gene compensated all growth defects and pathogenic effects on tomato plants, what indicates that the two genes have the same functions.

The enzyme VdThi4 is not only required for vitamin B1 biosynthesis but also for an appropriate oxidative stress response. Lack of this dual-function enzyme impairs plant pathogenicity of the fungus. An attractive hypothesis is that the fungus requires primarily the thiamine biosynthetic function in the lower parts of the plant and the UV-damage repair function in the upper parts when exposed to sunlight and UV primarily. In addition, Thi4 might contribute to the ROS-mediated plant response systems (sum up in Figure 34). For further analysis it would be interesting to detect if supplementation of thiamine in a plant-infection assay to the THI4 deletion strain by watering would complement the pathogenicity effect.

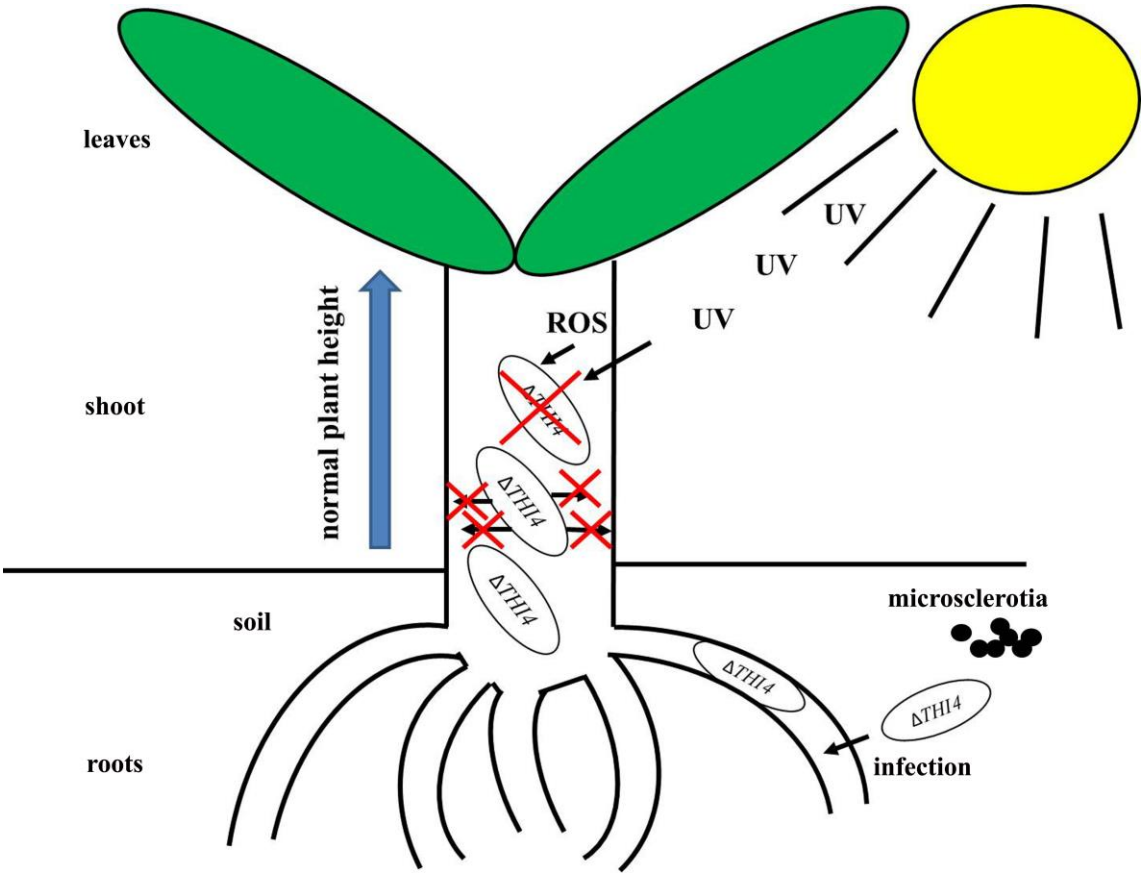

Figure 34: ***VdTHI4* encodes a protein with function in thiamine synthesis that has additional repair function and is required to induce disease on tomato.** *Verticillium* Thi4 is required for thiamine synthesis, in respone to DNA damage agents (like UV or oxidative stress), and to induce disease on tomato. *VdΔTHI4* still enters the plants and grows inside but is apathogenic. No stunting symptoms are detectable. In the model this is shown by the red rectangles covering the arrows. The importance of the *Verticillium* Thi4 protein for DNA damage repair could result in a high mutation rate caused by the UV light emitted by the sun or by ROS. This could lead to a higher frequency of respiration-deficient cells in the upper parts of the plants (red rectangle covering the whole fungal cell).

4.2 The secreted Pa14_2 is involved in melanization and in response to ROS of *Verticillium dahliae*

Besides the intracellular thiamine pathway protein VdThi4, a secreted protein of the *Verticillium* exoproteome called VdPa14_2 was investigated in this study. In plant pathogenic fungi secreted proteins are often involved in the infection process in different ways. Glycosidases or glucanases for example directly affect the host by degrading the polysaccharides of plant cell walls (Albersheim *et al.*, 1969; Hasan *et al.*, 2013). Secreted structural proteins are incorporated into the plasma membrane as well as the cell wall, where they may be involved in recognition processes (Peberdy, 1994). The importance of secreted proteins for the infection of host plants was recently shown in *V. dahliae*, where a cell wall degrading, secreted protein was identified, that is required for pathogenicity (Liu *et al.*, 2013b).

The protein, which is analysed in this study was detected in the exoproteome of *V. longisporum* and named after its PA14_2 containing domain, which is related to a lectin-like binding domain. This PA14 domain can be found in a variety of fungal adhesins like the *S. cerevisiae* flocculins, in bacterial and eukaryotic glycosidases as well as glycosyl transferases like bacterial toxins, enzymes, adhesins and signaling molecules (Kobayashi *et al.*, 1998; Linder & Gustafsson, 2008; Rigden *et al.*, 2004; Zupancic *et al.*, 2008). In addition, this domain is involved in carbohydrate binding.

VdPa14_2 is less conserved in other organisms, whereas only 38% of the functional domain is identical with proteins in other plant pathogenic fungi. However, for PA14 domain containing proteins it was shown that they do not need highly sequence similarities to belong to the same protein family. The sequences of the β-galactosidases from *Kluveromonas fragilis* (Raynal *et al.*, 1987), *Agrobacterium tumefaciens* (Castle *et al.*, 1992), *Clostridium stercorarium* (Schwarz *et al.*, 1989) and *Thermotoga neapolitana* (Zverlov *et al.*, 1997) share a pairwise identity of about 40% and the proteins belong to the same family of glycosidases (glycoside hydrolases) (Henrissat, 1991). *Verticillium* Pa14_2 seems to be specific and highly conserved in *V. dahliae*, *V. albo-atrum* and *V. longisporum*, but might share the function with hypothetic proteins of the phytopathogenic fungi *Colloetrichium gloeospoioides* and *Gaeumannomyces graminis*. Most proteins described for the related PA14 domain contain more than one functional domain (Rigden *et al.*, 2004). However, no additional conserved domain was detected by Interpro scan for *Verticillium* Pa14_2 protein. Interestingly the amino acid sequence GLEYA (which is named after the containing amiono acids) is localized N-terminally of the functional PA14_2 domain. In case of described proteins, this sequence is

located inside the PA14_2 domain (Linder & Gustafsson, 2008). This led to the hypothesis that the GLEYA sequence of VdPa14_2 might act as a second domain, which is needed to be analyzed in further investigations.

In addition, sequencing data and Southern hybridization (Figure 17 and Figure 22) propose only one gene in the allodiploid *V. longisporum*. These results might be due to the fact that the sequences of the putative parental strains *V. dahliae* and *V. albo-atrum* (Clewes *et al.*, 2008; Collado-Romero *et al.*, 2010; Inderbitzin *et al.*, 2011b; Tran *et al.*, 2013) are highly similar, which is very difficult to discriminate for the assembly programs. In the transcriptomic datasets for *V. longisporum* 43 seems to be a hint for a second isogene, but this includes only one half of the gene.

A signal peptide cleavage site suggested the VdPa14_2 protein can be secreted. The protein was predicted by YLoc+ (Briesemeister *et al.*, 2010) and a localization at the membrane was shown by Gfp-tagging (Figure 23). This localization could be a hint for being functionally involved in adherence to interaction partners. An adhesion assay in *S. cerevisiae* revealed that VdPa14_2 is not involved in surface adherence. Presumably, the protein is not directly located in the membrane due to the fact that it does not contain any transmembrane helices or a GPI anchor; possibly it interacts with a membrane-bound protein. However, the direct cell wall attachment without GPI anchor was described for proteins containing a GLEYA domain (Linder & Gustafsson, 2008) and could also occur for VdPa14_2.

This *Verticillium* protein might have a function in carbohydrate metabolism and/or binding. These functions were shown for proteins containing the experimentally characterized related lectin-like ligand-binding PA14 domain (de Groot & Klis, 2008; Rigden *et al.*, 2004; Yoshida *et al.*, 2010). Pa14_2 mutants deficiency in producing the typical black color of melanized microsclerotia (Pegg & Brady, 2002) (Figure 19) assuming a functional role of the protein in the melanin biosynthesis pathway by a putative function in the carbohydrate metabolism and/or binding affecting the melanin production. Carbohydrate metabolism is highly important for the fungus. In the transcriptomic approach of *Verticillium in situ* growth, carbohydrate active enzymes (CAZys) were detected to be highly expressed (see 3.3). A deficiency in carbohydrate metabolism concerning of *PA14_2* deletion, seems to affect cellular processes like melanization. Another possibility is that the melanin synthesis, produced by polyketide biosynthesis, still works but the last step of polymerization of 1,8-dihydroxynaphthalene (DHN) is disturbed and melanin is not turned to black color. The DHN melanin has been implicated as a pathogenicity factor in some fungal plant diseases and animal mycoses (Geis *et al.*, 1984; Kubo *et al.*, 1982; Wheeler & Stipanovic, 1985; Wolkow

et al., 1983; Woloshuk *et al.*, 1983). In *Colletotrichum lagenarium* for example the induced inhibition of appressoria pigmentation by tricyclazole resulted in a phenotype, where the colorless appressoria germinated laterally and, consequently, could not penetrate nitrocellulose membranes (Kubo *et al.*, 1982). Furthermore, in the rice blast disease causing fungus *Magnaporthe grisae* it was shown that mutants defective in melanin biosynthesis are also not able to penetrate the host by appressoria (Chumley & Valent, 1990). Both fungi have a complete different infection mechanism compared to *Verticillium*, but all fungi need to enter the epidermis of their hosts. Black melanized microsclerotia have a central role in pathogen survival and in initiating the infection trough the plant roots. Therefore, the microsclerotia of could be targets for disease control (Duressa *et al.*, 2013). Real-time PCR revealed an influence of VdPa14_2 in the polyketide biosynthesis, which produces melanin. No polyketide synthase 1 (*PKS1*) gene was expressed in VdPa14_2 deletion strain, in contrast to *V. dahliae* wild type (Figure 20). Furthermore, *PKS1* is also not expressed in the not completely black colored complementation strains. This could be due to the fact of the complicated arrangement of clusters like the *PKS1* cluster. If the chromosomal structure is not exactly arranged like in wild type, the cluster is maybe not functional. Possibly, the insertion of the second exogenous inserted *VdPA14_2* copy disturbs the expression of the *PKS1* cluster. This might be an explanation for this partial complementation phenotype. Or this second copy in the complementation strain evokes an overexpression of *VdPA14_2*, which results in the slightly black partial complementation phenotype.

Interestingly, the deletion of Pa14_2 in *V. dahliae* shows increased resistance to the reactive oxygen species menadione (Figure 24). The membrane bound protein negatively affects the cellular response to ROS being involved either directly or as a co-factor bound to a protein. This would be interesting to find out in further investigations. It was not possible to complement the decrease of resistance against oxidative stress in the *VlPA14_2-1* heterologous complemented strain. This effect could be influenced by the additional integrated ectopical gene copy. In general, the gene complementation strains are confirmed by the regaining pathogenicity to host plants (3.2.4). The two cellular functions of VdPa14_2 in melanization and the decrease in resistance to oxidative stress are shown in a model (Figure 35).

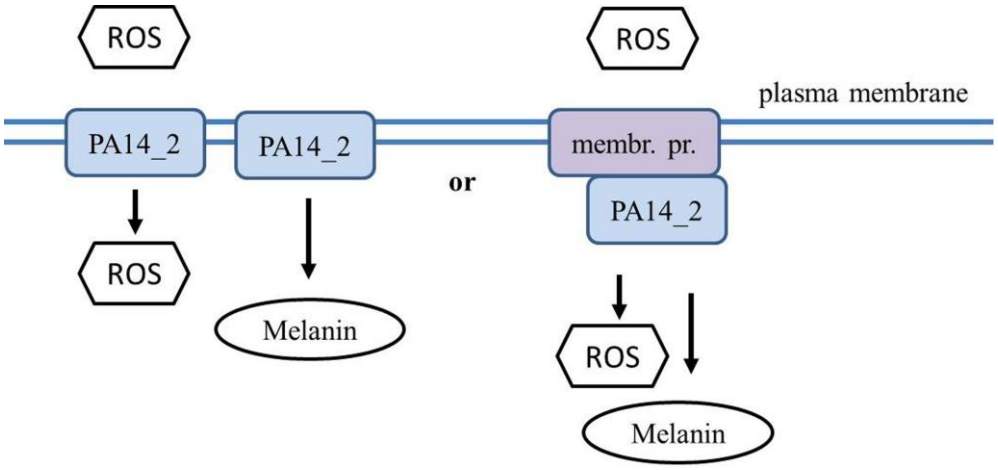

Figure 35: **Pa14_2 is involved in melanization and reduces resistance against ROS.** The membrane-bound Pa14_2 protein is either directly bound to the membrane or bound to a membrane protein. It affects the response to ROS negatively, resulting in a reduced phenotype growth. Beside this function, the protein is needed for the synthesis of black colored melanin in the cell. This was observed by a non-melanizing knockout that does not express the *PKS1*, which is important for melanin synthesis

4.2.1 *Verticillium dahliae* Pa14_2 mutant is impaired in infection process on host plants

The infection assay on *Solanum lycopersicum* plants reveals that the *V. dahliae* PA14_2 deletion strain is deficient in entering the host plants (3.2.4). This is obvious by detecting only 1/10 of the fungal DNA amount on infected plant material for the knockout strain, than for wild type strain. In this less abundance, the Pa14_2 deletion strain is not able to induce infection symptoms on host plants. Both effects, the stunting symptoms as well as the high amount of fungal DNA could be complemented homologous (with *VdPA14_2*) and heterologous (with *VlPA14_2-1*) confirming the accuracy of the mutant.

The deficiencys in the melanin synthesis might handicap the *VdPA14_2* deletion strain entering the host plants epidermis during infection process. Infection of susceptible plants by *Verticillium* occurs either at the root tip, via wounds or at the sites of lateral root formation (Bishop & Cooper, 1983). The fungus has to cross the epidermis of the roots and inside the endodermis to enter the central cylinder. It was shown that the melanin deficient mutant of the rice blast disease causing fungus *M. grisae*, which is no longer able to penetrate the epidermis, successfully infected plants through wounds in the leaf epidermis (Chumley & Valent, 1990). During the used laboratory process of infection by root dipping, most likely the roots have been wounded. The small amount of VdPa14_2 mutant fungal DNA in infected plant material leads to the hypothesis that the non-melanizing fungus is impaired in the infection process directly, but could enter the host plants through these lesions in the root epidermis. The slightly melanizing complementation strains infect the host plants like the

wild type strain again. This indicates that a small amount of black coloured melanin is sufficient for the infection process on the plants. For further analyses it would be interesting to investigate, if melanin or microslerotia are produced by the *VdPA14_2* mutant strain and how much is produced in the complementation strains.

In this study, an effect on melanin production for the membrane located VdPa14_2 protein was revealed, which is important for plant infection on tomato plants. As a second function the protein might indicate a negative effect to the cellular response to ROS, which has to be further investigated. These analyzed functions of VdPa14_2 on host plants are shown in a model (Figure 36).

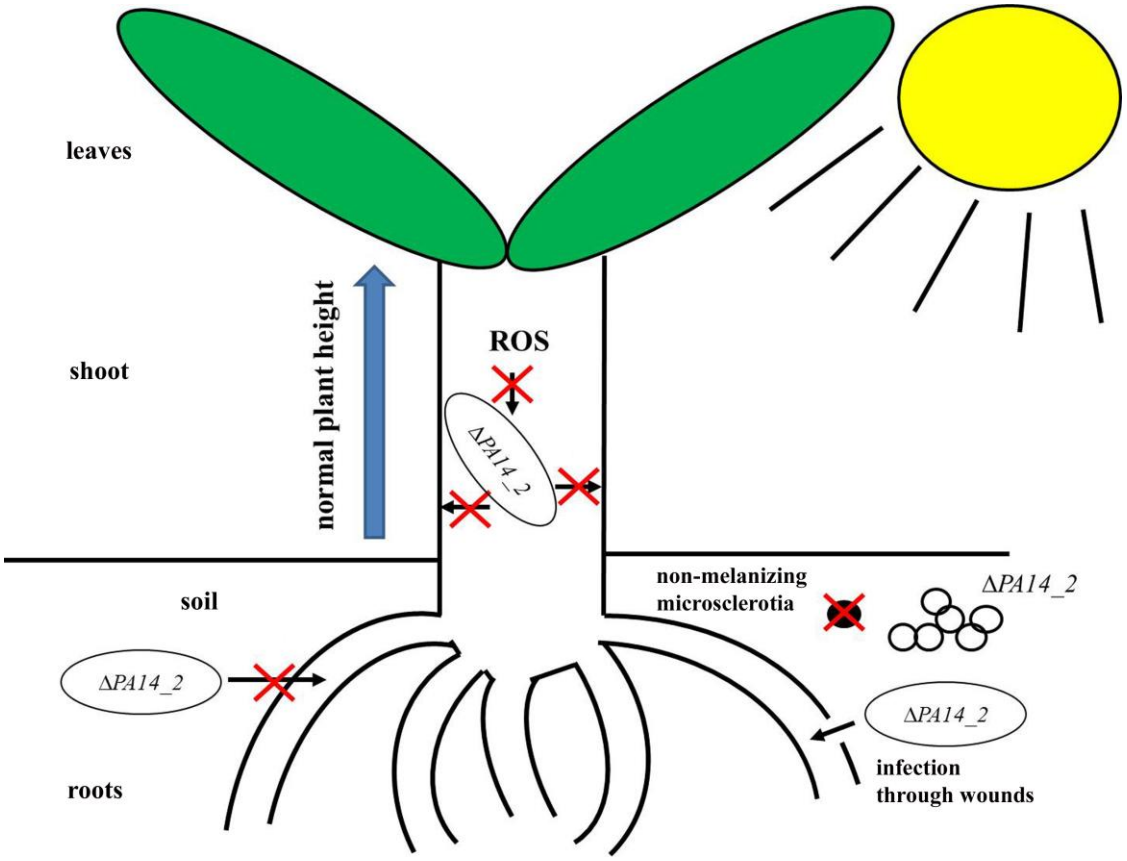

Figure 36: **Non-melanizing Δ*PA14_2* mutant lost the ability to infect the host.** The non-melanizing Pa14_2 mutant strain (shown with white microsclerotia inside the soil) is impaired in infecting the host plant. This is shown on the left side of the model, where the fungus can not enter the roots. The deletion strain is putatively only able to enter the roots through wounds in the cortex (right side of the model in the soil). A small amount of the fungus enters the central cylinder, which is too less for inducing infection symptoms (red crosses over the arrows). Inside the cell, the loss of the Pa14_2 protein increases the resistance against ROS, what leads to the assumption that the putative carbohydrate metabolism protein negatively affects the cellular response to ROS.

4.3 Protoplastation as established DNA transformation method in *Verticillium dahliae*

DNA transformation in *Verticillium* was performed until now by *Agrobacterium tumefaciens*-mediated transformation (ATMT) (Jyothishwaran *et al.*, 2007; Singh *et al.*, 2010; Singh *et al.*, 2012; Timpner *et al.*, 2013; Tran *et al.*, 2013; Zhou *et al.*, 2013a). Using this method, a binary vector with the knockout or silencing cassette has to be constructed before inserting it in *A. tumefaciens*. For RNAi processes in the allodiploid fungus *Verticillium longisporum* this is the only established technique for transformation.

In this study the protocol for DNA insertion via protoplastation in *Verticillium dahliae* was adjusted. This protoplastation based DNA transformation method was used to perform knockout construction or other integrations (Punt & van den Hondel, 1992) in the haploid fungi. This method is faster and easier to use compared to the *Agrobacterium*-mediated transformation method. On the one hand, the integration cassette is transformed linear into the fungus and no binary vector has to be constructed, which has to be first transformed into *A. tumefaciens*. On the other hand, transformants grow up in 7-9 days on the plate and the whole transformation process can be performed on one day with overnight grown mycelium.

The numbers of positive transformants is nearly equal to the output of positive transformants using the *A. tumefaciens*-mediated transformation. In this study the two different techniques were compared when performing a knockout of two genes in *V. dahliae* (data not shown).

It points out that the rate of positive transformants depends essentially on the gene of interest. In the case of *VdΔTHI4* 38% of the ATMT transformants were positive. Using the protoplastation method 27% of the screened closes were positive. In order to screen for a *VdPA14_2* mutant, in total 44 transformants from ATMT (25 clones) and protoplastation transformation (19 clones) were tested to find two positive clones only by the protoplastation based method. This is a success rate of 10%. For *GFP*-tagged *THI4* 40% (two of five) of the tested clones made by protoplastation based transformation were positive.

Finally, DNA integration by protoplastation based transformation is an effective method that is easy to use for haploid *Verticillium* strains.

4.4 *Verticillium longisporum* 43 specific and core-set regulated transcripts belong to the same protein familys

Verticillium longisporum is a host specific soil-borne plant pathogenic fungus that infects only *Brassicaceae*. Disease cycle as well as its biotrophical growth inside the vascular system is already known. In contrast, the transcriptional regulation in *V. longisporum* is yet not analyzed. It is unknown which genes are specific up-regulated inside the host and which belong to the core-set of the fungus. Furthermore, the question why the allodiploid *V. longisporum* is host specific to *Brassicaceae* and the putative parental strains *V. dahliae* and *V. albo-atrum* (Clewes *et al.*, 2008; Collado-Romero *et al.*, 2010; Inderbitzin *et al.*, 2011b; Tran *et al.*, 2013) are not, is still unanswered. At the end of these findings a putative point of attack on the fungus usable for agriculture would be desirable.

The new high-throughput sequencing systems have revolutionized genome sequencing as well as expression analysis (Lister *et al.*, 2009; Rusk & Kiermer, 2008). It enables to compare transcript abundance quantitatively among many samples with relatively low costs and can be used even on organisms with less analyzed genomes. The investigation on transcriptome by deep sequencing of *V. longisporum* 43 growing *in situ* in harvested *B. napus* xylem-sap compared with the *in vitro* growth in the synthetic SXM medium (Neumann & Dobinson, 2003) is a part of the global investigations that includes genome sequencing as well as transcriptomic, proteomic and metabolomic analyses.

For the putative parental strain *V. dahliae*, several studies have characterized transcriptomic changes in cotton defense response by hybridization- or sequence-based approaches (Hill *et al.*, 1999; Zuo *et al.*, 2005). However, the polyploid cotton genome is highly complicated, and the limited information cannot provide a comprehensive understanding of the cotton defense response to *V. dahliae*. In the fungus extracted from the infected *Gossyphium barbadense* cotton plants, 3,442 defense responsive genes were identified by deep sequencing and qPCR methods. Furthermore, 211 unique genes were differentially identified in the *G. barbadense* response to *V. dahliae* by combining hybridization experiments and microarray (Xu *et al.*, 2011). Recently, transcriptome profiling of *V. dahliae* and tomato interaction has been performed to study incompatible and tolerant interactions and further, to identify genes playing a role in host defense (Robb *et al.*, 2007; Van Esse *et al.*, 2009). RNA-seq studies on *V. dahliae* microsclerotia revealed microsclerotia specific up-regulated genes, which might be new targets for disease control (Duressa *et al.*, 2013).

Cultivating the allodiploid *V. longisporum* under *in situ* and *in vitro* conditions, in toal 21,192 transcripts were detected in this thesis to be regulated. In the haploid putative parental *V. dahliae* 10,500 genes were predicted to be regulated in total (Klosterman *et al.*, 2011). This is about half of the gene amount of *V. longisporum*. In this allodiploid fungus about 38% (8,121) of these detected transcripts were unchanged or weakly regulated and therefore defined as the core-set of genes being expressed in all conditions. Transcripts being *in situ* or *in vitro* expressed in *V. longisporum*, revealed a specific expression in total of about 15% (1,500 genes each) under both investigated conditions in the plant pathogenic fungus.

About 9700 transcripts were not described. These are transcripts being detected with RPKM data of transcripts that are regulated different in the same cultivation condition. This was detected for the transcripts of *Verticillium THI4*, which is described in this thesis to be involved in the thiamine synthesis and to be a pathogenic relevant gene in *Verticillium*. Its transcripts are not included in the groups of specific up- or core regulated transcripts. This gene is much more expressed under *in vitro* cultivation conditions than under *in situ* with a varying expression in SXM between RPKMs of about 60 and 160 for *VlTHI4-1* and 30-80 for *VlTHI4-2*.

4.4.1 Core-regulated transcripts

Most predicted proteins of the core-set of genes in *V. longisporum* are localized in the cytoplasm of the cell and in the nucleus, what was expected because there most of the metabolism reactions and the transcription of genes occurs. The detection of localization in detail was quite different in output of the two used tool WoLF PSORT (Horton *et al.*, 2007) and YLoc+ (Briesemeister *et al.*, 2010). This could be explained by the different algorithms of the tools and by the fact that these predictions are dependent on different parameter settings.

Most of the equally expressed transcripts were predicted to encode for proteins of the functional category “metabolism”, especially C-compound and carbohydrate metabolism. Lots of those proteins were found to be CAZys (carbohydrate active enzymes). By Pfam analysis and categorization it was shown that ribosomal proteins with functions in RNA-synthesis and lots of transcription factors as well as binding proteins and enzymes like kinases and peptidases are needed in high amounts by the fungus. Furthermore, proteins for transport seem to belong to the most needed proteins in the core-set of *V. longisporum*. These findings were expected for a living organism. In the cell, carbohydrate-active enzymes are important for enzymatic reactions. The CAZy classification includes all enyzmes being involved in the synthesis, metabolism and transport of carbohydrates (Cantarel *et al.*, 2009). The transcription factors

always acting as master switches by controlling the expression of series of genes with slight changes in expression to regulate different plant development or response to biotic and abiotic stresses (Singh *et al.*, 2002). In general, the analysis by categorization of the transcripts by "Hivi" tool and the analysis of Pfam domains confirm each other.

4.4.2 Specific regulated transcripts

This study on *V. longisporum* revealed that xylem-sap and SXM are highly different to each other and an overview of the HCA (hierarchical cluster analysis) as well as the 1D self-organizing map of all transcripts from *in situ* (xylem-sap) and *in vitro* (SXM) cultivation vizualizes the high disparties of the media. The simulated xylem medium (SXM) was designed by Neumann and Robinson to reflect the nutritional conditions of the vascular fluid (Neumann & Dobinson, 2003). Specific gene expression in SXM and xylem-sap grown fungus are highly different, what revealed that the SXM does not reflect the nutritional conditions of the *in vivo* vascular fluid inside host plants. Hence, for further global analyses these distinctions between *in situ* cultivation in xylem-sap and *in vitro* cultivation in SXM medium should be receiving attention.

The analyses of media specific expressed transcripts compared gene regulation in *V. longisporum* grown *in situ* and *in vitro* revealed differences and similarities in the gene functions. In the complex *in vitro* medium more transcripts for metabolism predicted proteins are specific up-regulated. Growing in this medium the fungus seem to need genes encoding especially for amino acid biosynthesis (like transferases, oxidases, transketolases, deacetylases, transaminases and dehydrogenases as well as biosynthetic proteins), and nitrogen sulfur and selenium (like oxigenases, synthases, lyases, GTPases, aminotransferases, reductases, transferases, a desulfurizing enzyme, allantoicase and a nitrogen permease regulator) as well and proteins for C-compound and carbohydrate predicted proteins (like reductases, dehydogenases, hydolases, oxidases, transport proteins, precursor proteins, dehydratases, thiolases and transferases). As expected, this study reveals also enzymes, which seem to be needed specifically by *V. longisporum* for growing in the pectin-rich medium. Growing, under these *in vitro* cultivation conditions the highly expressed family of peptidases that can hydrolyze the peptide bonds linking amino acids in the polypeptide chain of proteins (Rawlings *et al.*, 2010), contains important enzymes. Besides these proteins, peptidases were detected as it was expected. In general, more genes being predicted for a protein synthesis function seem to be highly specific expressed in the full medium SXM compared to xylem-sap.

Nearly for all detected functional groups, more transcripts expressed in SXM were predicted. On the one hand this could be attributed to the higher number of specific expressed transcripts in SXM and on the other hand this leads to the conclusion that the supposed full medium SXM is not a perfect medium for the fungus and especially is not identical to the xylem-sap.
Further analyses in *V. dahliae* extracted from infected plant material revealed, that most of the expressed genes belong to "metabolic processes" directly followed by genes involved in "nitrogen compound metabolic" and "secondary metabolism" (Xu *et al.*, 2011). For *V. longisporum*, in this study it was detected that genes with nitrogen and secondary metabolism functions were specifically up-regulated under *in situ* cultivation condition, what fits nicely to the results from the vascular grown *V. dahliae* strain. Furthermore, most needed proteins for the life in the vascular system, are proteins of metabolism. In this vascular medium, the highest number of the predicted proteins was localized in the cytoplasm of the cell and in the nucleus, where most of the metabolism reactions and the transcription of genes, occur. In comparison to the SXM specific up-regulated putative proteins, more CAZys and especially transcription factors were found to be specific for xylem-sap. The detection of a high number of medium specific up-regulated transcripts which encode for CAZys was expectable. This is due to the fact, that both media contain different carbon sources.
Most specific up-regulated genes of *in situ* cultivation are predicted to be putative proteins for transcription and its regulation such as splicing factors, proteins of transcription activator complex, transcriptional regulators, RNA polymerase subunits, putative RNA helicases, repressors, activators and Zn_finger proteins. This might result in the assumption that xylem-sap is a kind of "minimal medium" for the fungus. Inside the vascular host plants system the fungus could take up less nutrients from this medium meaning that the filamentous fungus needs to synthesize all essential nutrients itself for survivial and pathogenicity. This synthesis of essential nutrients while living inside the vascular system was demonstrated in former studies that revealed a bradytrophic mutant of *V. longisporum* with reduced pathogenicity on *B. napus* in a strain with reduced activity of the aromatic amino acid enzyme chorismate synthase (vl43-au16.g15076) (Singh *et al.*, 2010). Furthermore, deletion of the thiamine pathway involved *THI4* gene in this study was shown to cause growth deficiencies and apathogenicity of the fungus (3.1). Unfortunately, *VlTHI4* (vl43-au6.g10019.t1 and vl43au16.g10016.t2) is not included in the functional analyses of specific up-regulated or in the core regulated transcripts. The RPKM data revealed the transcripts to be regulated differenty when growing under SXM cultivation condition. This unstable expression pattern was also detected for the chorismate synthase gene likewise. Hence, this pathogen relevant gene,

which is required for life inside the xylem vessels, was not included in the specific up- or core-regulated analyses approaches.

The analysis of the transcriptomic dataset by sorting the associated Pfam domains of putative encoded proteins (Mulder *et al.*, 2005; Sonnhammer *et al.*, 1997) is a different approach of categorization. By this analysis 1257 domains were detected to be assigned specifically in xylem-sap and 1377 in SXM. In general it was expected to detect differences of the expressed transcripts, when comparing two different cultivation conditions. In this approach we could raveal the SXM medium not to simulate the xylem-sap artificially.
When growing inside the xylem vessels, the fungus needs to produce lots of its own nutrients. The Pfam domain predicition reveals that most of the putative proteins specific up-regulated in xylem-sap or SXM are (Zn_cluster) transcription factors. Also protein kinase and CAZy domains were detected among the specifically up-regulated genes. Interestingly growing in xylem-sap the fungus needs more CAZys expressed, than under *in vitro* growth conditions. It seems that the fungus needs to express more genes to use the carbon sources when growing in the vascular system, than when growing in the artificial SXM medium. This approach of analysis confirms the described categorization method. As expected, in the pectin and casein rich medium SXM, domains for pectinases and peptidases seem to appear in much higher amounts than in the *in situ* medium. Pectinases are highly important for plant pathogenic fungi. The plant cell walls consist mainly of polysaccharides (i.e. cellulose, hemicelluloses and pectins), which could be degraded by secreted fungal pectiases. Pectinases are pectin degrading enzymes, playing an important role in the plant-pathogen interaction (Juge, 2006).
In general, the analyses of protein domains by Pfam analyses have advantages compared with the analyses of predicted functional categories via annotation by *Fusarium graminearum* genes, which are used by the "Hivi" tool. On the account, using *F. graminearum* for annotation, all *Verticillium* specific genes are not included in the analyses, because they can not be annotated. This was the case for the core regulated *Verticillium PA14_2* (vl43-au16.g5346) gene, which is *Verticillium* specific and shown in this study to be relevant for pathogenicity. The transcript of the *PA14_2* gene is not highly but core expressed. This reveals pathogenic genes not to be xylem-sap specific. Besides *Verticillium* specific genes, all genes, which are not accurate annotated in *F. graminearum*, were missing in this analysis approach. *V. longisporum CPC1* (vl43-au16.g19783 and vl43-au16.g20638) (Timpner *et al.*, 2013) is conserved in *F. graminearum* (FGSG_0928, GenRE) with more than 50% of its

amino acid sequence, but its annotation is only predicted in that fungus. Obvious this core regulated gene was not included for annotation.

To penetrate and use the plant cell wall nutritions, pathogens secrete a remarkable array of polysaccharide degrading enzymes. Deep sequencing of *V. dahliae* response to cotton plants revealed that the defense-responsive genes were classified into 22 biological processes, including metabolism, transport, catabolic process, response to stress and stimulus, biosynthetic process, regulation, cell communication, and others (Xu *et al.*, 2011). In further analyses it would be interesting to investigate the fungal response of *V. longisporum* 43 to plant response of *B. napus*, when growing inside the vascular system in order to identify effector proteins in transcriptomic approaches on *B. napus* infected plants.

5 References

Agrios G (2005) Plant pathology, 5th edn. *Elsevier academic press, USA.*

Ahn IP, Kim S, Lee YH (2005) Vitamin B1 functions as an activator of plant disease resistance. *Plant physiology* 138: 1505-1515

Ahrazem O, Prieto A, Gimenez-Abian MI, Leal JA, Jimenez-Barbero J, Bernabe M (2006) Structural elucidation of fungal polysaccharides isolated from the cell wall of *Plectosphaerella cucumerina* and *Verticillium* spp. *Carbohydrate research* 341: 246-252

Albersheim P, Jones TM, English PD (1969) Biochemistry of the cell wall in relation to infective processes. *Annual review of phytopathology* 7: 171-194

Albersheim P, Valent BS (1974) Host-Pathogen Interactions: VII. Plant Pathogens Secrete Proteins which Inhibit Enzymes of the Host Capable of Attacking the Pathogen. *Plant physiology* 53: 684-687

Altschul SF, Gish W, Miller W, Myers EW, Lipman DJ (1990) Basic local alignment search tool. *Journal of molecular biology* 215: 403-410

Amyotte SG, Tan X, Pennerman K, Jimenez-Gasco Mdel M, Klosterman SJ, Ma LJ, Dobinson KF, Veronese P (2012) Transposable elements in phytopathogenic *Verticillium* spp.: insights into genome evolution and inter- and intra-specific diversification. *BMC genomics* 13: 314

Babadoost M, Chen W, Bratsch AD, Eastman CE (2004) Plant Pathology. *Plant pathology journal* 53: 669–676

Bahler J, Wu JQ, Longtine MS, Shah NG, McKenzie A, 3rd, Steever AB, Wach A, Philippsen P, Pringle JR (1998) Heterologous modules for efficient and versatile PCR-based gene targeting in *Schizosaccharomyces pombe*. *Yeast* 14: 943-951

Balasubramanian V, Vashisht D, Cletus J, Sakthivel N (2012) Plant beta-1,3-glucanases: their biological functions and transgenic expression against phytopathogenic fungi. *Biotechnology letters* 34: 1983-1990

Bandeiras TM, Freitas MC, Petrasch D, Kletzin A, Frazao C (2013) SAD phasing towards structure determination of a thermostable Rieske ferredoxin with a novel stabilizing disulfide bridge. *Acta crystallographica section F, structural biology and crystallization communications* 69: 555-558

Barbara DJ, Clewes E (2003a) Plant pathogenic *Verticillium species*: how many of them are there? *Molecular plant pathology* 4: 297–305

Barbara DJ, Clewes E (2003b) Plant pathogenic Verticillium species: how many of them are there? *Molecular plant pathology* 4: 297-305

Bartnicki-Garcia S (1968) Cell wall chemistry, morphogenesis, and taxonomy of fungi. *Annual review of microbiology* 22: 87-108

Bedwell DM, Strobel SA, Yun K, Jongeward GD, Emr SD (1989) Sequence and structural requirements of a mitochondrial protein import signal defined by saturation cassette mutagenesis. *Molecular and cellular biology* 9: 1014-1025

Begley TP (1996) The biosynthesis and degradation of thiamin (vitamin B1). *Natural product reports* 13: 177-185

Belanger FC, Leustek T, Chu B, Kriz AL (1995) Evidence for the thiamine biosynthetic pathway in higher-plant plastids and its developmental regulation. *Plant molecular biology* 29: 809-821

Bell AA, Wheeler MH (1986) Biosynthesis and Functions of Fungal Melanins. *Annual review of phytopathology* 24: 411-451

Berlanger I, Powelson ML (2000) Verticillium wilt, *The plant health instructor*.

Bhat RG, Smith RF, Koike ST, Wu BM, Subbarao KV (2003) Characterization of *Verticillium dahliae* isolates and wilt epidemics of pepper. *Plant disease* 87: 789-797

Bishop CD, Cooper RM (1983) An ultrastructural study of root invasion in three vascular wilt diseases, Vol. 22, *Physiological plant pathology*.

Bocobza SE, Malitsky S, Araujo WL, Nunes-Nesi A, Meir S, Shapira M, Fernie AR, Aharoni A (2013) Orchestration of thiamin biosynthesis and central metabolism by combined action of the thiamin pyrophosphate riboswitch and the circadian clock in *Arabidopsis*. *The plant cell* 25: 288-307

Briesemeister S, Rahnenfuhrer J, Kohlbacher O (2010) Going from where to why--interpretable prediction of protein subcellular localization. *Bioinformatics* 26: 1232-1238

Brown GM (1970) Merabolic Pathways, Vol. 4 (Ed.: D. M. Greenberg).

Brown GM (1971) Comprehensive Biochemistry, Vol. 21 . (Eds.: M. Florkin, E. H. Stotz).

Busch S, Eckert SE, Krappmann S, Braus GH (2003) The COP9 signalosome is an essential regulator of development in the filamentous fungus *Aspergillus nidulans*. *Molecular microbiology* 49: 717-730

Butterworth RF (2003) Thiamin deficiency and brain disorders. *Nutrition research reviews* 16: 277-284

Cantarel BL, Coutinho PM, Rancurel C, Bernard T, Lombard V, Henrissat B (2009) The Carbohydrate-Active EnZymes database (CAZy): an expert resource for Glycogenomics. *Nucleic acids research* 37: D233-238

Castle LA, Smith KD, Morris RO (1992) Cloning and sequencing of an *Agrobacterium tumefaciens* beta-glucosidase gene involved in modifying a vir-inducing plant signal molecule. *Journal of bacteriology* 174: 1478-1486

Castroverde CDM, R.N. N, Robb J (2010) Defence genes in tomato., *Nova science publishers inc, Hauppauge.*

Chatterjee A, Abeydeera ND, Bale S, Pai PJ, Dorrestein PC, Russell DH, Ealick SE, Begley TP (2011) *Saccharomyces cerevisiae* THI4p is a suicide thiamine thiazole synthase. *Nature* 478: 542–546

Chatterjee A, Jurgenson CT, Schroeder FC, Ealick SE, Begley TP (2006) Thiamin biosynthesis in eukaryotes: characterization of the enzyme-bound product of thiazole synthase from *Saccharomyces cerevisiae* and its implications in thiazole biosynthesis. *Journal of the american chemical society* 128: 7158-7159

Cheah MT, Wachter A, Sudarsan N, Breaker RR (2007) Control of alternative RNA splicing and gene expression by eukaryotic riboswitches. *Nature* 447: 497-500

Choi GH, Marek ET, Schardl CL, Richey MG, Chang SY, Smith DA (1990) *sti35*, a stress-responsive gene in *Fusarium* spp. *Journal of bacteriology* 172: 4522-4528

Christakopoulos P, Kekos D, Macris BJ, Claeyssens M, Bhat MK (1995) Purification and characterization of a less randomly acting endo-1,4-beta-D-glucanase from the culture filtrates of *Fusarium oxysporum*. *Archives of biochemistry and biophysics* 316: 428-433

Christakopoulos P, Nerinckx W, Kekos D, Macris B, Claeyssens M (1996) Purification and characterization of two low molecular mass alkaline xylanases from *Fusarium oxysporum* F3. *Journal of biotechnology* 51: 181-189

Chumley FG, Valent B (1990) Genetic analysis of melanin-deficient, nonpathogenic mutants of *Magnaporthe grisea*. *Molecular plant-microbe interactions* 3: 135-143

Clewes E, Edwards SG, Barbara DJ (2008) Direct molecular evidence supports long-spored microsclerotial isolates of *Verticillium* from crucifers being interspecific hybrids. *Plant pathology journal* 75: 1047-1057

Collado-Romero M, Jimenez-Diaz RM, Mercado-Blanco J (2010) DNA sequence analysis of conserved genes reveals hybridization events that increase genetic diversity in *Verticillium dahliae*. *Fungal biology* 114: 209-218

Cormack BP, Ghori N, Falkow S (1999) An adhesin of the yeast pathogen *Candida glabrata* mediating adherence to human epithelial cells. *Science* 285: 578-582

Croft MT, Moulin M, Webb ME, Smith AG (2007) Thiamine biosynthesis in algae is regulated by riboswitches. *Proceedings of the national academy of sciences of the United States of America* 104: 20770-20775

Davis JR, Huisman OC, Westermann DT, Hafez SL, Everson DO, Sorensen LH, Schneider AT (1996) Effects of green manures on *Verticillium* wilt of potato. *Phytopathology* 86: 444-453

de Groot PW, Klis FM (2008) The conserved PA14 domain of cell wall-associated fungal adhesins governs their glycan-binding specificity. *Molecular microbiology* 68: 535-537

de Jonge R, Bolton MD, Kombrink A, van den Berg GC, Yadeta KA, Thomma BP (2013) Extensive chromosomal reshuffling drives evolution of virulence in an asexual pathogen. *Genome research* 23: 1271-1282

Dobinson KF, Harrington MA, Omer M, Rowe RC (2000) Molecular Characterization of Vegetative Compatibility Group 4A and 4B Isolates of *Verticillium dahliae* Associated with Potato Early Dying. *Plant disease* 84: 1241-1245

Duressa D, Anchieta A, Chen D, Klimes A, Garcia-Pedrajas MD, Dobinson KF, Klosterman SJ (2013) RNA-seq analyses of gene expression in the microsclerotia of *Verticillium dahliae*. *BMC genomics* 14: 607

Eastburn DM, Chang RJ (1994) *Verticillium dahliae*: A causal agent of root discoloration of horseradish in Illinois. *Plant disease* 78: 496-498

Elena K (1999) Genetic Relationships Among *Verticillium* dahliae Isolates from Cotton in Greece Based on Vegetative Compatibility. *European journal of plant pathology* 105: 609-616

Enjo F, Nosaka K, Ogata M, Iwashima A, Nishimura H (1997) Isolation and characterization of a thiamin transport gene, *THI10*, from *Saccharomyces cerevisiae*. *The journal of biological chemistry* 272: 19165-19170

Eynck C, Koopmann B, Grunewaldt-Stoecker G, Karlovsky P, von Tiedemann A (2007) Differential interactions of *Verticillium longisporum* and *V. dahliae* with *Brassica napus* detected with molecular and histological techniques. *European journal of plant pathology* 118: 259–274

Faou P, Tropschug M (2003) A novel binding protein for a member of CyP40-type Cyclophilins: *N.crassa* CyPBP37, a growth and thiamine regulated protein homolog to yeast Thi4p. *Journal of molecular biology* 333: 831-844

Faou P, Tropschug M (2004) *Neurospora crassa* CyPBP37: a cytosolic stress protein that is able to replace yeast Thi4p function in the synthesis of vitamin B1. *Journal of molecular biology* 344: 1147-1157

Feldbrügge M, Kellner R, Schipper K (2013) The biotechnological use and potential of plant pathogenic smut fungi. *Applied microbiology and biotechnology* 97: 3253-3265

Fradin EF, Thomma BP (2006) Physiology and molecular aspects of *Verticillium* wilt diseases caused by *V. dahliae* and *V. albo-atrum*. *Molecular plant pathology* 7: 71-86

Fradin EF, Zhang Z, Juarez Ayala JC, Castroverde CD, Nazar RN, Robb J, Liu CM, Thomma BP (2009) Genetic dissection of *Verticillium* wilt resistance mediated by tomato Ve1. *Plant physiology* 150: 320-332

Frieman MB, McCaffery JM, Cormack BP (2002) Modular domain structure in the *Candida glabrata* adhesin Epa1p, a beta1,6 glucan-cross-linked cell wall protein. *Molecular microbiology* 46: 479-492

Fujii I, Mori Y, Watanabe A, Kubo Y, Tsuji G, Ebizuka Y (2000) Enzymatic synthesis of 1,3,6,8-tetrahydroxynaphthalene solely from malonyl coenzyme A by a fungal iterative type I polyketide synthase PKS1. *Biochemistry* 39: 8853-8858

Fulton TR, Ibrahim N, Losada MC, Grzegorski D, Tkacz JS (1999) A melanin polyketide synthase (PKS) gene from *Nodulisporium* sp. that shows homology to the *pks1* gene of *Colletotrichum lagenarium*. *Molecular & general genetics* 262: 714-720

Geis PA, Wheeler MH, Szaniszlo PJ (1984) Pentaketide metabolites of melanin synthesis in the dematiaceous fungus *Wangiella dermatitidis*. *Archives of microbiology* 137: 324-328

Gerke J, Bayram O, Feussner K, Landesfeind M, Shelest E, Feussner I, Braus GH (2012) Breaking the silence: protein stabilization uncovers silenced biosynthetic gene clusters in the fungus *Aspergillus nidulans*. *Applied and environmental microbiology* 78: 8234-8244

Goossens K, Willaert R (2010) Flocculation protein structure and cell-cell adhesion mechanism in *Saccharomyces cerevisiae*. *Biotechnology letters* 32: 1571-1585

Goud JK, Termorshuizen AJ, Gams W (2003) Morphology of *Verticillium dahliae* and *V. tricorpus* on semi-selective media used for the detection of *V. dahliae* in soil. *Mycological research* 107: 822-830

Guthrie C, Fink GR (2004) Guide to yeast genetics and molecular and cell biology, Part A. Methods in Enzymology. *Elsevier academic press*

Hanahan D, Jessee J, Bloom FR (1991) Plasmid transformation of *Escherichia coli* and other bacteria. *Methods in enzymology* 204: 63-113

Hasan S, Ahmad A, Purwar A, Khan N, Kundan R, Gupta G (2013) Production of extracellular enzymes in the entomopathogenic fungus *Verticillium lecanii*. *Bioinformation* 9: 238-242

Hastie AC (1973) Hybridization of *Verticillium albo-atrum* and *Verticillium dahliae*. *Transactions of the british mycological society* 60: 5II-523

Heale JB, Karapapa VK (1999) The *Verticillium* threat to Canada's major oilseed crop: canola. *Canadian journal of plant pathology* 21: 1-7

Henrissat B (1991) A classification of glycosyl hydrolases based on amino acid sequence similarities. *The biochemical journal* 280 (Pt 2): 309-316

Hill MK, Lyon KJ, Lyon BR (1999) Identification of disease response genes expressed in *Gossypium hirsutum* upon infection with the wilt pathogen *Verticillium dahliae*. *Plant molecular biology* 40: 289-296

Horie T, Horie R, Chan WY, Leung HY, Schroeder JI (2006) Calcium regulation of sodium hypersensitivities of sos3 and athkt1 mutants. *Plant & cell physiology* 47: 622-633

Horton P, Park KJ, Obayashi T, Fujita N, Harada H, Adams-Collier CJ, Nakai K (2007) WoLF PSORT: protein localization predictor. *Nucleic acids research* 35: W585-587

Huisman OC (1982) Interrelations of Root Growth Dynamics to Epidemiology of Root-Invading Fungi. *Annual review of phytopathology* 20: 303-327

Ielasi FS, Decanniere K, Willaert RG (2012) The epithelial adhesin 1 (Epa1p) from the human-pathogenic yeast *Candida glabrata*: structural and functional study of the carbohydrate-binding domain. *Acta crystallographica section D, biological crystallography* 68: 210-217

Inderbitzin P, Bostock RM, Davis RM, Usami T, Platt HW, Subbarao KV (2011a) Phylogenetics and taxonomy of the fungal vascular wilt pathogen *Verticillium*, with the descriptions of five new species. *PloS one* 6: e28341

Inderbitzin P, Davis RM, Bostock RM, Subbarao KV (2011b) The ascomycete *Verticillium longisporum* is a hybrid and a plant pathogen with an expanded host range. *PloS one* 6: e18260

Inoue H, Nojima H, Okayama H (1990) High efficiency transformation of *Escherichia coli* with plasmids. *Gene* 96: 23-28

Isaac I (1947) A comparative study of pathogenic isolates of *Verticillium*. *Transactions of the british mycological society* 32: 137–157

Isaac I (1949) *Verticillium* wilt of sainfoin. *Annals of applied biology* 33: 28-34

Ito H, Fukuda Y, Murata K, Kimura A (1983) Transformation of intact yeast cells treated with alkali cations. *Journal of bacteriology* 153: 163-168

Jacob-Wilk D, Goldschmidt EE, Riov J, Sadka A, Holland D (1997) Induction of a Citrus gene highly homologous to plant and yeast thi genes involved in thiamine biosynthesis during natural and ethylene-induced fruit maturation. *Plant molecular biology* 35: 661-666

Jansen BCP (1972) The Viraniins Chemisrry, Physiology, Pathology, Methods, Vol. 5 (Eds.: W. H. Sebrell, Jr.. R. S. Harris), *Academic press, New York.*

Jansen BCP, Donath WF (1926) On the isolation of antiberiberi vitamin. *Proc kon ned akad wet* 29: 1390–1400

Jimenez-Diaz RM, Mercado-Blanco J, Olivares-Garcia C, Collado-Romero M, Bejarano-Alcazar J, Rodriguez-Jurado D, Gimenez-Jaime A, Garcia-Jimenez J, Armengol J (2006) Genetic and Virulence Diversity in *Verticillium dahliae* Populations Infecting Artichoke in Eastern-Central Spain. *Phytopathology* 96: 288-298

Joaquim TR, Rowe RC (1990) Reassessment of vegetative compatibility relationships among strains of Verticillium dahliae using nitrate-nonutilizing mutants. *Phytopathology* 80: 1160-1166

Joaquim TR, Rowe RC (1991) Vegetative compatibility and virulence of strains of *Verticillium dahliae* from soil and potato plants. *Phytopathology* 81: 552-558

Jonkers W, Rodrigues CD, Rep M (2009) Impaired colonization and infection of tomato roots by the Deltafrp1 mutant of *Fusarium oxysporum* correlates with reduced CWDE gene expression. *Molecular plant-microbe interactions* 22: 507-518

Juge N (2006) Plant protein inhibitors of cell wall degrading enzymes. *Trends in plant science* 11: 359-367

Jurgenson CT, Begley TP, Ealick SE (2009) The structural and biochemical foundations of thiamin biosynthesis. *Annual review of biochemistry* 78: 569-603

Jurgenson CT, Chatterjee A, Begley TP, Ealick SE (2006) Structural insights into the function of the thiamin biosynthetic enzyme Thi4 from *Saccharomyces cerevisiae*. *Biochemistry* 45: 11061-11070

Jyothishwaran G, Kotresha D, Selvaraj K, Srideshikan SM, Rajvanshi PK, Jayabaskaran C (2007) A modified freeze–thaw method for efficient transformation of *Agrobacterium tumefaciens*. *Current science* 93: 770-772

Kaever A, Landesfeind M, Possienke M, Feussner K, Feussner I, Meinicke P (2012) MarVis-Filter: ranking, filtering, adduct and isotope correction of mass spectrometry data. *Journal of biomedicine & biotechnology* 2012: 263910

Kaever A, Lingner T, Feussner K, Gobel C, Feussner I, Meinicke P (2009) MarVis: a tool for clustering and visualization of metabolic biomarkers. *BMC bioinformatics* 10: 92-92

Karapapa VK, Brainbridge BW, Heale JB (1997) Morphological and molecular characterization of *Verticillium longisporum* comb. nov., pathogenic to oilseed rape. *Mycological research* 101: 1281-1294

Katan T (2000) Vegetative compatibility in populations of *Verticillium* – An overview. *American phytopathological society*: 69-86

Kim JT, Park IH, Lee HB, Hahm YI, Yu SH (2001) Identification of *Verticillium dahliae* and *V. albo-atrum* causing wilt of tomato in Korea. *Plant pathology journal* 17: 222-226

Klosterman SJ, Atallah ZK, Vallad GE, Subbarao KV (2009) Diversity, Pathogenicity, and Management of *Verticillium* Species. *Annual review of phytopathology* 47: 39–62

Klosterman SJ, Subbarao KV, Kang S, Veronese P, Gold SE, Thomma BP, Chen Z, Henrissat B, Lee YH, Park J, Garcia-Pedrajas MD, Barbara DJ, Anchieta A, de Jonge R, Santhanam P, Maruthachalam K, Atallah Z, Amyotte SG, Paz Z, Inderbitzin P, Hayes RJ, Heiman DI, Young S, Zeng Q, Engels R, Galagan J, Cuomo CA, Dobinson KF, Ma LJ (2011) Comparative genomics yields insights into niche adaptation of plant vascular wilt pathogens. *PLoS pathogens* 7: e1002137

Kobayashi O, Hayashi N, Kuroki R, Sone H (1998) Region of FLO1 proteins responsible for sugar recognition. *Journal of bacteriology* 180: 6503-6510

Koike ST, Subbarao KV, Davis RM, Gordon TR, Hubbard JC (1994) *Verticillium* Wilt of Cauliflower in California. *Plant disease* 78: 1116-1121

Kolar M, Punt PJ, van den Hondel CA, Schwab H (1988) Transformation of *Penicillium chrysogenum* using dominant selection markers and expression of an *Escherichia coli* lacZ fusion gene. *Gene* 62: 127–134

Kowalska E, Kujda M, Wolak N, Kozik A (2012) Altered expression and activities of enzymes involved in thiamine diphosphate biosynthesis in *Saccharomyces cerevisiae* under oxidative and osmotic stress. *Federation of european microbiological societies* 12: 534–546

Kubo Y, Suzuki K, Furusawa I, Yamamoto M (1982) Effect of Tricyclazole on Appressorial Pigmentation and Penetration from Appressoria of *Colletotrichum lagenarium*. *Phytopathology* 72: 1198-1200

Kubodera T, Watanabe M, Yoshiuchi K, Yamashita N, Nishimura A, Nakai S, Gomi K, Hanamoto H (2003) Thiamine-regulated gene expression of *Aspergillus oryzae thiA* requires splicing of the intron containing a riboswitch-like domain in the 5'-UTR. *FEBS letters* 555: 516-520

Kumar A, Agarwal S, Heyman JA, Matson S, Heidtman M, Piccirillo S, Umansky L, Drawid A, Jansen R, Liu Y, Cheung KH, Miller P, Gerstein M, Roeder GS, Snyder M (2002) Subcellular localization of the yeast proteome. *Genes & development* 16: 707-719

Kwak YS, Han S, Thomashow LS, Rice JT, Paulitz TC, Kim D, Weller DM (2011) Saccharomyces cerevisiae genome-wide mutant screen for sensitivity to 2,4-diacetylphloroglucinol, an antibiotic produced by *Pseudomonas fluorescens*. *Applied and environmental microbiology* 77: 1770-1776

Lazo GR, Stein PA, Ludwig RA (1991) A DNA transformation-competent *Arabidopsis* genomic library in *Agrobacterium*. *Biotechnology (N Y)* 9: 963-967

Leder IG (1975) Metabolic Pathways, Vol. 7 (Ed : D. M. Greenberg).

Leslie JF (1993) Fungal vegetative compatibility. *Annual review of phytopathology* 31: 127-150

Leslie M (2013) Molecular biology. 'Dead' enzymes show signs of life. *Science* 340: 25-27

Linder T, Gustafsson CM (2008) Molecular phylogenetics of ascomycotal adhesins--a novel family of putative cell-surface adhesive proteins in fission yeasts. *Fungal genetics and biology* 45: 485-497

Lister R, Gregory BD, Ecker JR (2009) Next is now: new technologies for sequencing of genomes, transcriptomes, and beyond. *Current opinion in plant biology* 12: 107-118

Liu D, Li J, Zhao S, Zhang R, Wang M, Miao Y, Shen Y, Shen Q (2013a) Secretome diversity and quantitative analysis of cellulolytic *Aspergillus fumigatus* Z5 in the presence of different carbon sources. *Biotechnology for biofuels* 6: 149

Liu SY, Chen JY, Wang JL, Li L, Xiao HL, Adam SM, Dai XF (2013b) Molecular characterization and functional analysis of a specific secreted protein from highly virulent defoliating *Verticillium dahliae*. *Gene* 529: 307-316

Mace ME, Bell AA, Beckman CH (1981) Fungal wilt diseases of plants. *Academic press, New York*

Machado CR, de Oliveira RL, Boiteux S, Praekelt UM, Meacock PA, Menck CF (1996) *Thi1*, a thiamine biosynthetic gene in *Arabidopsis thaliana*, complements bacterial defects in DNA repair. *Plant molecular biology* 31: 585-593

Machado CR, Praekelt UM, de Oliveira RC, Barbosa AC, Byrne KL, Meacock PA, Menck CF (1997) Dual role for the yeast *THI4* gene in thiamine biosynthesis and DNA damage tolerance. *Journal of molecular biology* 273: 114-121

Mahuku GS, Platt HW (2002) Molecular evidence that *Verticillium ablo-atrum* Grp 2 isolates are distinct from *V. albo-atrum* Grp 1 and *V. tricorpus*. *Molecular plant pathology* 3: 71-79

Mandal M, Boese B, Barrick JE, Winkler WC, Breaker RR (2003) Riboswitches control fundamental biochemical pathways in Bacillus subtilis and other bacteria. *Cell* 113: 577-586

Manetti AG, Rosetto M, Maundrell KG (1994) *nmt2* of fission yeast: a second thiamine-repressible gene co-ordinately regulated with *nmt1*. *Yeast* 10: 1075-1082

Marchler-Bauer A, Anderson JB, Cherukuri PF, DeWeese-Scott C, Geer LY, Gwadz M, He S, Hurwitz DI, Jackson JD, Ke Z, Lanczycki CJ, Liebert CA, Liu C, Lu F, Marchler GH, Mullokandov M, Shoemaker BA, Simonyan V, Song JS, Thiessen PA, Yamashita RA, Yin JJ, Zhang D, Bryant SH (2005) CDD: a Conserved Domain Database for protein classification. *Nucleic acids research* 33: D192-196

Michielse CB, Reijnen L, Olivain C, Alabouvette C, Rep M (2012) Degradation of aromatic compounds through the beta-ketoadipate pathway is required for pathogenicity of the tomato wilt pathogen *Fusarium oxysporum* f. sp. *lycopersici*. *Molecular plant pathology* 13: 1089-1100

Moeller W, Amons R (1985) Phosphate-binding sequences in nucleotide-binding proteins. *FEBS letters* 186: 1-7

Mojzita D, Hohmann S (2006) *Pdc2* coordinates expression of the *THI* regulon in the yeast *Saccharomyces cerevisiae*. *Molecular genetics and genomics* 276: 147-161

Mortazavi A, Williams BA, McCue K, Schaeffer L, Wold B (2008) Mapping and quantifying mammalian transcriptomes by RNA-Seq. *Nature methods* 5: 621-628

Morton A, Carder JH, Barbara DJ (1995) Sequences of the internal transcribed spacers of the ribosomal RNA genes and relationships between isolates of *Verticillium albo-atrum* and *V. dahliae*. *Plant pathology journal* 44: 183–190

Mulder NJ, Apweiler R, Attwood TK, Bairoch A, Bateman A, Binns D, Bradley P, Bork P, Bucher P, Cerutti L, Copley R, Courcelle E, Das U, Durbin R, Fleischmann W, Gough J, Haft D, Harte N, Hulo N, Kahn D, Kanapin A, Krestyaninova M, Lonsdale D, Lopez R, Letunic I, Madera M, Maslen J, McDowall J, Mitchell A, Nikolskaya AN, Orchard S, Pagni M, Ponting CP, Quevillon E, Selengut J, Sigrist CJ, Silventoinen V, Studholme DJ, Vaughan R, Wu CH (2005) InterPro, progress and status in 2005. *Nucleic acids research* 33: D201-205

Mullaney EJ, Hamer JE, Roberti KA, Yelton MM, Timberlake WE (1985) Primary structure of the trpC gene from *Aspergillus nidulans*. *Molecular and general genetics* 199: 37-45

Müller M, Gocke D, Pohl M (2009) Thiamin diphosphate in biological chemistry: exploitation of diverse thiamin diphosphate-dependent enzymes for asymmetric chemoenzymatic synthesis. *The FEBS journal* 276: 2894-2904

Neumann MJ, Dobinson KF (2003) Sequence tag analysis of gene expression during pathogenic growth and microsclerotia development in the vascular wilt pathogen *Verticillium dahliae*. *Fungal genetics and biology* 38: 54-62

Onuchic LF, Furu L, Nagasawa Y, Hou X, Eggermann T, Ren Z, Bergmann C, Senderek J, Esquivel E, Zeltner R, Rudnik-Schoneborn S, Mrug M, Sweeney W, Avner ED, Zerres K, Guay-Woodford LM, Somlo S, Germino GG (2002) *PKHD1*, the polycystic kidney and hepatic disease 1 gene, encodes a novel large protein containing multiple immunoglobulin-like plexin-transcription-factor domains and parallel beta-helix 1 repeats. *American journal of human genetics* 70: 1305-1317

Peberdy JF (1994) Protein secretion in filamentous fungi--trying to understand a highly productive black box. *Trends in biotechnology* 12: 50-57

Pegg GF, Brady BL (2002) Verticillium wilts., *CABI publishing, New York.*

Pegg GF, Young DH (1981) Changes in glycosidase activity and their relationship to fungal colonization during infection of tomato by *Verticillium albo-atrum*. *Physiological plant pathology* 19: 371–382

Praekelt UM, Byrne KL, Meacock PA (1994) Regulation of *THI4* (*MOL1*), a thiamine-biosynthetic gene of *Saccharomyces cerevisiae*. *Yeast* 10: 481-490

Praekelt UM, Meacock PA (1992) *MOL1*, a *Saccharomyces cerevisiae* gene that is highly expressed in early stationary phase during growth on molasses. *Yeast* 8: 699-710

Puhalla JE, Hummel M (1983) Vegetative compatibility groups within *Verticillium dahliae*. *Genetics* 73: 1305-1308

Punt PJ, van den Hondel CA (1992) Transformation of filamentous fungi based on hygromycin B and phleomycin resistance markers. *Methods in enzymology* 216: 447-457

Punt PJ, Veldhuisen G, van den Hondel CA (1994) Protein targeting and secretion in filamentous fungi. A progress report. *Antonie van leeuwenhoek* 65: 211-216

Rapala-Kozik M, Kowalska E, Ostrowska K (2008) Modulation of thiamine metabolism in *Zea mays* seedlings under conditions of abiotic stress. *Journal of experimental botany* 59: 4133-4143

Rapala-Kozik M, Wolak N, Kujda M, Banas AK (2012) The upregulation of thiamine (vitamin B1) biosynthesis in *Arabidopsis thaliana* seedlings under salt and osmotic stress conditions is mediated by abscisic acid at the early stages of this stress response. *BMC plant biology* 12: 2

Ratzinger A, Riediger N, von Tiedemann A, Karlovsky P (2009) Salicylic acid and salicylic acid glucoside in xylem sap of *Brassica napus* infected with *Verticillium longisporum*. *Journal of plant research* 122: 571-579

Rawlings ND, Barrett AJ, Bateman A (2010) MEROPS: the peptidase database. *Nucleic acids research* 38: D227-233

Raynal A, Gerbaud C, Francingues MC, Guerineau M (1987) Sequence and transcription of the beta-glucosidase gene of *Kluyveromyces fragilis* cloned in *Saccharomyces cerevisiae*. *Current genetics* 12: 175-184

Reinke J, Berthold G (1879) Die Zersetzung der Kartoffel durch Pilze. *Untersuchungen aus dem botanischen Laboratorium der Universität Göttingen*: 1-127

Rep M (2005) Small proteins of plant-pathogenic fungi secreted during host colonization. *FEMS microbiology letters* 253: 19-27

Ribeiro A, Praekelt U, Akkermans AD, Meacock PA, van Kammen A, Bisseling T, Pawlowski K (1996) Identification of agthi1, whose product is involved in biosynthesis of the thiamine precursor thiazole, in actinorhizal nodules of *Alnus glutinosa*. *The plant journal* 10: 361-368.

Rigden DJ, Mello LV, Galperin MY (2004) The PA14 domain, a conserved all-beta domain in bacterial toxins, enzymes, adhesins and signaling molecules. *Trends in biochemical sciences* 29: 335-339

Robb J, Lee B, Nazar RN (2007) Gene suppression in a tolerant tomato-vascular pathogen interaction. *Planta* 226: 299-309

Robb J, Moukhamedov R, Hu X, Platt H, Nazar RN (1993) Putative subgroups of *Verticillium albo-atrum* distinguishable by PCR-based assays. *Physiological and molecular plant pathology* 43: 423–436

Robinson N, Platt HW, Hale LR (2007) *Verticillium dahliae* interactions with *V. albo-atrum* 'Group 2' and *V. tricorpus* and their effects on *Verticillium* wilt disease development in potato. *American journal of potato research* 84: 229-235

Rodriguez A, Perestelo F, Carnicero A, Regalado V, Perez R, De la Fuente G, Falcon MA (1996) Degradation of natural lignins and lignocellulosic substrates by soil-inhabiting fungi imperfecti. *FEMS microbiology ecology* 21: 213–219

Roise D, Schatz G (1988) Mitochondrial presequences. *The Journal of biological chemistry* 263: 4509-4511

Rowe RC (1987) Potato early dying: causal agents and management strategies. *Plant disease* 71

Rowe RC, Powelson ML (2002) Potato Early Dying: Management Challenges in a Changing Production Environment. *The american phytopathological society* 68: 1184-1193

Ruiz-Roldan C, Puerto-Galan L, Roa J, Castro A, Di Pietro A, Roncero MI, Hera C (2008) The *Fusarium oxysporum sti35* gene functions in thiamine biosynthesis and oxidative stress response. *Fungal genetics and biology* 45: 6-16

Rusk N, Kiermer V (2008) Primer: Sequencing--the next generation. *Nature methods* 5: 15

Samal BB, Karan B, Boone TC, Osslund TD, Chen KK, Stabinsky Y (1990) Isolation and characterization of the gene encoding a novel, thermostable serine proteinase from the mould *Tritirachium album Limber*. *Molecular microbiology* 4: 1789-1792

Sambrook J, Fritsch EF, Maniatis T (1989) Molecular Cloning: A Laboratory Manual. *Cold spring harbour laboratory.*

Sasse C, Bignell EM, Hasenberg M, Haynes K, Gunzer M, Braus GH, Krappmann S (2008) Basal expression of the *Aspergillus fumigatus* transcriptional activator CpcA is sufficient to support pulmonary aspergillosis. *Fungal genetics and biology* 45: 693-704

Schmidt CL, Shaw L (2001) A comprehensive phylogenetic analysis of Rieske and Rieske-type iron-sulfur proteins. *Journal of bioenergetics and biomembranes* 33: 9-26

Schwarz W, Jauris S, Kouba M, Bronnenmeier K, Staudenbauer WL (1989) Cloning and expression of *Clostridium stercorarium* cellulase genes in *Escherichia coli*. *Biotechnology letters* 11: 461-466

Sewell GWF, Wilson JF (1964) Occurrence and dispersal of *Verticillium* conidia in xylem sap of hop (*Humulus lupulus L.*). *Nature* 204: 901

Sheppard DC, Yeaman MR, Welch WH, Phan QT, Fu Y, Ibrahim AS, Filler SG, Zhang M, Waring AJ, Edwards JE, Jr. (2004) Functional and structural diversity in the Als protein family of *Candida albicans*. *The journal of biological chemistry* 279: 30480-30489

Shokolenko I, Venediktova N, Bochkareva A, Wilson GL, Alexeyev MF (2009) Oxidative stress induces degradation of mitochondrial DNA. *Nucleic acids research* 37: 2539-2548

Singh K, Foley RC, Onate-Sanchez L (2002) Transcription factors in plant defense and stress responses. *Current opinion in plant biology* 5: 430-436

Singh S, Braus-Stromeyer SA, Timpner C, Tran VT, Lohaus G, Reusche M, Knufer J, Teichmann T, von Tiedemann A, Braus GH (2010) Silencing of *Vlaro2* for chorismate synthase revealed that the phytopathogen *Verticillium longisporum* induces the cross-pathway control in the xylem. *Applied microbiology and biotechnology* 85: 1961-1976

Singh S, Braus-Stromeyer SA, Timpner C, Valerius O, von Tiedemann A, Karlovsky P, Druebert C, Polle A, Braus GH (2012) The plant host *Brassica napus* induces in the pathogen *Verticillium longisporum* the expression of functional catalase peroxidase which is required for the late phase of disease. *Molecular plant-microbe interactions* 25: 569-581

Singleton CK (1997) Identification and characterization of the thiamine transporter gene of *Saccharomyces cerevisiae*. *Gene* 199: 111-121

Smith G (1949) The effect of adding trace elements to Czapek-Dox medium. *Transactions of the british mycological society* 32: 280–283

Snyder WC, Hansen HN (1940) The species concept in *Fusarium*. *American journal of botany* 27: 64-67

Sonnhammer EL, Eddy SR, Durbin R (1997) Pfam: a comprehensive database of protein domain families based on seed alignments. *Proteins* 28: 405-420

Spenser ID, White RL (1997) Biosynthesis of Vitamin B1 (Thiamin): An Instance of Biochemical Diversity. *Angewandte chemie internationale edition (English)* 36: 1032–1046

Stark C (1961) Das Aufreten der *Verticillium*: Tracheomykosen in Hamburger Gartenbaukulturen. *Gartenbauwissenschaft* 26: 493-528

Steventon LA, Fahelson J, Quiong H, Dixelius C (2002) Identification of the causal agent of *Verticillium wilt* of winter oilseed rape in Sweden, *V. longisporum*. *Mycological research* 106: 570–578

Sudarsan N, Barrick JE, Breaker RR (2003) Metabolite-binding RNA domains are present in the genes of eukaryotes. *RNA* 9: 644-647

Sutherland JB, Pometto ALI, Crawford DL (1983) Lignocellulose degradation by *Fusarium* species. *Canadian journal of botany* 61: 1194-1198

Takano Y, Kubo Y, Shimizu K, Mise K, Okuno T, Furusawa I (1995) Structural analysis of *PKS1*, a polyketide synthase gene involved in melanin biosynthesis in *Colletotrichum lagenarium*. *Molecular and general genetics* 249: 162-167

Thanonkeo P, Akiyama K, Jain S, Takata R (2000) Targeted disruption of *sti35*, a stress-responsive gene in phytopathogenic fungus *Fusarium oxysporum*. *Current microbiology* 41: 284-289

Thore S, Leibundgut M, Ban N (2006) Structure of the eukaryotic thiamine pyrophosphate riboswitch with its regulatory ligand. *Science* 312: 1208-1211

Timpner C, Braus-Stromeyer SA, Tran VT, Braus GH (2013) The Cpc1 regulator of the cross-pathway control of amino acid biosynthesis is required for pathogenicity of the vascular pathogen *Verticillium longisporum*. *Molecular plant-microbe interactions* 26: 1312-1324

Tjamos EC, Beckman CH (1989) Vascular wilt diseases of plants: Basic studies and control, *Springer-Verlag*.

Tran VT, Braus-Stromeyer SA, Timpner C, Braus GH (2013) Molecular diagnosis to discriminate pathogen and apathogen species of the hybrid Verticillium longisporum on the oilseed crop Brassica napus. *Applied microbiology and biotechnology* 97: 4467-4483

Tunc-Ozdemir M, Miller G, Song L, Kim J, Sodek A, Koussevitzky S, Misra AN, Mittler R, Shintani D (2009) Thiamin confers enhanced tolerance to oxidative stress in *Arabidopsis*. *Plant physiology* 151: 421-432

Van den Hondel CAMJJ, Punt PJ (1991) Gene transfer systems and vector development for filamentous fungi. *BSM symposium series, applied molecular genetics of fungi* 18: 1-29

Van den Hondel CAMJJ, Punt PJ, Van Goreom RFM (1991) Heterologous gene expression in filamentous fungi. In: Bennett JW & Lasure LL (Eds) More gene manipulation in fungi. *Academic press, San Diego, CA*: 396-428

Van Esse HP, Fradin EF, de Groot PJ, de Wit PJ, Thomma BP (2009) Tomato transcriptional responses to a foliar and a vascular fungal pathogen are distinct. *Molecular plant-microbe interactions* 22: 245-258

Van Loon LC, Rep M, Pieterse CM (2006) Significance of inducible defense-related proteins in infected plants. *Annual review of phytopathology* 44: 135-162

Vida TA, Emr SD (1995) A new vital stain for visualizing vacuolar membrane dynamics and endocytosis in yeast. *The journal of cell biology* 128: 779-792

Ward CJ, Hogan MC, Rossetti S, Walker D, Sneddon T, Wang X, Kubly V, Cunningham JM, Bacallao R, Ishibashi M, Milliner DS, Torres VE, Harris PC (2002) The gene mutated in autosomal recessive polycystic kidney disease encodes a large, receptor-like protein. *Nature genetics* 30: 259-269

Wheeler MH, Stipanovic RD (1985) Melanin biosynthesis and the metabolism of flaviolin and 2-hydroxyjuglone in *Wangiella dermatitidis*. *Archives of microbiology* 142: 234-241

White RL, Spenser ID (1979a) Biosynthesis of vitamin B1 in yeast. Origin of the thiazole unit. *Journal of the american chemical society* 101: 5102-5104

White RL, Spenser ID (1979b) Thiamin biosynthesis in *Saccharomyces cerevisiae*. Origin of carbon-2 of the thiazole moiety. *The Biochemical journal* 179: 315-325

White RL, Spenser ID (1982) Thiamin biosynthesis in yeast. Origin of the five-carbon unit of the thiazole moiety. *Journal of the american chemical society* 104: 4934-4943

Wilhelm S (1955) Longevity of the *Verticillium* wilt fungus in the laboratory and field. *Phytopathology* 45: 180-182

Williams RR, Spies RD (1938) VifaminB, (Thiamin) andirs Use in Medicine. *MacMillan New York*: 138-143

Winkler W, Nahvi A, Breaker RR (2002) Thiamine derivatives bind messenger RNAs directly to regulate bacterial gene expression. *Nature* 419: 952-956

Wolkow PM, Sisler HD, Vigil EL (1983) Effect of inhibitors of melanin biosynthesis on structure and function of appressoria of *Colletotrichum lindemuthianum*. *Physiological plant pathology* 23: 55–71

Woloshuk CP, Sisler HD, Vigil EL (1983) Action of the antipenetrant, tricyclazole, on appressoria of *Pyricularia oryzae*. *Physiological plant pathology* 22: 245–259

Woodcock DM, Crowther PJ, Doherty J, Jefferson S, DeCruz E, Noyer-Weidner M, Smith SS, Michael MZ, Graham MW (1989) Quantitative evaluation of *Escherichia coli* host strains for tolerance to cytosine methylation in plasmid and phage recombinants. *Nucleic acids research* 17: 3469-3478

Xiong H, Chen Y, Yi Y, Tsuchiya K, Moeckel G, Cheung J, Liang D, Tham K, Xu X, Chen XZ, Pei Y, Zhao ZJ, Wu G (2002) A novel gene encoding a TIG multiple domain protein is a positional candidate for autosomal recessive polycystic kidney disease. *Genomics* 80: 96-104

Xu L, Zhu L, Tu L, Liu L, Yuan D, Jin L, Long L, Zhang X (2011) Lignin metabolism has a central role in the resistance of cotton to the wilt fungus *Verticillium dahliae* as revealed by RNA-Seq-dependent transcriptional analysis and histochemistry. *Journal of experimental botany* 62: 5607-5621

Yoshida E, Hidaka M, Fushinobu S, Koyanagi T, Minami H, Tamaki H, Kitaoka M, Katayama T, Kumagai H (2010) Role of a PA14 domain in determining substrate specificity of a glycoside hydrolase family 3 beta-glucosidase from *Kluyveromyces marxianus*. *The biochemical journal* 431: 39-49

Young DH, Pegg GF (1982) The action of tomato and *Verticillium albo-atrum* glycosidases on the hyphal wall of *V. albo-atrum*. *Physiological plant pathology* 21: 411-423

Young DW (1986) The biosynthesis of the vitamins thiamin, riboflavin, and folic acid. *Natural product reports* 3: 395-419

Zare R, Gams W, Starink-Willemse M, Summerbell RC (2007) *Gibellulopsis*, a suitable genus for *Verticillium nigrescens*, and *Musicillium*, a new genus for *V. theobromae*. *Nova hedwigia* 85: 463—489

Zeise K, von Tiedemann A (2001) Morphological and physiological differentiation among vegetative compatibility groups of *Verticillium dahliae* in relation to *V. longisporum*. *Journal of phytopathology* 149: 469–475

Zeise K, von Tiedemann A (2002) Host Specialization among Vegetative Compatibility Groups of *Verticillium dahliae* in Relation to *Verticillium longisporum*. *Journal of phytopathology* 150: 112-119

Zhou L, Zhao J, Guo W, Zhang T (2013a) Functional analysis of autophagy genes via *Agrobacterium*-mediated transformation in the vascular Wilt fungus *Verticillium dahliae*. *Journal of genetics and genomics* 40: 421-431

Zhou P, Chen Z, Yan Q, Yang S, Hilgenfeld R, Jiang Z (2013b) The structure of a glycoside hydrolase family 81 endo-beta-1,3-glucanase. *Acta crystallographica section D* 69: 2027-2038

Zuo K, Wang J, Wu W, Chai Y, Sun X, Tang K (2005) Identification and characterization of differentially expressed ESTs of *Gossypium barbadense* infected by *Verticillium dahliae* with suppression subtractive hybridization. *Molekuliarnaia biologiia* 39: 214-223

Zupancic ML, Frieman M, Smith D, Alvarez RA, Cummings RD, Cormack BP (2008) Glycan microarray analysis of *Candida glabrata* adhesin ligand specificity. *Molecular microbiology* 68: 547-559

Zverlov VV, Volkov IY, Velikodvorskaya TV, Schwarz WH (1997) *Thermotoga neapolitana bglB* gene, upstream of *lamA*, encodes a highly thermostable beta-glucosidase that is a laminaribiase. *Microbiology* 143: 3537-3542

6 Appendices

6.1 Specific up-regulated transcripts – top 20 of most different main categories

Table 16: Transcripts up-regulated in xylem-sap or SXM medium

Category / Transcripts upregulated in this cathegory	xylem-Sap vs. SXM	
	xylS up	SXM up
Metabolism	196	305
Cellular transport, transport facilitation and transport routes	107	159
Protein with binding function or co-factor requirement (structural or catalytic)	97	156
Transcription	88	70
Protein fate (folding, modification, destination)	69	138
Cell rescue, defense and virulence	53	131
Cell cycle and DNA processing	68	96
Interaction with the environment	37	83
Energy	36	75
Biogenesis of cellular components	50	70
Cellular communication/signal transduction mechanism	28	27
Cell type differentiation	32	31
Protein synthesis	27	49
Cell fate	11	22
Regulation of metabolism and protein function	9	24
Development (systemic)	2	-
Systemic interaction with the environment	2	1
Organ differentiation	-	3
Transposable elements, viral and plasmid proteins	1	-
	913	1440

The most differences between xylem-sap and SXM different up-regulated transcripts were marked in red. The first 20 transcripts contained in these categories, were shown in the following tables.

Table 17: "Metabolism" top 20 Transcripts up-regulated in xylem-sap

Metabolism xylem-sap up	
id	function (annot. *F. graminearum*)
vl43-au16.g10009.t1	related to proline oxidase
vl43-au16.g12308.t1	probable TRANSKETOLASE
vl43-au16.g13162.t1	related to DAHP synthase class II
vl43-au16.g13443.t2	probable protein MET-10
vl43-au16.g14645.t1	related to D-amino acid oxidase
vl43-au16.g14671.t1	probable acyl-CoA dehydrogenase
vl43-au16.g216.t1	related to acetoacetyl-CoA synthetase
vl43-au16.g3450.t1	probable cpc-3 protein
vl43-au16.g5139.t1	related to asparagine synthases
vl43-au16.g8139.t1	related to D-amino acid hydantoin hydrolase (hydantoinase)
vl43-au16.g5214.t1	probable GFA1 - glucosamine--fructose-6-phosphate transaminase
vl43-au16.g8396.t1	probable GFA1 - glucosamine--fructose-6-phosphate transaminase
vl43-au16.g13860.t2	probable ZWF1 - glucose-6-phosphate dehydrogenase
vl43-au16.g3737.t1	probable fatty-acyl-CoA synthase, beta subunit
vl43-au16.g2330.t1	probable glutamate synthase (NADPH)
vl43-au16.g3288.t1	probable glutamate synthase (NADPH)
vl43-au16.g3737.t1	probable fatty-acyl-CoA synthase, beta subunit
vl43-au16.g12483.t1	probable aldehyde dehydrogenase
vl43-au16.g5358.t1	related to dihydrodipicolinate synthase
vl43-au16.g6223.t1	related to dihydrodipicolinate synthase

For transcripts 21-383 mapping in this main category and below categories see attached data on CD (SXM_vs_xylS_xylem-sap_up-regulated_HIVI_cutoff_50). In total, the number of mappings is higher than the number of genes in this category. This is caused by the fact, that some genes were assigned to multiple subcategories, and by that were counted twice ore more.

Table 18: "Metabolism" top 20 Transcripts up-regulated in SXM

Metabolism SXM up	
id	function (annot. *F. graminearum*)
vl43-au16.g556.t1	probable aspartate aminotransferase, cytoplasmic
vl43-au16.g990.t1	related to aryl-alcohol dehydrogenases
vl43-au16.g10483.t1	probable MXR1 - responsible for the reduction of methionine sulfoxide
vl43-au16.g13480.t1	probable L-amino-acid oxidase
vl43-au16.g15149.t1	probable TRANSKETOLASE
vl43-au16.g1629.t1	related to gamma-glutamyltransferase
vl43-au16.g3031.t1	related to glu/asp-tRNA amidotransferase subunit A
vl43-au16.g4472.t1	probable DTD1 - D-Tyr-tRNA(Tyr) deacylase activity
vl43-au16.g4586.t1	probable DTD1 - D-Tyr-tRNA(Tyr) deacylase activity
vl43-au16.g5004.t1	probable TRANSKETOLASE
vl43-au16.g5501.t1	probable alanine transaminases
vl43-au16.g5591.t1	probable methyltransferase DPH5
vl43-au16.g6035.t1	conserved hypothetical protein
vl43-au16.g7849.t1	conserved hypothetical protein
vl43-au16.g9644.t1	probable methyltransferase DPH5
vl43-au16.g14378.t1	related to acetyltransferase
vl43-au16.g13860.t3	probable ZWF1 - glucose-6-phosphate dehydrogenase
vl43-au16.g10564.t1	probable URA2 - multifunctional pyrimidine biosynthesis protein
vl43-au16.g5405.t1	probable glutamate dehydrogenase (NADP+)
vl43-au16.g8716.t1	probable fatty-acyl-CoA synthase, beta subunit

For transcripts 21-616 mapping in this main category and below see attached data on CD (SXM_vs_xylS_SXM_up-regulated_HIVI_cutoff_50). In total, the number of mappings is higher than the number of genes in this category. This is caused by the fact, that some genes were assigned to multiple subcategories, and by that were counted twice ore more.

Table 19: "Protein fate" top 20 Transcripts up-regulated in xylem-sap

Protein fate (folding, modification, destination) xylem-sap up	
id	function (annot. *F. graminearum*)
vl43-au16.g5358.t1	related to histone-lysine N-methyltransferase
vl43-au16.g1354.t1	related to midasin (AAA ATPase)
vl43-au16.g15709.t1	related to peptidylprolyl isomerase (cyclophilin)-like
vl43-au16.g3164.t1	probable CCT2 - chaperonin of the TCP1 ring complex, cytosolic
vl43-au16.g10151.t1	related to vacuolar protein sorting-associated protein VPS13
vl43-au16.g11474.t1	probable ran GTPase activating protein 1
vl43-au16.g117.t1	probable novel protein of ras superfamily KREV-1
vl43-au16.g14957.t1	related to Sls2 protein
vl43-au16.g14983.t1	related to phosphatidylinositol 4-phosphate 5-kinase
vl43-au16.g2026.t1	related to protein carrier KAP123
vl43-au16.g4791.t1	related to importin beta homolog Kap119p
vl43-au16.g5358.t1	related to SIGNAL RECOGNITION PARTICLE 72 KDA PROTEIN
vl43-au16.g7415.t1	related to protein kinase homolog VPS15
vl43-au16.g777.t1	related to Sls2 protein
vl43-au16.g8244.t1	related to vacuolar protein sorting-associated protein VPS13
vl43-au16.g8253.t1	related to phosphatidylinositol 4-phosphate 5-kinase
vl43-au16.g8713.t1	related to GTP-binding protein Rab5c
vl43-au16.g9620.t1	related to SLS1 protein precursor
vl43-au16.g10079.t1	related to regulator of mitochondrial iron homeostasis
vl43-au16.g1113.t1	related to fructosyl amino acid oxidase

For transcripts 21-82 mapping in this main category and below see attached data on CD (SXM_vs_xylS_xylem-sap_up-regulated_HIVI_cutoff_50). In total, the number of mappings is higher than the number of genes in this category. This is caused by the fact, that some genes were assigned to multiple subcategories, and by that were counted twice ore more.

Table 20: "Protein fate" top 20 Transcripts up-regulated in SXM

Protein fate (folding, modification, destination) SXM up	
id	function (annot. *F. graminearum*)
vl43-au16.g11418.t1	relatedto NonF protein, involved in nonactin biosynthesis
vl43-au16.g13674.t1	related to bacterial leucyl aminopeptidase
vl43-au16.g15256.t1	related to bacterial leucyl aminopeptidase
vl43-au16.g4895.t1	probable 26S proteasome regulatory particle chain RPT5
vl43-au16.g4908.t1	probable 26S proteasome regulatory particle chain RPT5
vl43-au16.g10487.t1	probable peptidylprolyl isomerase precursor, mitochondrial (cyclophilin B)
vl43-au16.g12377.t1	probable LYS7 - copper chaperone for superoxide dismutase Sod1p
vl43-au16.g13076.t1	related to hsp70 protein
vl43-au16.g13450.t1	probable chaperonin ClpB
vl43-au16.g13718.t1	related to stress-induced protein STI1
vl43-au16.g13773.t1	related to midasin (AAA ATPase)
vl43-au16.g1380.t1	probable heat shock protein 80
vl43-au16.g14383.t1	related to antioxidant protein andmetal homeostasis factor
vl43-au16.g14569.t1	related to COX17 protein
vl43-au16.g15605.t1	conserved hypothetical protein
vl43-au16.g2417.t1	probable heat shock protein HSP104 (endopeptidase Clp ATP-binding chain HSP104)
vl43-au16.g3295.t1	related to tetratricopeptide repeat protein 2
vl43-au16.g4585.t1	probable CPR6 - member of the cyclophilin family
vl43-au16.g4929.t1	probable chaperonin ClpB
vl43-au16.g5332.t1	probable FPR3 - prolyl cis-trans isomerase

For transcripts 21-229 mapping in this main category and below see attached data on CD (SXM_vs_xylS_SXM_up-regulated_HIVI_cutoff_50). In total, the number of mappings is higher than the number of genes in this category. This is caused by the fact, that some genes were assigned to multiple subcategories, and by that were counted twice ore more.

Table 21: "Cell rescue" top 20 Transcripts up-regulated in xylem-sap

Cell rescue, defense and virulence xylem-sap up	
id	function (annot. *F. graminearum*)
vl43-au16.g10008.t1	related to gamma-glutamyltransferase
vl43-au16.g13860.t2	probable ZWF1 - glucose-6-phosphate dehydrogenase
vl43-au16.g15018.t1	related to isoflavone reductase homolog A622
vl43-au16.g10079.t1	probable AAA protease IAP-1 (mitochondrial intermembrane space)
vl43-au16.g11006.t1	probable DNA-directed RNA polymerase II chain Rpb7
vl43-au16.g11771.t1	related to AP1-like transcription factor
vl43-au16.g13860.t2	probable ZWF1 - glucose-6-phosphate dehydrogenase
vl43-au16.g7028.t1	probable AAA protease IAP-1 (mitochondrial intermembrane space)
vl43-au16.g7984.t1	related to splicing factor 3B subunit 3 (spliceosomal protein sap130)
vl43-au16.g8743.t1	probable TPS1 - alpha,alpha-trehalose-phosphate synthase, 56 KD subunit
vl43-au16.g10079.t1	related to regulator of mitochondrial iron homeostasis
vl43-au16.g11111.t1	probable 1,4-Benzoquinone reductase
vl43-au16.g371.t1	related to peroxiredoxin 5, mitochondrial precursor
vl43-au16.g11578.t2	related to phosphotyrosyl phosphatase activator PTPA
vl43-au16.g11619.t1	probable profilin
vl43-au16.g1212.t1	related to aldo-keto reductase YPR1
vl43-au16.g2349.t1	related to Na+/H+ antiporter CNH1
vl43-au16.g4582.t1	related to human and mouse neutral sphingomyelinase
vl43-au16.g4626.t1	related to members ofthe aldo/keto reductase family
vl43-au16.g540.t1	related to aldo-keto reductase YPR1

For transcripts 21-70 mapping in this main category and below see attached data on CD (SXM_vs_xylS_xylem-sap_up-regulated_HIVI_cutoff_50). In total, the number of mappings is higher than the number of genes in this category. This is caused by the fact, that some genes were assigned to multiple subcategories, and by that were counted twice ore more.

Table 22: "Cell rescue" top 20 Transcripts up-regulated in SXM

Cell rescue, defense and virulence SXM up	
id	function (annot. *F. graminearum*)
vl43-au16.g10659.t1	probable arsenite translocating ATPase (ASNA1)
vl43-au16.g13860.t3	probable ZWF1 - glucose-6-phosphate dehydrogenase
vl43-au16.g1629.t1	related to gamma-glutamyltransferase
vl43-au16.g3788.t2	related to vacuolar membrane protein HMT1
vl43-au16.g6370.t1	probable arsenite translocating ATPase (ASNA1)
vl43-au16.g10487.t1	probable peptidylprolyl isomerase precursor, mitochondrial (cyclophilin B)
vl43-au16.g10848.t1	probable TPS1 - alpha,alpha-trehalose-phosphate synthase, 56 KD subunit
vl43-au16.g11466.t1	related to SSD1 protein
vl43-au16.g13076.t1	related to hsp70 protein
vl43-au16.g13093.t1	conserved hypothetical protein
vl43-au16.g13694.t1	probable ubiquitin-protein ligase
vl43-au16.g13860.t3	probable ZWF1 - glucose-6-phosphate dehydrogenase
vl43-au16.g14047.t1	probable calcium P-type ATPase NCA-1
vl43-au16.g14780.t1	probable Snz-type pyridoxine vitamin B6 biosynthetic protein SNZ1
vl43-au16.g1522.t1	conservedhypothetical protein
vl43-au16.g2417.t1	probable AAA protease IAP-1 (mitochondrial intermembrane space)
vl43-au16.g2762.t1	related to RPN12 - 26S proteasome regulatory subunit
vl43-au16.g3650.t1	probable calcium P-type ATPase NCA-1
vl43-au16.g4363.t1	conservedhypothetical protein
vl43-au16.g4585.t1	probable peptidylprolyl isomerase precursor, mitochondrial (cyclophilin B)

For transcripts 21-176 mapping in this main category and below see attached data on CD (SXM_vs_xylS_SXM_up-regulated_HIVI_cutoff_50). In total, the number of mappings is higher than the number of genes in this category. This is caused by the fact, that some genes were assigned to multiple subcategories, and by that were counted twice ore more.

Table 23: "Interaction with the environment" top 20 Transcripts up-regulated in xylem-sap

Interaction with the environment xylem-sap up	
id	function (annot. *F. graminearum*)
vl43-au16.g14470.t1	probable amino acid permease NAAP1
vl43-au16.g14470.t1	probable amino acid permease NAAP1
vl43-au16.g14470.t1	probable amino acid permease NAAP1
vl43-au16.g14470.t1	probable amino acid permease NAAP1
vl43-au16.g14470.t1	probable amino acid permease NAAP1
vl43-au16.g14470.t1	probable amino acid permease NAAP1
vl43-au16.g14470.t1	probable amino acid permease NAAP1
vl43-au16.g14470.t1	probable amino acid permease NAAP1
vl43-au16.g14470.t1	probable amino acid permease NAAP1
vl43-au16.g11494.t1	probable potassium transporter TRK-1
vl43-au16.g12360.t1	probable siderophore regulation protein (GATA factor)
vl43-au16.g12602.t1	related to vacuolar Ca2+/H+ antiporter
vl43-au16.g14578.t1	related to PHO36 - regulatory role in lipid and phosphate metabolism
vl43-au16.g1540.t1	related to PHO36 - regulatory role in lipid and phosphate metabolism
vl43-au16.g216.t1	related to nonribosomal peptide synthetase MxcG (component of the myxochelin iron transport regulon)
vl43-au16.g2349.t1	related to Na+/H+ antiporter CNH1
vl43-au16.g3260.t1	related to vacuolar Ca2+/H+ antiporter
vl43-au16.g3609.t1	related to tetratricopeptide repeat protein tpr1
vl43-au16.g371.t1	related to peroxiredoxin 5, mitochondrial precursor
vl43-au16.g6288.t1	probable amino acid transport proteinGAP1

For transcripts 21-47 mapping in this main category and below see attached data on CD (SXM_vs_xylS_xylem-sap_up-regulated_HIVI_cutoff_50). In total, the number of mappings is higher than the number of genes in this category. This is caused by the fact, that some genes were assigned to multiple subcategories, and by that were counted twice ore more.

Table 24: "Interaction with the environment" top 20 Transcripts up-regulated in SXM

Interaction with the environment SXM up	
id	function (annot. *F. graminearum*)
vl43-au16.g11788.t1	probable myosin I heavy chain
vl43-au16.g4585.t1	probable CPR6 - member of the cyclophilin family
vl43-au16.g15122.t1	probable AAD14 - strong similarity to aryl-alcohol reductase
vl43-au16.g15123.t1	probable AAD14 - strong similarity to aryl-alcohol reductase
vl43-au16.g2083.t1	probable SMF1 - Manganese transporter of the plasma membrane
vl43-au16.g3086.t1	related to na+/k+/2cl- cotransporter
vl43-au16.g4853.t1	probable PHO89 - Na+/phosphate co-transporter
vl43-au16.g8722.t1	probable PHO89 - Na+/phosphate co-transporter
vl43-au16.g8767.t1	probable DUR3 - Urea permease
vl43-au16.g10346.t1	probable Na+-transporting ATPase ENA-1
vl43-au16.g10541.t1	probable lysine permease
vl43-au16.g11034.t1	probable Na+-transporting ATPase ENA-1 (sodium P-type ATPase ENA-1)
vl43-au16.g12296.t1	probable potassium channel beta subunit protein
vl43-au16.g12377.t1	probable LYS7 - copper chaperone for superoxide dismutase Sod1p
vl43-au16.g12672.t1	related to copper transport protein
vl43-au16.g13109.t1	related to ferric reductase
vl43-au16.g13113.t1	probable lysine permease
vl43-au16.g13227.t1	probable Na+-transporting ATPase ENA-1
vl43-au16.g13883.t1	probable peroxisomal membrane protein

For transcripts 21-96 mapping in this main category and below see attached data on CD (SXM_vs_xylS_SXM_up-regulated_HIVI_cutoff_50). In total, the number of mappings is higher than the number of genes in this category. This is caused by the fact, that some genes were assigned to multiple subcategories, and by that were counted twice ore more.

Table 25: "Energy" top 20 Transcripts up-regulated in xylem-sap

Energy xylem-sap up	
id	function (annot. *F. graminearum*)
vl43-au16.g11125.t1	related to ALCOHOL DEHYDROGENASE I - ADH1
vl43-au16.g12308.t1	probable TRANSKETOLASE
vl43-au16.g13860.t2	probable ZWF1 - glucose-6-phosphate dehydrogenase
vl43-au16.g14794.t1	related to alcohol dehydrogenase, class C
vl43-au16.g1705.t1	related to ALCOHOL DEHYDROGENASE I - ADH1
vl43-au16.g8355.t1	probable L-serine dehydratase 2
vl43-au16.g11050.t2	related to 6-phosphofructo-2-kinase
vl43-au16.g11148.t1	probable alpha-glucosidase (maltase)
vl43-au16.g540.t1	probable formate dehydrogenase
vl43-au16.g10914.t1	probable cig2 protein (putative GDP-GTP exchange factor)
vl43-au16.g12076.t1	related toribokinase
vl43-au16.g12308.t1	probable TRANSKETOLASE
vl43-au16.g15406.t1	related to 3-hydroxyisobutyrate dehydrogenase
vl43-au16.g9593.t1	related to 3-hydroxyisobutyrate dehydrogenase
vl43-au16.g13860.t2	probable ZWF1 - glucose-6-phosphate dehydrogenase
vl43-au16.g9605.t1	related to malate dehydrogenase
vl43-au16.g9605.t2	related to malate dehydrogenase
vl43-au16.g3838.t1	probable NADH2 dehydrogenase (ubiquinone) 10.5K chain
vl43-au16.g5837.t1	related to NADH oxidase
vl43-au16.g4222.t1	related to lactate 2-monooxygenase

For transcripts 21-49 mapping in this main category and below see attached data on CD (SXM_vs_xylS_xylem-sap_up-regulated_HIVI_cutoff_50). In total, the number of mappings is higher than the number of genes in this category. This is caused by the fact, that some genes were assigned to multiple subcategories, and by that were counted twice ore more.

Table 26: **“**Energy” top 20 Transcripts up-regulated in SXM

Energy SXM up	
id	function (annot. *F. graminearum*)
vl43-au16.g10363.t1	probable L-serine dehydratase 2
vl43-au16.g10848.t1	probable 3-isopropylmalate dehydrogenase beta
vl43-au16.g10882.t1	probable acetyl-CoA synthetase
vl43-au16.g12207.t1	related to SER3 - 3-phosphoglycerate dehydrogenase
vl43-au16.g13860.t3	probable ZWF1 - glucose-6-phosphate dehydrogenase
vl43-au16.g15149.t1	probable TRANSKETOLASE
vl43-au16.g15605.t1	probable PYC2 - pyruvate carboxylase 2
vl43-au16.g2422.t1	probable acetyl-CoA synthetase
vl43-au16.g4220.t1	related to alcohol dehydrogenase
vl43-au16.g4637.t1	related to glycerol-3-phosphate dehydrogenase precursor
vl43-au16.g5004.t1	probable TRANSKETOLASE
vl43-au16.g714.t1	probableglyceraldehyde 3-phosphate dehydrogenase (ccg-7)
vl43-au16.g7632.t1	probable ALCOHOL DEHYDROGENASE I - ADH1
vl43-au16.g604.t1	related to aldehyde reductase II
vl43-au16.g396.t1	related to several transaminases
vl43-au16.g10876.t1	related to xylulose-5-phosphate/fructose-6-phosphate phosphoketolase
vl43-au16.g12207.t1	related to SER3 - 3-phosphoglycerate dehydrogenase
vl43-au16.g1437.t1	related to ribokinase
vl43-au16.g15149.t1	probable TRANSKETOLASE
vl43-au16.g3026.t1	probable xylulose-5-phosphate phosphoketolase

For transcripts 21-118 mapping in this main category and below see attached data on CD (SXM_vs_xylS_xylem-sap_up-regulated_HIVI_cutoff_50). In total, the number of mappings is higher than the number of genes in this category. This is caused by the fact, that some genes were assigned to multiple subcategories, and by that were counted twice ore more.

6.2 Specific and core regulated transcript functional categories comparison

Table 27: Functional protein categories of regulated transcripts

Category / Transcripts upregulated in this cathegory	xylS up	SXM up	both up
Metabolism	196	305	1331
Cellular transport, transport facilitation and transport routes	107	159	792
Protein with binding function or Co-factor requirement (structural or catalytic)	97	156	843
Transcription	88	70	657
Protein fate (folding, modification, destination)	69	138	762
Cell rescue, defense and virulence	53	131	375
Cell cycle and DNA processing	68	96	594
Interaction with the environment	37	83	275
Energy	36	75	272
Biogenesis of cellular components	50	70	428
Cellular communication/signal transduction mechanism	28	27	250
Cell type differentiation	32	31	216
Protein synthesis	27	49	415
Cell fate	11	22	160
Regulation of metabolism and protein function	9	24	157
Development (systemic)	2	-	39
Systemic interaction with the environment	2	1	10
Organ differentiation	-	3	2
Transposable elements, viral and plasmid proteins	1	-	3
	913	1440	7581

6.3 Specific up-regulated transcripts – regulated subcategories only in xylem-sap

Table 28: First 30 up-regulated KEGG functional subcategories for xylem-sap (XylS) and SXM specific up-regulated transcripts

Category with subcategories / genes in this category	xylem-Sap vs. SXM	
	xylS up	SXM up
Metabolism	*196*	*305*
amino acid metabolism	41	77
nitrogen, sulfur and selenium metabolism	-	23
nucleotide/nucleoside/nucleobase metabolism	23	-
phosphate metabolism	25	43
C-compound and carbohydrate metabolism	94	160
lipid, fatty acid and isoprenoid metabolism	43	68
metabolism of vitamins, co-factors, and prosthetic groups	18	24
secondary metabolism	28	49
extracellular metabolism	14	-
Energy	-	*75*
fermentation	-	25
Cell cycle and DNA processing	*68*	*96*
DNA processing	33	55
cell cycle	44	60
Transcription	*88*	*70*
RNA synthesis	64	56
RNA processing	33	24
Protein fate (folding, modification, destination)	*69*	*138*
protein folding and stabilization	-	23
protein targeting, sorting and translocation	14	31
protein modification	36	69
protein/peptide degradation	17	66
Protein with binding function or Co-factor requirement (structural or catalytic)	*97*	*156*
protein binding	14	36
nucleic acid binding	32	37
metal binding	13	-
nucleotide/nucleoside/nucleobase binding	33	53
complex Co-factor/cosubstrate/vitamine binding	-	32
Cellular transport, transport facilitation and transport routes	*107*	*159*
transported compounds (substrates)	71	115
transport facilities	38	59
transport routes	72	89
Cellular communication/signal transduction mechanism	*97*	-
cellular signalling	21	-

Category with subcategories / genes in this category	xylem-Sap vs. SXM	
	xylS up	SXM up
Cell rescue, defense and virulence	*53*	*131*
stress response	20	82
disease, virulence and defense	21	35
detoxification	15	34
Interaction with the environment	*37*	*83*
homeostasis	23	42
cellular sensing and response to external stimulus	18	44
Cell fate	-	-
cell growth / morphogenesis	-	-
Biogenesis of cellular components	*50*	*70*
cell wall	16	27
nucleus	13	-
Cell type differentiation	-	*31*
fungal/microorganismic cell type differentiation	-	30

Table 29: **“**Nucleotide/nucleoside/nucleobased metabolism”

nucleotide/nucleoside/nucleobase metabolism	
id	function (annot. *F. graminearum*)
vl43-au16.g14375.t1	probable ADP, ATP carrier protein (ADP/ATP translocase)
vl43-au16.g11186.t1	probable IMP dehydrogenase
vl43-au16.g11192.t1	probable IMP dehydrogenase
vl43-au16.g1402.t1	probable IMP dehydrogenase
vl43-au16.g14497.t1	probable ribose-phosphate diphosphokinase catalytic chain I
vl43-au16.g6693.t1	related to phosphoribosylformylglycinamidine synthase
vl43-au16.g1675.t1	probable RIB2 - DRAP deaminase
vl43-au16.g14497.t1	probable ribose-phosphate diphosphokinase catalytic chain I
vl43-au16.g10221.t1	MAC1 - probable adenylate cyclase
vl43-au16.g12854.t1	MAC1 - probable adenylate cyclase
vl43-au16.g14387.t1	MAC1 - probable adenylate cyclase
vl43-au16.g1675.t1	probable RIB2 - DRAP deaminase
vl43-au16.g10381.t1	conserved hypothetical protein
vl43-au16.g11484.t1	related topurine utilization positive regulator
vl43-au16.g11950.t1	related topurine utilization positive regulator
vl43-au16.g4429.t1	related to 3`,5`-cyclic-nucleotide phosphodiesterase
vl43-au16.g4870.t2	related topurine utilization positive regulator
vl43-au16.g6027.t1	related to purine-cytosine permease
vl43-au16.g6657.t1	related topurine utilization positive regulator
vl43-au16.g6662.t1	related topurine utilization positive regulator
vl43-au16.g4195.t1	related to 3`-5` exonuclease
vl43-au16.g4791.t1	related to importin beta homolog Kap119p
vl43-au16.g1209.t1	related to lariat-debranching enzyme
vl43-au16.g14277.t1	related to protein involved in ribosomal RNA processing, component of the exosome complex responsible for 3` end processing and degradation of many RNA species
vl43-au16.g4355.t1	related to RNA helicase

In Table 29 to Table 33 the transcripts and their function of the functional subcategories shown in Table 28 (marked with red rectangle) and only found to be up-regulated in *V. longisporum* cultivated in xylem-sap were listed.

Table 30: **“**Extracellular metabolism”

	extracellular metabolism
id	function (annot. *F. graminearum*)
vl43-au16.g15018.t1	related tochitin binding protein
vl43-au16.g2731.t1	probable endoglucanase IV
vl43-au16.g3977.t1	related to beta-1,3 exoglucanase precursor
vl43-au16.g4222.t1	probable beta-1,3 exoglucanase precursor
vl43-au16.g4230.t1	related to chitin binding protein
vl43-au16.g5067.t1	related to endoglucanase IV precursor
vl43-au16.g6149.t1	probable beta-1,3 exoglucanase precursor
vl43-au16.g8098.t1	probable pectate lyase
vl43-au16.g8937.t1	related to chitin binding protein
vl43-au16.g950.t1	related to chitin binding protein
vl43-au16.g13689.t1	related tocarboxypeptidase
vl43-au16.g10924.t1	related to 1-phosphatidylinositol phosphodiesterase precursor
vl43-au16.g2731.t1	probable acetylxylan esterase
vl43-au16.g12693.t1	related to laccase precursor
vl43-au16.g6867.t1	related to laccase precursor
vl43-au16.g8937.t1	conserved hypothetical protein
vl43-au16.g950.t1	conserved hypothetical protein

Table 31: **“**Metal binding”

	metal binding
id	function (annot. *F. graminearum*)
vl43-au16.g10887.t1	conserved hypothetical protein
vl43-au16.g14578.t1	related to PHO36 - regulatory role in lipid and phosphate metabolism
vl43-au16.g1540.t1	related to PHO36 - regulatory role in lipid and phosphate metabolism
vl43-au16.g14375.t1	probable ADP, ATP carrier protein (ADP/ATP translocase)
vl43-au16.g9340.t1	related to annexin XIV
vl43-au16.g4582.t1	related to human and mouse neutral sphingomyelinase
vl43-au16.g10079.t1	probable AAA protease IAP-1 (mitochondrial intermembrane space)
vl43-au16.g11006.t1	related to isoleucine tRNA ligase
vl43-au16.g11125.t1	related to ALCOHOL DEHYDROGENASE I - ADH1
vl43-au16.g11876.t1	probable GTP cyclohydrolase I
vl43-au16.g12955.t1	related to vacuolar membrane protein HMT1 (heavy metal tolerance protein)
vl43-au16.g1696.t1	related to zinc finger protein crol gamma
vl43-au16.g1705.t1	related to ALCOHOL DEHYDROGENASE I - ADH1

Table 32: **“**Cellular signalling”

cellular signalling	
id	function (annot. *F. graminearum*)
vl43-au16.g10660.t1	related to hexamer-binding protein HEXBP
vl43-au16.g11578.t2	related to phosphotyrosyl phosphatase activator PTPA
vl43-au16.g117.t1	probable novel protein of ras superfamily KREV-1
vl43-au16.g12529.t1	related to RIM15 - protein kinase involved in expression of meiotic genes
vl43-au16.g14926.t1	probable NADPH oxidase heavy chain subunit
vl43-au16.g1498.t1	related to CELL DIVISION CYCLE 2-RELATED PROTEIN KINASE 7
vl43-au16.g15775.t1	related to CELL DIVISION CYCLE 2-RELATED PROTEIN KINASE 7
vl43-au16.g1647.t1	related to protein histidine kinase
vl43-au16.g2606.t1	related to cyclin dependent kinase C
vl43-au16.g300.t1	related to archipelago beta form (F-box-WD40 repeat protein)
vl43-au16.g4910.t1	related to dock180 protein
vl43-au16.g8713.t1	related to GTP-binding protein Rab5c
vl43-au16.g12052.t1	related to COP9 signalosome complex subunit 1 (G protein pathway suppressor 1)
vl43-au16.g129.t1	related to UNR-interacting protein STRAP (serine-threonine kinase receptor-associated protein)
vl43-au16.g5272.t1	related totetratricopeptide repeat protein 2
vl43-au16.g117.t1	probable novel protein of ras superfamily KREV-1
vl43-au16.g300.t1	related to archipelago beta form (F-box-WD40 repeat protein)
vl43-au16.g6620.t1	related to E. coli elongation factor-type GTP-binding protein lepa
vl43-au16.g8713.t1	related to GTP-binding protein Rab5c
vl43-au16.g10221.t1	MAC1 - probable adenylate cyclase
vl43-au16.g12854.t1	MAC1 - probable adenylate cyclase
vl43-au16.g14387.t1	MAC1 - probable adenylate cyclase
vl43-au16.g4582.t1	related to human and mouse neutral sphingomyelinase
vl43-au16.g4582.t1	related to human and mouse neutral sphingomyelinase
vl43-au16.g9929.t1	conserved hypothetical protein

Table 33: **“**Nucleus”

	nucleus
id	function (annot. *F. graminearum*)
vl43-au16.g10476.t1	probable ATPase component of chromatin remodeling complex (ISW1)
vl43-au16.g12056.t1	related to structural maintenance of chromosome protein (SMC)
vl43-au16.g14496.t1	probable ATPase component of chromatin remodeling complex (ISW1)
vl43-au16.g14497.t1	related to the component Tra1 of the SAGA complex
vl43-au16.g1875.t2	probable ATPase component of chromatin remodeling complex (ISW1)
vl43-au16.g1905.t1	related to the component Tra1 of the SAGA complex
vl43-au16.g2865.t1	related to transcriptional regulator CHD1
vl43-au16.g2871.t2	related to transcriptional regulator CHD1
vl43-au16.g3609.t1	related to the component Tra1 of the SAGA complex
vl43-au16.g3663.t1	related to transcriptional regulator CHD1
vl43-au16.g5214.t1	related to proliferation associated SNF2-like protein
vl43-au16.g5886.t1	related to the component Tra1 of the SAGA complex
vl43-au16.g8396.t1	related to proliferation associated SNF2-like protein

6.4 Pfam domains of xylem-sap and SXM specific up-regulated transcripts

Table 34: First 120 domains of different up-regulated transcripts

Part 1 domains of different up-regulated transcripts

No	PFAM		xylem-sap	SXM	difference
1	Zn_clus	Zinc finger domain	46	16	30
2	Fungal_trans	Fungal specific transcription factor	39	9	30
3	Pkinase	Protein kinase	20	4	16
4	Ank	Ankyrin repeat	15	2	13
5	RRM_1	RNA recignition motiv	13	1	12
6	p450	Cytochrome P450	21	10	11
7	Glyco_hydro_3	Glycosyl hydrolase family 3	11	0	11
8	Helicase_C	Helicase conserved C-terminal domain	10	0	10
9	Beta-lactamase	Beta-lactamase	9	0	9
10	PP-binding	Phosphopantetheine attachment site	9	0	9
11	Response_reg	Response regulator reciever domain	9	0	9
12	AMP-binding	AMP-binding enzyme	12	4	8
13	HET	Heterokaryon incompatibility protein	11	3	8
14	Amino_oxidase	Flavin containing amine oxidoreductase	10	2	8
15	Glyco_hydro_3_C	Glycoside hydrolase family 3	10	2	8
16	NACHT	NACHT domain	9	1	8
17	Acyl_transf_1	Acyl transferase domain	8	0	8
18	AA_permease	Amino acid permease	11	4	7
19	CBM_20	Carbohydrate-binding module	7	0	7
20	DEAD	DEAD/DEAH box helicase	7	0	7
21	HisKA	His Kinase A (phospho-acceptor) domain	7	0	7
22	ketoacyl-synt	Beta-ketoacyl synthase, N-terminal domain	7	0	7
23	Ketoacyl-synt_C	Beta-ketoacyl synthase, C-terminal domain	7	0	7
24	HATPase_c	Histidine kinase-, DNA gyrase B-, and HSP90-like ATPase	7	1	6
25	Abhydrolase_3	Alpha/beta hydrolase fold	6	0	6
26	PDR_CDR	CDR ABC transporter	6	0	6
27	WD40	WD or beta-transducin repeat	9	4	5
28	ABC2_membrane	ABC-2 type transporter	7	2	5
29	APH	Phosphotransferase enzyme family	7	2	5
30	Melibiase	Melibiase	6	1	5

Part 2 domains of different up-regulated transcripts

No	PFAM		xylem-sap	SXM	difference
31	Glyco_hydro_15	Glycoside hydrolase family 15	5	0	5
32	KR	KR domain	5	0	5
33	Mito_carr	Mitochondrial carriers	5	0	5
34	GMC_oxred_N	glucose-methanol-choline oxidoreductase family	9	5	4
35	NPP1	Necrosis inducing protein	7	3	4
36	zf-C2H2	Zinc finger, C2H2 type	6	2	4
37	SNF2_N	SNF2 family N-terminal domain	5	1	4
38	7tm_2	Secretin receptor family of 7 transmembrane receptors	4	0	4
39	AAA_5	AAA domain (dynein-related subfamily)	4	0	4
40	Alpha-amylase	Alpha amylase, catalytic domain	4	0	4
41	Condensation	Condensation domain	4	0	4
42	Cu-oxidase	Multicopper oxidase	4	0	4
43	Cu-oxidase_2	Multicopper oxidase	4	0	4
44	Cu-oxidase_3	Multicopper oxidase	4	0	4
45	DUF2235	Uncharacterized alpha/beta hydrolase domain	4	0	4
46	FAD_binding_7	FAD binding domain of DNA photolyase	4	0	4
47	Glyco_transf_34	galactosyl transferase GMA12/MNN10 family	4	0	4
48	Na_Ca_ex	Sodium/calcium exchanger protein	4	0	4
49	NB-ARC	NB-ARC domain	4	0	4
50	Peptidase_M20	Peptidase family M20/M25/M40	4	0	4
51	Phospholip_A2_3	Prokaryotic phospholipase A2	4	0	4
52	ADH_zinc_N	Zinc-binding dehydrogenase	16	13	3
53	DAO	FAD dependent oxidoreductase	6	3	3
54	Chitin_bind_3	carbohydrate-binding module	4	1	3
55	DUF3425	Domain of unknown function (DUF3425)	4	1	3
56	Patatin	Patatin-like phospholipase	4	1	3
57	Chromo	CHRromatin Organisation MOdifier domain	3	0	3
58	DNA_photolyase	DNA photolyase	3	0	3
59	DUF3433	Protein of unknown function (DUF3433)	3	0	3
60	DUF676	Putative serine esterase (DUF676)	3	0	3

Part 3 domains of different up-regulated transcripts

No	PFAM		xylem-sap	SXM	difference
61	Fmp27	Mitochondrial protein from FMP27	3	0	3
62	GCV_T_C	Glycine cleavage T-protein C-terminal barrel domain	3	0	3
63	Git3	G protein-coupled glucose receptor regulating Gpa2	3	0	3
64	Glu_synthase	Conserved region in glutamate synthase	3	0	3
65	Glyco_hydro_71	Glycoside hydrolase family 71	3	0	3
66	HA2	Helicase associated domain	3	0	3
67	IMPDH	IMP dehydrogenase / GMP reductase domain	3	0	3
68	Ldh_2	Malate/L-lactate dehydrogenase	3	0	3
69	LRR_1	Leucine Rich Repeat	3	0	3
70	PalH	PalH/RIM21	3	0	3
71	Pex24p	Integral peroxisomal membrane peroxin	3	0	3
72	Pirin	Pirin	3	0	3
73	S1		3	0	3
74	Sec7	Sec7 domain	3	0	3
75	TrkH	Cation transport protein	3	0	3
76	Acetyltransf_1	Acetyltransferase (GNAT) family	7	5	2
77	GMC_oxred_C	Glucose-methanol-choline oxidoreductase family	7	5	2
78	NAD_binding_1	Oxidoreductase NAD-binding domain	4	2	2
79	SH3_1	SH3 domain	4	2	2
80	DUF1605	Helicase associated domain (HA2)	3	1	2
81	Exo_endo_phos	Endonuclease/Exonuclease/phosphatase family	3	1	2
82	3HCDH_N	3-hydroxyacyl-CoA dehydrogenase, NAD binding domain	2	0	2
83	6PF2K	6-phosphofructo-2-kinase	2	0	2
84	ABC_membrane_2	ABC transporter transmembrane region 2	2	0	2
85	Ad_cyc_g-alpha	Adenylate cyclase G-alpha binding domain	2	0	2
86	Adaptin_N	Adaptin N terminal region	2	0	2
87	Ammonium_transp	Ammonium transporter	2	0	2
88	Apt1	Golgi-body localisation protein domain	2	0	2
89	Asparaginase	Asparaginase	2	0	2
90	BTB	BTB/POZ domain	2	0	2

Part 4 domains of different up-regulated transcripts

No	PFAM		xylem-sap	SXM	difference
91	Cation_efflux	Cation efflux family	2	0	2
92	CGI-121	Kinase binding protein CGI-121	2	0	2
93	Chitin_bind_1	Chitin recognition protein	2	0	2
94	Choline_sulf_C	Choline sulfatase enzyme C terminal	2	0	2
95	Cpn60_TCP1	TCP-1/cpn60 chaperonin family	2	0	2
96	Cyt-b5	Cytochrome b5-like Heme/Steroid binding domain	2	0	2
97	DHC_N1	Dynein heavy chain, N-terminal region 1	2	0	2
98	Dioxygenase_N	Catechol dioxygenase N terminus	2	0	2
99	DUF1162	Protein of unknown function (DUF1162)	2	0	2
100	DUF1966	Domain of unknown function (DUF1966)	2	0	2
101	DUF2405	Domain of unknown function (DUF2405)	2	0	2
102	DUF2420	Protein of unknown function (DUF2420)	2	0	2
103	DUF3517	Domain of unknown function (DUF3517)	2	0	2
104	DUF3659	Protein of unknown function (DUF3659)	2	0	2
105	DUF3712	Protein of unknown function (DUF3712)	2	0	2
106	DUF917	Protein of unknown function (DUF917)	2	0	2
107	FAT	FAT domain	2	0	2
108	Flavodoxin_1	Flavodoxin	2	0	2
109	Fmp27_SW	RNA pol II promoter Fmp27 protein domain	2	0	2
110	Fmp27_WPPW	RNA pol II promoter Fmp27 protein domain	2	0	2
111	GATase_2	Glutamine amidotransferases class-II	2	0	2
112	GCV_T	Aminomethyltransferase folate-binding domain	2	0	2
113	Glu_syn_central	Glutamate synthase central domain	2	0	2
114	Glyco_hydro_45	Glycoside hydrolase family 45	2	0	2
115	Glyco_transf_54	N-Acetylglucosaminyltransferase-IV (GnT-IV) conserved region	2	0	2
116	HMG_box	HMG (high mobility group) box	2	0	2
117	HSA	HSA	2	0	2
118	HsbA	Hydrophobic surface binding protein A	2	0	2
119	HSF_DNA-bind	Heast Shock Factor-type DNA-binding	2	0	2
120	Hydrolase_4	Putative lysophospholipase	2	0	2

Erklärung

Hiermit erkläre ich an Eides Statt, dass die Dissertation mit dem Titel „Characterization of the pathogenicity relevant genes *THI4* and *PA14_2* in *Verticillium dahliae*" selbständig und ohne unerlaubte Hilfe angefertigt wurde.

Göttingen, Oktober 2013

Clara Elisabeth Hoppenau

Danksagung

An erster Stelle möchte ich Herrn Prof. Gerhard Braus für die Möglichkeit danken, an diesem spannenden Thema in seiner Arbeitsgruppe zu arbeiten und dort meine Doktorarbeit anzufertigen. Ich danke ihm und Frau Prof. Ursula Kües für die gute Betreuung während dieser Zeit.

Frau Dr. Susanna Braus-Stromeyer, die mich während meiner Promotion umfassend betreute, danke ich für die anregenden Diskussionen und Gespräche. Des Weiteren gilt mein Dank Dr. Harald Kusch und Dr. Van Tran Tuan für ihre allzeitige Unterstützung.
Meinen Kollegen Christian Timpner, Anika Kühn, Christiane Oberthür und Kai Nesemann möchte ich auf diesem Wege für die sehr gute Zusammenarbeit während unserer gemeinsamen Experimente in Labor und Gewächshaus danken. Auf diesem Wege bedanke ich mich auch bei den Kolleginnen Dr. Mareike Possienke, Dr. Kirstin Feussner und Dr. Stefanie König (Abteilung Prof. Dr. Feussner) für die erfolgreiche, gemeinsame Arbeit an den großen Infektionsexperimenten. Ich möchte Alexander Kaever, Dr. Tonatiuh Pena Centeno und den anderen Bioinformatikern von BioFung, insbesondere Kathrin Aßhauer und Manuel Landesfeind, danken, für ihre Hilfe bei der Transkriptomdaten-Berechnung. Ich danke Dr. Blagovesta Popova, Kerstin Schmitt, Verena Hofer-Preez und Dr. Oliver Valerius, die mich bei meinen Hefeexperimenten unterstützten. Besonderer Dank gilt Maria Meyer und Heidi Northemann, für die sehr angenehme Atmosphäre in unserem Labor sowie für die guten und aufmunternden Gespräche. Auf diesem Wege möchte ich ebenfalls Nicole Scheiter für die fantastische Unterstützung im logistischen Bereich danken. Vielen Dank auch an alle Mitarbeiter der AG Braus für die schöne und angenehme Zeit.

Mein besonderer Dank gilt Dr. Mareike Possienke, Dr. Jennifer Gerke, Rebekka Harting, Dr. Anne Dettmann, Dr. Christoph Sasse, Dr. Anna Sasse und Dipl-Jur. Cornelia Gorholt, die sich die Zeit nahmen diese Arbeit gegen zu lesen.

Zum Schluss möchte ich mich ganz herzlich bei meinen Eltern bedanken ohne deren Unterstützung diese Arbeit nicht möglich gewesen wäre.

Diese Arbeit wurde finanziell unterstützt vom Bundesministerium für Bildung und Forschung (BMBF).

Curriculum Vitae

Clara Elisabeth Hoppenau

Born on December the 15th, 1982 in Cologne, Germany

Education:

1988-1992	Primary Education in Hamburg
1992-2003	Secondary Education in Hamburg

Scientific background:

2004-2007	**Basic studies** at the University of Hamburg
2007-2009	**Advanced studies** at the Philipps-University of Marburg **Graduation** in biology with the diploma thesis "Reparatur von Thymindimeren in duplex DNA durch *Arabidopsis Cryptochrom* 3 mittels Elektronentransfer entlang des DNA Stranges", in the Institut für Pflanzenphysiologie und Photobiologie, Abteilung für Molekulare Pflanzenphysiologie und Photobiologie of Prof. Dr. A. Batschauer.
2009-2013	**Scientific assistent** at the Georg-August Universität Göttingen (Germany), in the Institut für Mikrobiologie und Genetik, Abteilung für Molekulare Mikrobiologie und Genetik of Prof. Dr. G.H. Braus.